



UNIVERSIDADE D
COIMBRA

Vitaliy Masliy

**SUSTAINABLE SYNTHESIS OF NATURAL-
BASED POTENTIAL FRAGRANCES VIA
FLOW CHEMISTRY**

**Dissertação no âmbito do Mestrado em Química na vertente de
Química Avançada e Industrial orientada pela Professora Doutora
Maria Miguéns Pereira e coorientada pelo Doutor Fábio M. S. Rodrigues
apresentada ao Departamento de Química da
Faculdade de Ciências e Tecnologia da Universidade de Coimbra.**

Setembro de 2022

Faculdade de Ciências e Tecnologia
da Universidade de Coimbra

**Sustainable synthesis of natural-based potential
fragrances via flow chemistry**

Vitaliy Masliy

Dissertação no âmbito do Mestrado em Química na vertente de Química Avançada e Industrial
orientada pela Senhora Professora Doutora Maria Miguéns Pereira, coorientada pelo Doutor
Fábio M. S. Rodrigues e apresentada ao Departamento de Química da Faculdade de Ciências e
Tecnologia da Universidade de Coimbra

Setembro de 2022



UNIVERSIDADE D
COIMBRA

“In chemistry also, we are now conscious of the continuity of man’s intellectual effort; no longer does the current generation view the work of its forerunners with a disdainful lack of appreciation; and far from claiming infallibility, each successive age recognises the duty of developing its heritage from the past.”

August Kekulé von Stradonitz (1821–1896)

Acknowledgments

Os últimos cinco anos passaram num momento, parece que foi ontem que entrei na licenciatura e fui para a minha primeira praxe, no entanto já acabei a licenciatura e agora estou a acabar a tese de mestrado. Gostaria de agradecer às pessoas que me ajudaram a crescer academicamente e pessoalmente.

Começando por agradecer à professora Mariette Pereira, a minha orientadora, por me oferecer todas as oportunidades para o desenvolvimento deste trabalho, pela orientação, por me encorajar a encontrar soluções para os problemas que enfrentei durante o meu trabalho e pela compreensão.

Ao Doutor Fábio Rodrigues, pelo apoio e orientação, pela paciência, ajuda em qualquer dificuldade a qualquer momento do dia.

Ao Pedro Cruz do serviço de Ressonância Magnética Nuclear do Centro de Química de Coimbra (CCC-NMR), agradeço a colaboração na obtenção dos espectros de RMN.

Ao grupo de Química-Física Molecular, realçando à professora Maria Paula Marques e à Clara Martins pela colaboração nos estudos *in vitro*.

A todos os meus colegas do grupo Catálise e Química Fina, pelo convívio diário, por todo o apoio na utilização do equipamento e metodologias, pelos cafés oferecidos, pelos ensinamentos que me foram oferecidos e pelo ambiente amigável.

À Silvia Gramacho pelo apoio moral e pela colaboração na obtenção dos espectros de GC-MS.

A todos os meus amigos, pelo imenso apoio e amizade que me ofereceram durante estes anos. Por todas as conversas sobre química, concelhos, por todas as correções no português e por todos os momentos felizes que partilhámos.

Нарешті, я хотів би подякувати своїм батькам за підтримку в усіх моїх рішеннях, за поради та підтримку протягом усіх цих років. Я дуже вдячний вам за це.

Index

Abbreviations and Symbols.....	i
Abstract.....	v
Resumo	vi
Nomenclature.....	vii
1. Introduction	1
1.1. Natural Fragrances.....	1
1.2. Flow Chemistry in Fragrance Synthesis	3
1.3. Epoxidations of Natural Products.....	7
1.4. CO ₂ Cycloaddition to Epoxides	13
1.5. Sequential Epoxidation-Carboxylation Reactions	18
1.6. Thesis Goals	25
1.7. References	26
2. Chemical Transformations of Eugenol.....	39
2.1. Synthesis of Metalloporphyrin-Based Catalysts.....	40
2.2. Eugenol Hydroxyl Group Protection	52
2.2.1. Eugenol Methylation.....	52
2.2.2. Eugenol Acetylation.....	53
2.2.3. Heterogenous Eugenol Acetylation	55
2.3. Epoxidation of Eugenol Derivatives	60
2.3.1. Prilejaev Epoxidation of Eugenol.....	60
2.3.2. Catalytic Epoxidation Using Oxygen as Oxidant	65
2.2.3. Catalytic Epoxidations Using Hydrogen Peroxide as Oxidant.....	67
2.4. Synthesis of Acetyeugenol Cyclic Carbonate.....	73
2.4.1. Cycloaddition of CO ₂ to Epoxides	73
2.4.2. Oxidative Carboxylation.....	77
2.5. Conclusion and Future Perspectives.....	80
2.6. References	83
3. Experimental Section.....	89
3.1. Solvents and Reagents.....	89
3.2. Instrumentation	90
3.3. Synthesis of Metalloporphyrin-Based Catalysts.....	94
3.3.1. Porphyrin Synthesis.....	94
3.3.2. Preparation of CAT1.....	96

3.3.3. Preparation of CAT2.....	97
3.3.4. Preparation of CAT1@NHSiO2.....	98
3.4. Synthesis of Eugenol Derivatives	99
3.4.1. Methyl Eugenol Synthesis	99
3.4.2. Acetyeugenol Synthesis	99
3.4.3. Acetyeugenol Epoxide Synthesis	101
3.4.4. Methyl eugenol Epoxide Synthesis	102
3.4.5 Acetyeugenol Carbonate Synthesis	103
3.4.6 Oxidative Carboxylation.....	104
3.5. Cytotoxic: MTT Assay	105
3.6 References	106
Annex.....	107

Abbreviations and Symbols

λ	Wavelength
δ	Chemical shifts
[M] ⁺	Molecular ion
¹³ C NMR	Carbon 13 nuclear magnetic resonance spectroscopy
¹⁹ F NMR	Fluorine 19 nuclear magnetic resonance spectroscopy
¹ H NMR	Proton nuclear magnetic resonance spectroscopy
s	Singlet
d	Doublet
dd	Doublet of doublets
ddt	Doublet of doublet of triplets
m	Multiplet
p	Pentet
J	Coupling constant
A/Abs	Absorbance
Ac	Acetyl
Acac	Acetylacetone
BPR	Back pressure regulator
C&FC	Catalysis and Fine Chemistry
Cat.	Catalyst
COSY	Correlation spectroscopy in nuclear magnetic resonance
DBU	1,8-Diazabicyclo[5.4.0]undec-7-ene
DME	Dimethoxyethane
DMF	Dimethylformamide
DMSO	Dimethyl sulfoxide

eq.	Equivalent
HRMS (ESI)	High resolution electrospray ionization mass spectrometry
Et	Ethyl
F&F	Flavor and Fragrances
GC	Gas chromatography
GC-MS	Gas chromatography–mass spectrometry
HSQC	Heteronuclear Single Quantum Coherence
HMQC	Heteronuclear multiple-quantum correlation
ICP-OES	Inductively coupled plasma - optical emission spectrometry
iPr	Isopropyl
IRA-120H	Amberlite 120H
K10	Montmorillonite K10
m/z	Mass/Charge relation
MALDI-TOF	Matrix-assisted laser desorption/ionization
MTT	2,5-diphenyltetrazolium bromide
mCPBA	<i>m</i> -chloroperoxybenzoic acid
Me	Methyl
MeTHF	2-Methyltetrahydrofuran
NBS	N-Bromosuccinimide
NOESY	Nuclear Overhauser effect spectroscopy
PBS	Phosphate-buffered saline
<i>p</i> -CF ₃ TPP	5,10,15,20-tetra(4-trifluoromethylphenyl)porphyrin
ppm	Parts per million
PPNCl	Bis(triphenylphosphine)iminium chloride
S _N 2	Bimolecular nucleophilic substitution

STY	Space-Time-Yield
TBAB	Tetrabutylammonium bromide
TBAC	Tetrabutylammonium chloride
TBAI	Tetrabutylammonium iodide
TBHP	Tert-Butyl hydroperoxide
TDCPP	5,10,15,20-tetra(2,6-dichlorophenyl)porphyrin
TDCPPS	5,10,15,20-tetra(2,6-dichloro-3-chlorosulfonyl-phenyl)porphyrin
TDCPPS@NHSiO ₂	TDCPPS immobilized onto aminopropyl functionalized silica particles
TGA	Thermogravimetric analysis
THF	Tetrahydrofuran
TLC	Thin-layer chromatography
TPP	Tetraphenylporphyrin
TS	Titanium silicates
TTBPP	Tris(3-tert-butylphenyl)phosphate
UV-VIS	Ultraviolet-visible spectroscopy

Abstract

The studies described in this MSc. thesis are focused on the development of novel synthetic routes, using batch and continuous flow processes, for the preparation of eugenol derivatives, with potential application as fragrances.

In chapter 1 a critical review of recent literature on the main topics of the thesis is presented. It includes selected papers about the preparation of fragrances using continuous flow systems, epoxidations, CO₂ cycloadditions and oxidative carboxylation reactions, under batch and continuous flow conditions.

Chapter 2 starts with the preparation of Mn(III) and Cr(III) porphyrin-based catalysts for epoxidation and CO₂ cycloaddition reaction, respectively. After appropriate functionalization, the MnOAcTDCPP catalyst was immobilized onto silica and the material was fully characterized.

After optimization of eugenol protection under batch and flow conditions, using both homogeneous and heterogeneous acid catalysts, the studies pursued with the optimization of epoxidation reactions using peroxy acids, O₂ or H₂O₂ as oxidants. The best system was the H₂O₂ with imidazole as co-catalyst, which afforded excellent selectivity for epoxide formation, with a space-time yield of 0.32 g min⁻¹ dm⁻³.

Regarding the preparation of potential fragrance of eugenol cyclic carbonate type, two approaches were developed and the CO₂ cycloaddition to epoxides revealed to be the best catalytic system, which lead to 91% isolated yield.

In chapter 3, the techniques, experimental procedures and characterization of all the materials and products are described.

Resumo

Os estudos descritos nesta dissertação de mestrado focam-se no desenvolvimento de novas vias sintéticas, usando processos em *batch* e em fluxo contínuo para preparação de derivados do eugenol, com potencial aplicação como fragâncias.

No capítulo 1 é apresentada uma revisão crítica da literatura recente sobre os principais tópicos da tese. Inclui artigos selecionados para preparação de fragâncias em sistemas de fluxo contínuo, epoxidações, cicloadições de CO₂ e reações de carboxilação oxidativa, em condições *batch* e fluxo contínuo.

O capítulo 2 inicia-se com a preparação de catalisadores de Mn(III) e Cr(III) porfirínicos, para reação de epoxidação e cicloadição de CO₂, respetivamente. Após funcionalização adequada, o catalisador MnOAcTDCPP foi imobilizado em sílica e o material foi totalmente caracterizado.

Após otimização da proteção do eugenol em condições de *batch* e fluxo contínuo, usando catalisadores ácidos homogêneos e heterogêneos, os estudos prosseguiram com a otimização das reações de epoxidação, usando perácidos, O₂ ou H₂O₂ como oxidantes. O sistema de H₂O₂ foi considerado o melhor, com um “*space-time-yield*” de 0,32 g min⁻¹ dm⁻³.

Relativamente à preparação das potencias fragrância do tipo carbonato cíclico de eugenol, duas abordagens foram desenvolvidas, sendo a cicloadição de CO₂ a epóxidos o melhor sistema catalítico, que levou a 91% de rendimento isolado.

No capítulo 3 são descritas as técnicas, procedimentos experimentais e caracterização de todos os materiais e produtos.

Nomenclature

In this MSc Thesis, International Union of Pure and Applied Chemistry (IUPAC) guidelines regarding numbering and naming of compounds were followed, except for the porphyrin rings, which are promptly referred in this section.

For the designation of the synthesized porphyrins in this Thesis, IUPAC numbering system was used, which consists in the numbering of all the carbon atoms from the macrocycle from 1 to 20 and the internal nitrogen from 21 to 24 (Figure I) Sometimes, Fischer's terminology which designates the positions 5, 10, 15, 20 as *meso* and the positions 2, 3, 7, 8, 12, 13, 17 and 18 as positions β (beta) will be adopted.¹

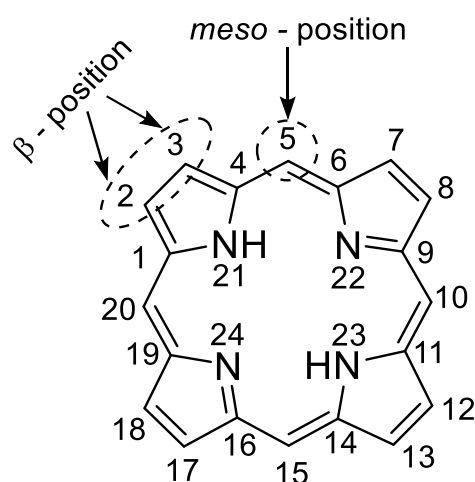


Figure I. IUPAC numbering system used for porphyrins and their respective designations according to Fischer's terminology.

1 Fischer, Hans, Hans Orth, and Adolf Stern. *Die Chemie Des Pyrrols*. Leipzig : Akademische Verlagsgesellschaft, 1937.

Introduction

1.1. Natural fragrances

The use of fragrances was documented, for the first time, in ancient Egypt and Mesopotamia about 4000 years ago.¹ In ancient Egypt, fragrances were made from oils obtained from plants, animal organs, or animal fat, such as ox, goose, cat, hippopotamus, and crocodile fats.^{1,2} These perfumes were more frequently used for religious rituals, magic and medicine.^{2,3} For private use, cinnamon, cardamom, myrrh, honey, wine or flowers were the main ingredients in perfume creation.^{1,2} Later, the perfume tradition and techniques were shared with ancient Greeks, who exported these products over the Eurasian continent and later to the rest of the world.^{1,2,4}

Until the 19th century, practically all fragrances were from natural sources, but with the development of chemistry, new aromas became possible to create by synthetic means. The new fragrances shook the well-established market, causing a quick rise of new fragrance-related companies.⁵ According to Grand View Research,⁶ the fragrance industry had an estimated market of \$23.35 billion in 2021, with over 4000 different fragrance molecules. Less than 5% of the reported fragrances are obtained directly from nature, the absolute majority are either fully synthetic molecules such as Velberry, a fruity-sweet fragrance developed by BASF, or simply natural compound derivatives, like the Frescolat, a menthol derivative patented by Symrise (Figure 1.1).⁷

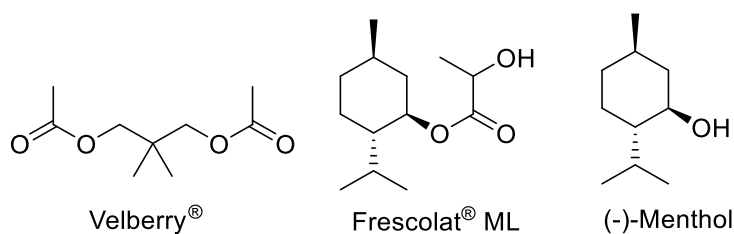


Figure 1.1. Fragrance molecules.⁷

Natural fragrances may smell better than other compounds, however, some of them also have biological activity.⁸⁻¹² In order to ensure the safety of the compounds, in-depth biological studies must be done.

Analyzing the long-term side effects of fragrances is quite a challenge, as many perfumes and cosmetics come with a complex mixture of compounds, which sometimes can count up to hundreds of volatile compounds, making it difficult to interpret the cause of the side effects of a given fragrance.¹³ Another factor that difficults the interpretation of the results is the law. Companies are allowed to hide the full list of ingredients as a trademark secret, including substances that can cause severe health problems.¹⁴ Such laws are different in the USA and Europe: the Federal Fair Packaging and Labeling Act of 1973 is the regulator for fragrances labeling in the USA, while in Europe the Regulation (EC) No 1223/2009 of 30/11/2009 is the law that only obligates the manufacturer to label fragrances which may trigger severe allergic reactions. With over 4000 different fragrances, only 27 of them must be listed on the European perfume labels.¹⁵

In 2010, Canadian Campaign for Safe Cosmetics published a report, in which 17 name-brand fragrance products were investigated for potentially dangerous fragrances, concluding that, while the fragrances that can trigger allergic reactions are labeled, hormone-disrupting chemicals are omitted. An average of four hormone-disrupting chemicals per product were reported, as they mimicked the estrogen and the thyroid hormones.¹⁶ The relationship between hormone-disrupting chemicals and cancer is well known, several individual fragrances were banned due to interference with the endocrine system.¹⁷

Among the most widely used natural compound for fragrance manufacturing, we highlight eugenol (Figure 1.2). It is one of the compounds used as a building block for the development of new fragrances and is the starting point of this work. Besides its pleasant flavor and aroma, eugenol also possesses antioxidant, antimutagenic, antigenotoxic, anti-inflammatory, and anticancer properties.¹⁸⁻²⁶ Due to its anti-inflammatory and antimicrobial properties, eugenol can be often found in inhalation and aerosol medicines, such as Aromatol, Amol, or Olbas.²⁷

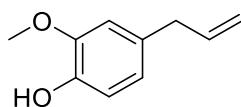


Figure 1.2. Chemical structure of eugenol (4-allyl-2-methoxyphenol).

Eugenol (4-allyl-2-methoxyphenol) is a natural volatile compound with fragrance properties, found in different plants, such as cinnamon, nutmeg, tea leaves, and clove.²⁸ Eugenol has many applications in the Flavors & Fragrances (F&F) industry, it can be commonly found in perfumes with fruity flavors, as a spicy flavoring in whisky, in ice creams, baked goods, and candies.²⁹ Since 2019, a great number of review articles (*ca.* 85) were published, regarding the extension of eugenol applications in the medicinal field. Therefore, many groups focused on the chemical modification of eugenol using hydroformylation,³⁰⁻³² epoxidation,³³⁻³⁵ and other reactions.³⁶

It should be noted that research in the area of chemical transformation of new fragrances has also undergone major developments in the search for sustainable processes, in line with the principles of green chemistry.³⁷ In this regard, we highlight flow chemistry that emerged as an alternative synthetic tool to perform the total synthesis of fragrance compounds. This is one of the main goals of the experimental work described in this thesis, in the next section, we present a critical literature review of the most relevant examples of fragrance development through continuous flow chemical processes.

1.2. Flow Chemistry in Fragrance Synthesis

Currently, batch synthetic methods are the most commonly used in industrial fragrance preparation although they present several limitations, particularly for scale-up production.³⁸ So, continuous-flow methods became a trendy alternative, allowing the efficient synthesis of a wide range of fragrances with higher yields, less waste and side-product formation and higher energetic efficiency, when compared with traditional batch synthetic methods.³⁹⁻⁴¹

Flow chemistry is a method of mixing reagents in a continuous flow process, pumping them through channels instead of reaction flasks/reactors, leading to a high surface to area ratio, allowing high heat and mass exchange. Additionally, the use of pumps in flow chemistry brings the possibility to pressurize the liquids, without other specialized equipment (Figure 1.3).⁴²⁻⁴⁴ The biggest interest in flow chemistry lies within the industrial sector, as reactions made using continuous flow processes are easy to scale up and they are overall safer when compared with industrial scale batch reactions.⁴⁵ The use of continuous flow methods allows the synthesis of diverse compounds without the need for intermediate purification, which decreases the use of solvents significantly, increasing the sustainability of this method.^{45, 46} All these issues led the companies such as Merck, Pfizer, BASF to give

high priority to flow chemistry in their R&D departments.⁴⁷ Among the most recent applications we highlight the use of flow chemistry for the microencapsulation of the Pfizer Covid vaccine, which increased the production of the vaccine several times.⁴⁸

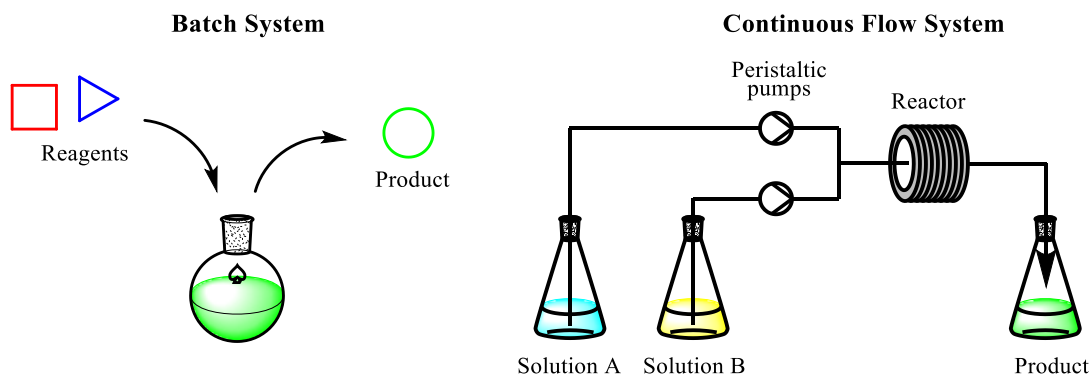
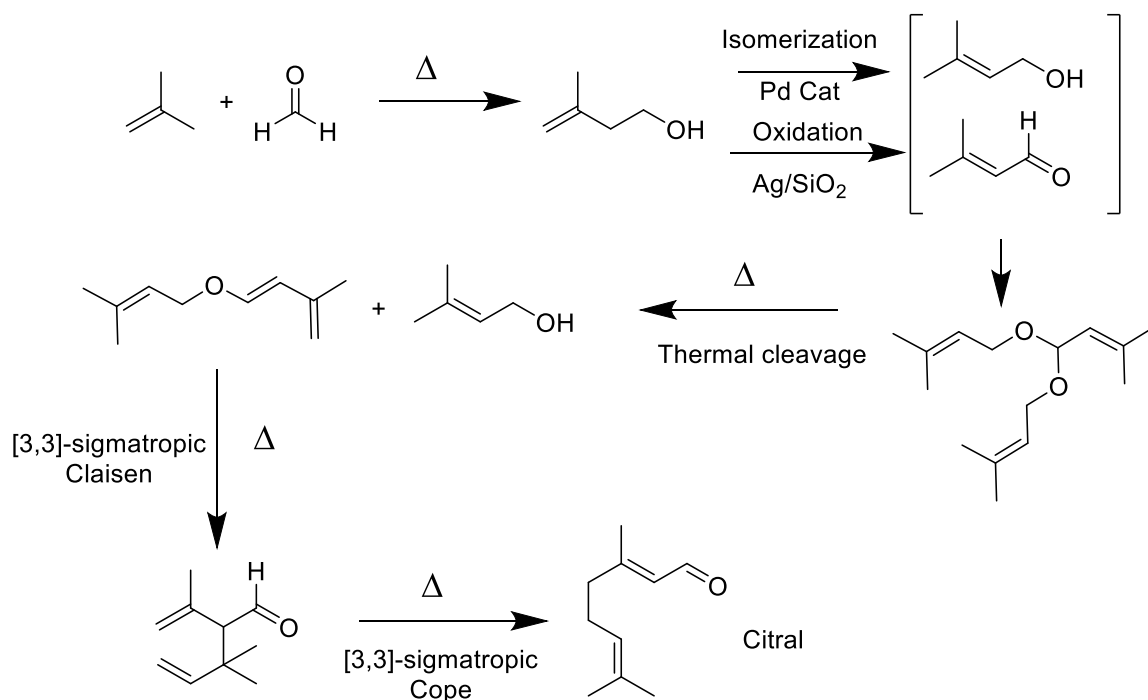


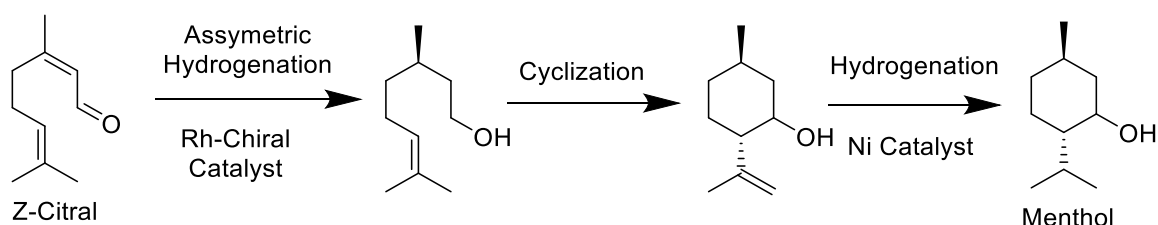
Figure 1.3. Schematic comparison between batch and continuous flow systems.

Regarding fragrance preparation and considering their high volatility, batch methods have low efficiency since parts of the reagents and product can evaporate during the process. This loss can be prevented by implementing a continuous flow system, as it is a pseudo-closed system, where heat distribution, pressure, and reaction time are strictly regulated.^{49, 50} The F&F industry was one of the first companies to implement continuous flow processes to solve this problem.⁴⁹ A remarkable example of continuous flow synthesis of fragrances was patented and then implemented by BASF in 2004 for the synthesis of citral from isobutylene and formaldehyde, producing 40,000 tons of citral per year (Scheme 1.1).⁵¹



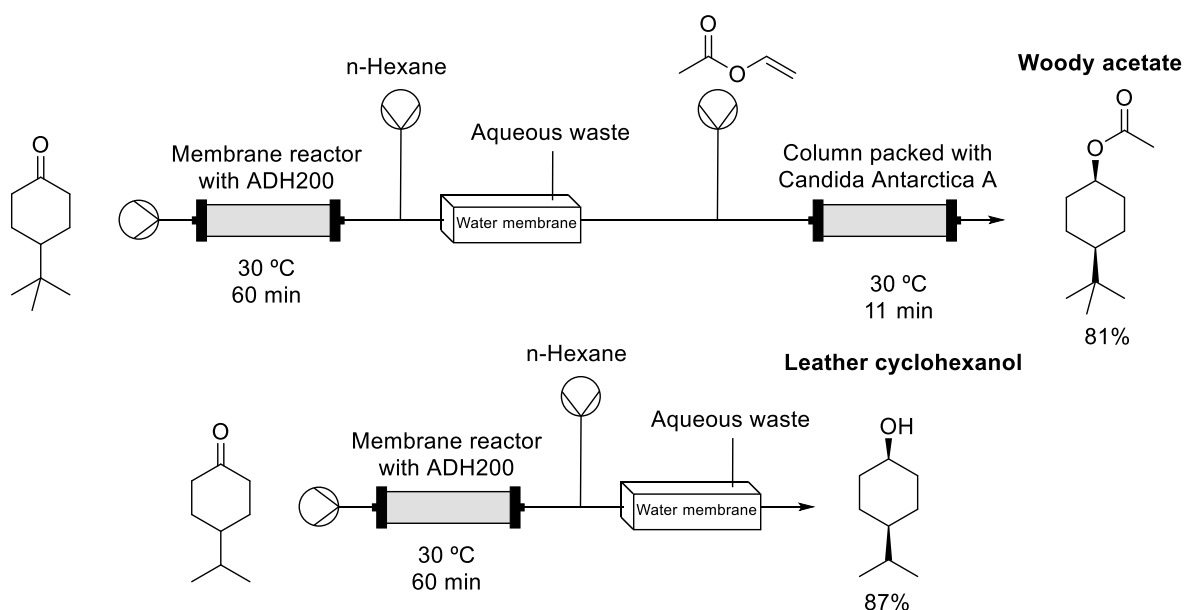
Scheme 1.1. Continuous flow process for the synthesis of Citral developed by BASF.⁵¹

Later, in 2012, BASF also developed and applied a continuous flow system for the synthesis of menthol from citral, in which higher product purity was obtained than previously developed batch products, Scheme 1.2.⁵²



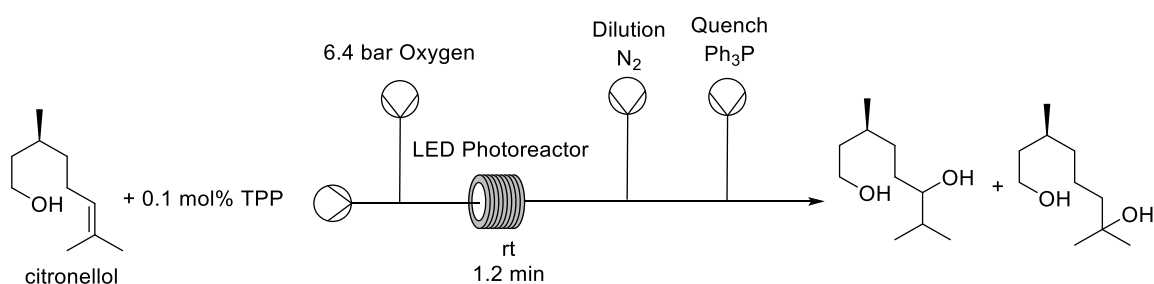
Scheme 1.2. Menthol commercial synthesis method developed by BASF.⁵²

Tessaro described the synthesis of leather cyclohexanol and woody acetate, known commercial fragrances.⁵³ For that purpose, the authors used commercially available enzymes (alcohol dehydrogenases) to stereoselectively reduce the corresponding ketones, as shown below (Scheme 1.3). Since different enantiomers have different aromas, the stereoselectivity of these processes is an extremely relevant parameter. Using this strategy, the authors reported, for leather cyclohexanol enantioselectivity of 87% with 90% yield, while woody acetate had 99% enantioselectivity with 81% yield.



Scheme 1.3. Woody acetate synthesis under flow conditions, described by D. Tessaro.⁵³

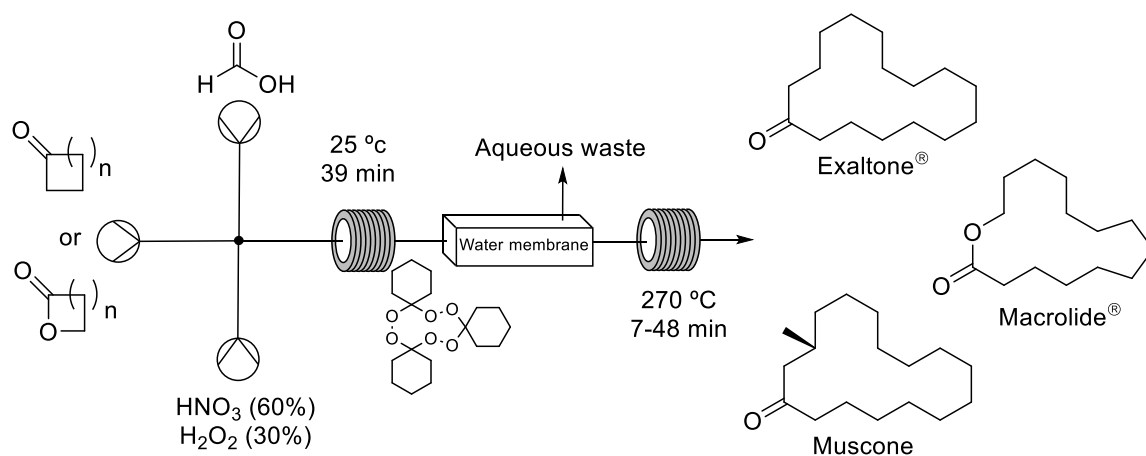
Réguillon described the photo-oxidation of citronellol under flow conditions. This reaction was used for the production of rose oxide di-hydroxylated precursors and is currently one of the few photo-oxidative processes that used flow chemistry at an industrial scale, producing around 100 tons per year.^{54, 55} Réguillon used TPP as photosensitizer and LEDs as light source (Scheme 1.4).⁵⁶ As the resulting products from this reaction are hydroperoxides, the authors had to adopt several precautions, including the *in-line* quenching, using triphenylphosphine to reduce the peroxide to alcohol and dilute the solution. For instance, for citronellol, the authors diluted the solution up to 0.05 M concentration to obtain ca. 95% conversion within 1.2 minutes.



Scheme 1.4. Photo-oxidation of citronellol under continuous flow described by Réguillon.⁵⁶

In 2021, Kirschning described the synthetic method for macrocyclic compounds, which are used in the fragrance industry due to their musk-like aroma (Scheme 1.5).⁵⁷

Using concentrated hydrogen peroxide, formic acid, and nitric acid mixture together with a ketone or lactone results in unstable triperoxides. These triperoxides can be pyrolyzed at temperatures above 230 °C, resulting in the desired macrocycles. Although this reaction is not new, its transposition from laboratory to industrial scale was impossible to date, as it requires extreme conditions, the use of dangerous reagent mixtures (30% H₂O₂, 65% HNO₃) and highly explosive triperoxide intermediates. However, with the use of flow conditions, the overall safety issues were minimized, since only small amounts of concentrated hydrogen peroxide and triperoxide intermediates are exposed to high temperatures, allowing its implementation at a higher scale.

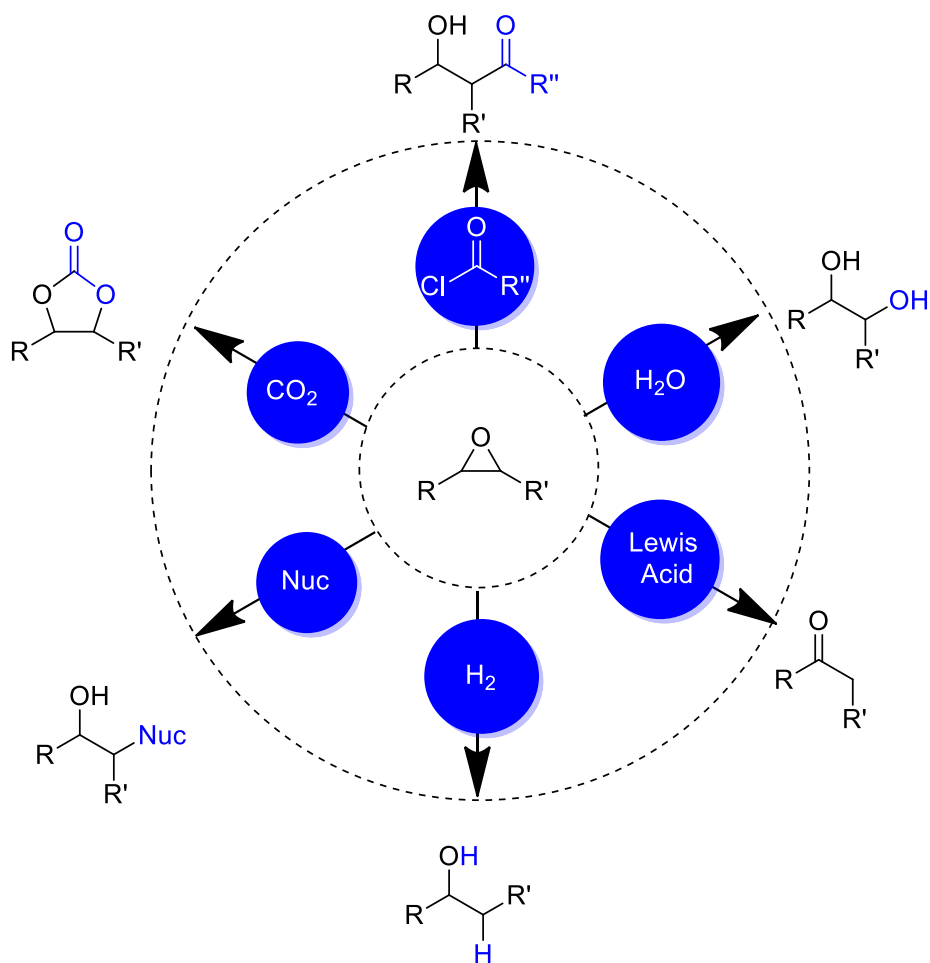


Scheme 1.5. Synthesis of ketone and lactone macrocycles under flow conditions described by Kirschning.⁵⁷

Among the multiple chemical transformations involved in the synthesis/functionalization of natural products for fragrance preparation, we highlight the catalytic epoxidation and CO₂ cycloaddition reactions, which are also the reactions studied in this thesis. Therefore, in the following sections, we present a literature review of batch *versus* continuous flow processes for the implementation of these catalytic reactions in natural product transformations.

1.3. Epoxidations of natural products

Epoxides are quite useful intermediates in fragrance synthetic chemistry, as they can react with nucleophiles leading to ring-opening reactions, can undergo cycloaddition reactions to CO₂ leading to the preparation of cyclic carbonates, rearrangement reactions, among others.⁵⁸⁻⁶⁰ (Scheme 1.6).



Scheme 1.6. Epoxide ring transformations.

Although the direct use of epoxide ring molecules in the perfume industry is rare, there are some examples of the application of terpenoid-based epoxides and the respective derivatives (ex. Folenox, Andrane, Ionone epoxide, Caryophyllene oxide) as fragrances (Figure 1.4).

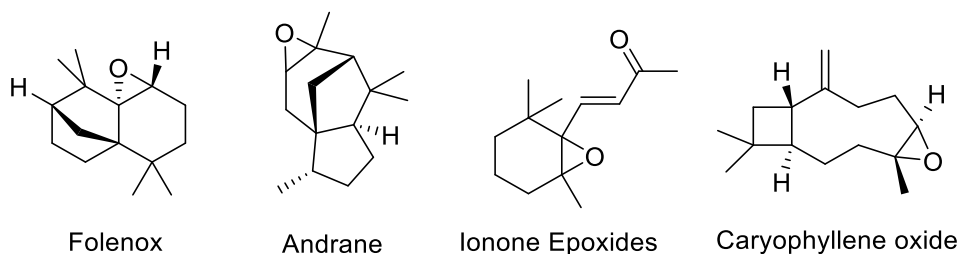


Figure 1.4. Examples of terpenoid-based epoxides fragrances.

The relevance of natural compound epoxidation is well illustrated by the publication of several reviews over the last few years,⁶¹⁻⁷¹ some of them describing the epoxidation of natural oils.⁷²⁻⁷⁴ Herein, we focus on the application of natural-product epoxidation reactions for the preparation of potential fragrances, reported over the last three years (Table 1.1). The epoxidation of high molecular weight compounds, such as fatty acids, were excluded since they have limited application in the fragrance industry.

An example of limonene epoxidation was described by F. Parrino.⁷⁵ Catalytic and photocatalytic epoxidations were described, using titanium and manganese nanoparticles immobilized in mesoporous silica as heterogeneous catalysts. Molecular oxygen was used as green oxidant, while isobutyraldehyde or *n*-hexanal have been used as “sacrificial” co-reductants. The best result was obtained with the bimetallic catalyst based on titanium oxide doped with manganese oxide, resulting in 90% conversion and 84% epoxide selectivity, at 60 °C. Regarding the photocatalytic process, carried at 25 °C and atmospheric pressure, 80% conversion and 50% selectivity for epoxide were obtained (Table 1.1, entry 1). Although the selectivity of the photocatalytic process was lower, it doesn't require the use of a co-reductant, which, in some cases, can be considered a more sustainable approach as it decreases waste.

Table 1.1. Epoxidation of natural compounds described over the past 3 years in batch conditions.

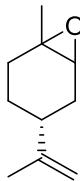
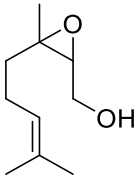
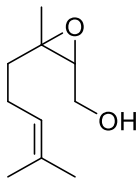
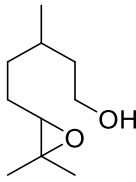
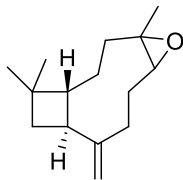
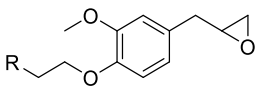
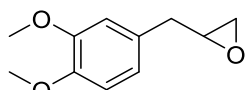
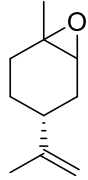
Entry	Products	Catalyst	Oxidant	Conditions & Results
1 ⁷⁵		TSMn-10	O ₂	<ul style="list-style-type: none"> • 2.5 eq of isobutyraldehyde • CH₂Cl₂ as solvent • 60 °C • 5 bar O₂ pressure • 0.5% of cat. • 3 h • 100% conversion • 40% selectivity to 1,2-epoxide
2 ⁷⁶		[Co ₃ (OH) ₂] ₆ (A-PW ₉ O ₃₄) ₂] ¹²⁻ Aliquat 336 as co-cat.	H ₂ O ₂	<ul style="list-style-type: none"> • CH₂Cl₂/H₂O (biphasic reaction) • 2.5 h • 15 °C • 0.5 mol% cat. • 94% conversion • 99% selectivity

Table 1.1. Epoxidation of natural compounds described over the past 3 years in batch conditions

Entry	Products	Catalyst	Oxidant	Conditions & Results
3 ⁷⁷		H ₃ PMo ₁₂ O ₄₀	H ₂ O ₂	<ul style="list-style-type: none">• 0.66 mol% of cat.• 1 eq of oxidant• 8 h• CH₃CN solvent• 25 °C• 96% conversion• 92% selectivity
4 ⁷⁸		titanosilicate	H ₂ O ₂	<ul style="list-style-type: none">• CH₃CN• 1 eq. of H₂O₂• 60 °C• 180 min• 16.6 conversion• 55% selectivity
5 ⁷⁹		Cu-based nanosheets	O ₂	<ul style="list-style-type: none">• THF• 60 °C• 18h• 1 bar of O₂• 0.1 eq. of TBHP• 87% yield
6 ⁸⁰		-----	mCPBA	<ul style="list-style-type: none">• CH₂Cl₂• 25 °C• 1.5 eq. of mCPBA• 7-67% yield
7 ⁸¹		-----	mCPBA	<ul style="list-style-type: none">• 6 eq. of mCPBA• CH₂Cl₂• 24 h• 25 °C• 69% yield
8 ⁸²		PW ₄ O ₂₄ [MeN ⁺ (C ₈ H ₁₇)] ₃	H ₂ O ₂	<ul style="list-style-type: none">• Neat• 1.6 eq. of H₂O₂• 50 °C• 16.7 min• Continuous flow• 89% conversion• 90% selectivity

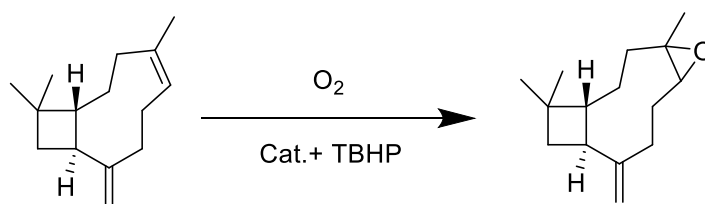
In 2020, Li did an in-depth study on allylic alcohols epoxidation using metallic phosphopolyoxotungstate anions as catalyst, Aliquat 336 as co-catalyst and H₂O₂ as

oxidant. (Table 1.1, entry 2).⁷⁶ Three different metallic ions were used in this study, resulting in the following poly-acids: $[\text{Ni}_3(\text{OH}_2)_3(\text{B-PW}_9\text{O}_{34})\text{WO}_5(\text{H}_2\text{O})]^{7-}$, $[\text{Co}_3(\text{OH}_2)_6(\text{A-PW}_9\text{O}_{34})_2]^{12-}$, and $[\text{WZn}(\text{Mn}(\text{OH})_2)_2(\text{B-ZnW}_9\text{O}_{34})_2]^{12-}$. They were evaluated in geraniol epoxidation being the cobalt catalyst the more efficient and selective, with 94% conversion and 99% selectivity for epoxide.

Later, in 2021, Silva described the use of Bronsted acids as catalysts for epoxidations of terpenes using H_2O_2 as green oxidant (Table 1.1, entry 3).⁷⁷ They obtained good conversions using phosphomolybdic acid and phosphotungstic acid, 95% conversion with 98% selectivity for epoxide in 1 hour for the phosphomolybdic acid, while the phosphotungstic acid conversion was 60% with 50% selectivity for the epoxide at the end of 8 hours. Other acids such as sulfuric and *p*-toluenesulfonic acid showed 20-40% conversion in 8 hours, with only 30-45% selectivity for the epoxide.

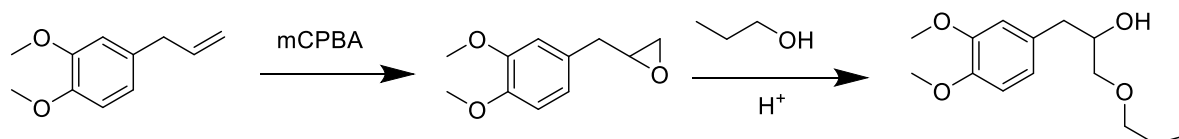
Zeolites have been also described in oxidation reactions, including epoxidations. Jan Přeč et al. described four different titanium silicates (TS) in the oxidation of citronellol, a terpene widely used as a fragrance (Table 1.1, entry 4).⁷⁸ The author describes the use of conventional morphology TS, mesoporous TS, layered TS, and silica-titania Pillared TS in epoxidation reactions using hydrogen peroxide as oxidant. The results with 1 equivalent of H_2O_2 in 180 minutes were 22% conversion with 71% selectivity for the conventional TS, with layered TS 17% conversion and 55% selectivity, with mesoporous 19% conversion with 68% selectivity, and for last, the pillared TS resulted in 30% conversion and 40% selectivity. Their selectivity was low in all the silicates due to ring-opening reactions with water. The use of zeolites is interesting from the Green Chemistry point of view, as they are an example of a reusable heterogeneous catalyst, easily prepared through eco-friendly reagents and conditions, although only moderate results were obtained in the epoxidation reactions.

A recent publication on β -caryophyllene epoxidation was reported by D. Yin and co-workers, using an heterogeneous copper-based catalyst, L-isoleucine aminoacid as ligand, molecular oxygen as oxidant and catalytic amounts of TBHP (Table 1.1, entry 5).⁷⁹ The molecular oxygen in the presence of the catalyst regenerates the used TBHP and then catalyzes the oxidation of the olefin. As a result, small amounts of TBHP are enough to obtain full conversion with 100% selectivity in 18 hours. Although the conversion for epoxide was 100%, the yield was 87% due to isomerization reactions. The copper catalyst was recycled 4 times without loss of catalytic activity, maintaining the same conversion and selectivity over time.



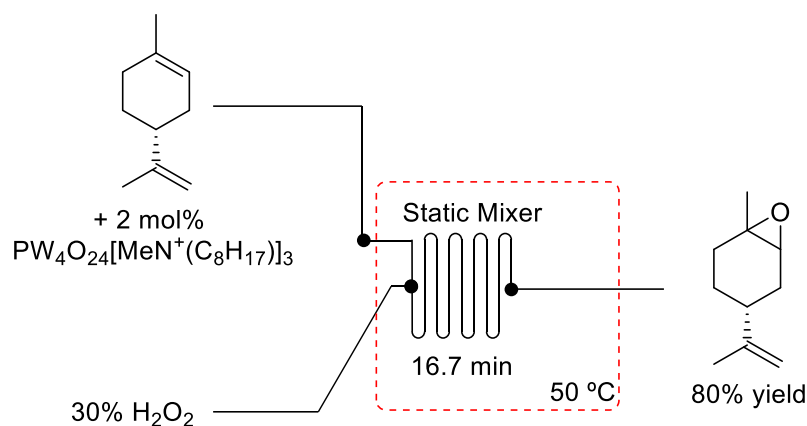
Scheme 1.7. Epoxidation of β -caryophyllene described by D. Yin.⁷⁹

In 2020, Gonçalves reported the epoxidation of eugenol derivatives to modulate the anti-cancer properties of these compounds. The epoxidation was performed using mCPBA, resulting in 7 to 67% yields in 24 hours (Table 1.1, entry 6).⁸⁰ A similar strategy was reported by Okopi and Affiku, in which methyl eugenol epoxide was synthesized, followed by the ring-opening in the presence of propanol, to compare the fragrance properties of each compound (Table 1.1, entry 7, Scheme 1.8).⁸¹ The authors concluded that the epoxide derivative had a strong floral aroma, while the corresponding hydroxy ether had a pungent glue-like smell.



Scheme 1.8. OKopi & Affiku methyl eugenol modifications.⁸¹

In 2021, S. Bull *et al.* developed a continuous flow epoxidation process of terpenoids using hydrogen peroxide as oxidant and a recyclable tungsten-based polyoxometalate as catalyst (Table 1.1, entry 8, Scheme 1.9). Using 2 mol% of catalyst and 1.6 equivalents of H_2O_2 as oxidant, 89% conversion with 90% selectivity was achieved for limonene oxide within 16.7 minutes. Although the authors state the possibility of catalyst recycling, catalyst reuse was not reported.

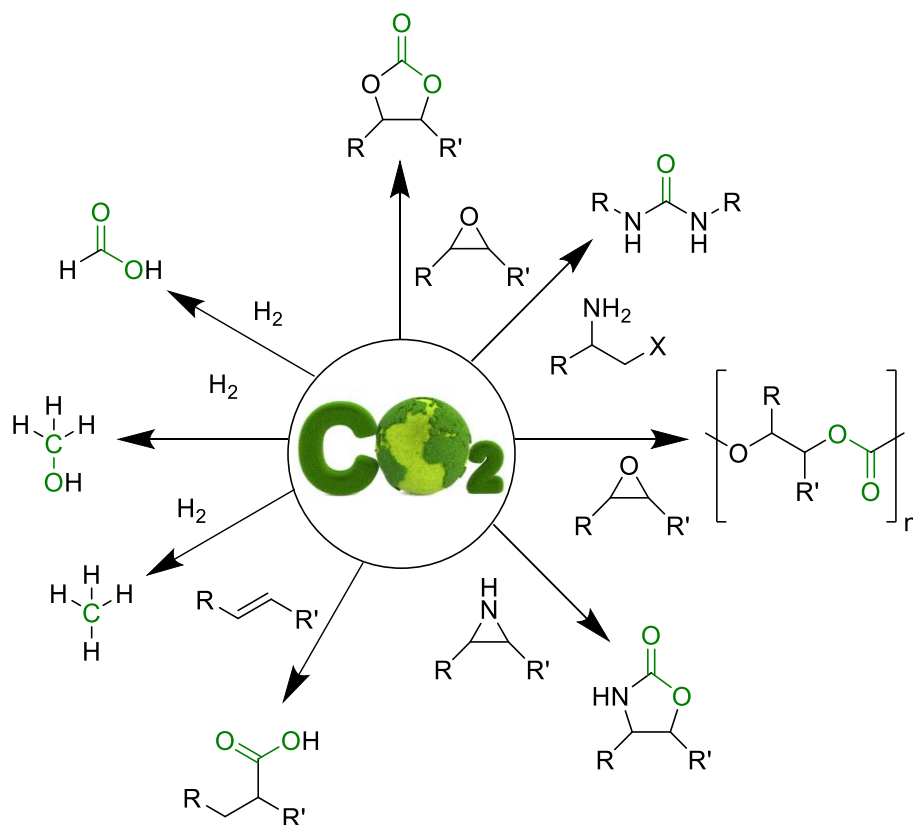


Scheme 1.9. Epoxidation of limonene under flow conditions proposed by S. Bull *et al.*⁸²

To the best of our knowledge, this was the only example of the application of natural products epoxidation under continuous flow conditions⁸³ for the preparation of potential fragrance and constitutes the starting point for the studies developed in this Master thesis.

1.4. CO_2 Cycloaddition to Epoxides

Over the past few decades, the use of carbon dioxide as a reagent has gained more and more attention. In early studies, the efficiency of the used catalysts for CO_2 activation reactions was low and, as result, extreme conditions were required.⁸⁴⁻⁸⁶ Nowadays, the reaction conditions are much milder due to the development of more active and selective catalysts. There are many applications for CO_2 , from the synthesis of methanol to polycarbonate polymer to biologically relevant urea compounds. Some examples of CO_2 applications are represented below (Scheme 1.10).



Scheme 1.10. Possible CO₂ application as C1 building block.

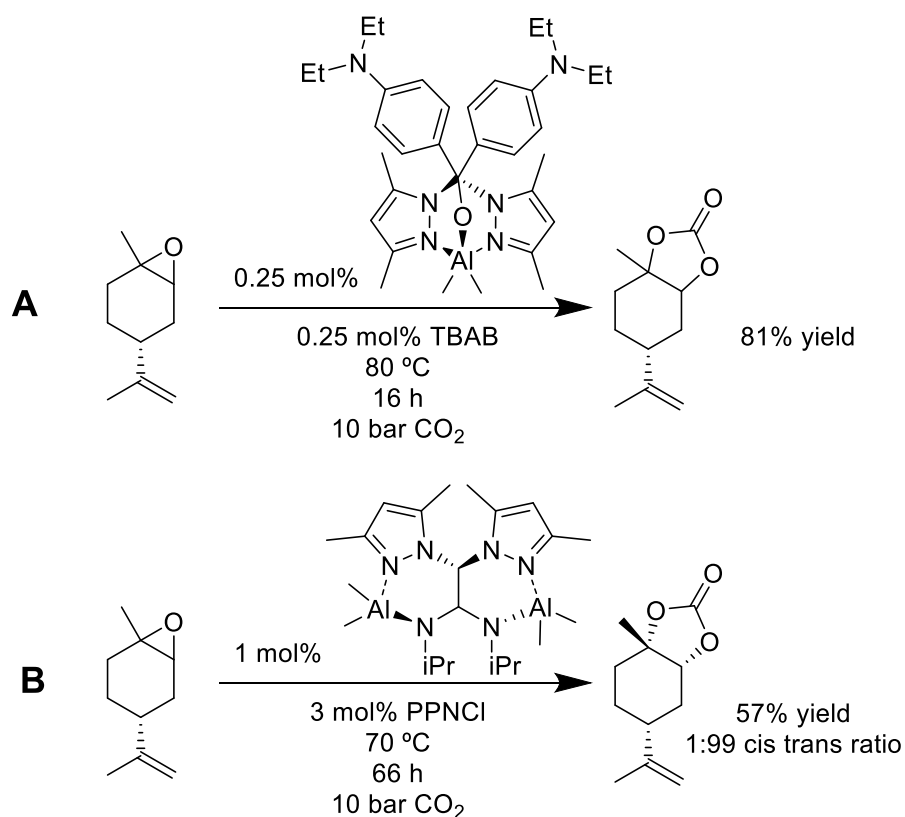
Cycloaddition reactions of CO₂ to epoxides are one of the most studied reactions as they yield cyclic carbonates, which find numerous applications, such as their use as green solvents, battery electrolytes or as relevant building blocks for the synthesis of both fine and bulk chemicals.⁸⁷ According to “web of science” database, over the past 3 years, *ca.* 430 articles related to CO₂ cycloaddition were published, which shows the relevance and high impact of this topic.⁸⁸⁻⁹⁵

Like the epoxidation reaction, CO₂ cycloadditions performed under batch processes are the most common way to obtain cyclic carbonates, and the vast majority of the substrates used so far belong to non-renewable sources. In Table 1.2, we present the list of cycloaddition reactions of CO₂ to natural-based epoxides, reported over the past 3 years. Once again, molecules with high molecular weight, such as fatty acids, were omitted since they are not relevant for fragrance manufacturing.

In 2019, Lacroix-Desmazes reported a study in which several derivatives of eugenol epoxide were used as monomers (Table 1.2, entry 1).⁹⁶ The authors used 3 mol% of tetrabutylammonium bromide as catalyst, 20 bar of CO₂ pressure and ethyl acetate as solvent, obtaining 66% yield of cyclic carbonate, after 48 h. Similar conditions were used

by Harvey for the cycloaddition reaction of CO₂ with 1,2-limonene oxide (Table 1.2, entry 2).⁹⁷ It should be noted that in the cycloaddition reaction of CO₂ to sterically hindered epoxides, such as 1,2-limonene oxide, the halide size had a significant influence on the overall conversion being chloride ion the most efficient. Additionally, the authors also observed a significant influence of the solvent on the catalytic activity, being the polar aprotic solvent the most efficient (DMF > propylene carbonate > acetonitrile > toluene). In the best conditions, 75% conversion and 100% selectivity toward the cyclic carbonate were obtained after 10 h, using DMF as solvent.

Sánchez reported CO₂ cycloaddition to several natural compound oxides, namely furfural, limonene, carvone, carvyl acetate, terpinen-4-ol, and ionone oxide, using aluminum scorpionates as catalysts and PPNBr or tetrabutylammonium bromide (TBAB) as co-catalyst. In all cases, full conversion with high selectivities were obtained (Table 1.2, entry 3, Scheme 1.11-A).⁹⁸ The effect of the co-catalyst was also described with the best results achieved using bromide ions (full conversion in 3 hours). Later, the same group released another aluminum-based scorpionate catalyst for the cycloaddition of CO₂ to limonene oxide, using PPNCl as co-catalyst (Table 1.2, Entry 4, Scheme 1.11-B).⁹⁹ This catalyst had lower activity than the previous one due to higher steric hindrance around the metal centers, achieving full conversion only for terminal epoxides. On the bright side, this catalyst was stereoselective toward the *trans* products, giving the desired carbonate with 99% stereoselectivity.



Scheme 1.11. CO₂ cycloaddition reactions to 1,2-limonene oxide, described by A. Sánchez group.^{98, 99}

An interesting approach for the synthesis of limonene cyclic carbonate was proposed by Nunes through CO₂ cycloaddition to 1,2-limonene epoxide, using an immobilized ionic catalyst (Table 1.2, Entry 5).¹⁰⁰ The ionic liquid [Aliquat][Cl] was supported into alginate and a silica aerogel matrix. The immobilization in silica completely deactivated the catalyst, while the alginate-supported ionic liquid catalysts gave 35% conversion. The authors did not present recycling and reuse studies.

Table 1.2. CO₂ Cycloaddition reaction to epoxides of natural products, described in the literature over the past 3 years.

Entry	Product	Catalyst	Conditions and Results
1 ⁹⁶		TBAB	<ul style="list-style-type: none"> • EtOAc • 80 °C • 3 wt% of cat. • 20 bar of CO₂ • 48 h • 66% yield
2 ⁹⁷		TBAC	<ul style="list-style-type: none"> • 20 h • 120 °C • 40 bar CO₂ • 6 mol% of cat • DMF • 87% conversion • cis/trans-isomers (40:60)
3 ⁹⁸		aluminum scorpionate	<ul style="list-style-type: none"> • 0.25 mol% of cat. • 0.25 mol% of TBAC • 80 °C • 16 h • 10 bar of CO₂ • 81% yield
4 ⁹⁹		aluminum scorpionate	<ul style="list-style-type: none"> • 10 bar CO₂ • 66 h • 1 mol% of cat. • 3 mol% of PPnCl • 70 °C • 76% yield • cis/trans 43:57
5 ¹⁰⁰		ionic liquid [Aliquat][Cl]	<ul style="list-style-type: none"> • 48 h • 80 °C • 40 bar of CO₂ • 35% conversion

Despite the recent advances on CO₂ cycloaddition to epoxides in continuous flow,¹⁰¹ to the best of our knowledge, there are no studies on the synthesis of cyclic carbonates using natural-based epoxides in continuous flow conditions, applied in fragrances synthesis. Thus, one of the main goals of this thesis is to synthesize cyclic carbonates

derived from natural compounds, using flow chemistry processes aiming the final production of potential fragrances.

1.5. Sequential epoxidation-carboxylation reactions

In the pursuit of a target molecule, an organic chemist must perform several reactions while isolating all intermediates so the subsequent transformations can be done without interferences. Aiming for the development of more sustainable chemical processes, sequential reactions were developed. They consist on the implementation of several distinct and consecutive transformations into one single sequence, without isolating the intermediates.¹⁰² Sequential reactions are well known for reducing the amount of chemical waste produced, labor, time, safety, and cost.¹⁰³

Quite often, sequential reactions involve multiple, highly selective, reactions. Many times, catalysts are employed in sequential reactions as they increase the selectivity of a given reaction. High selectivities can nullify the necessity to purify a reaction, motivating many groups to search for highly selective and efficient catalysts for those purposes.¹⁰²

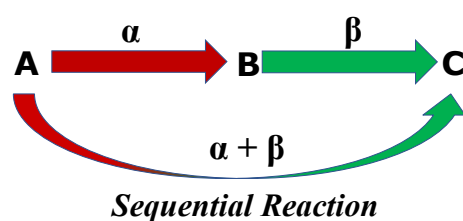
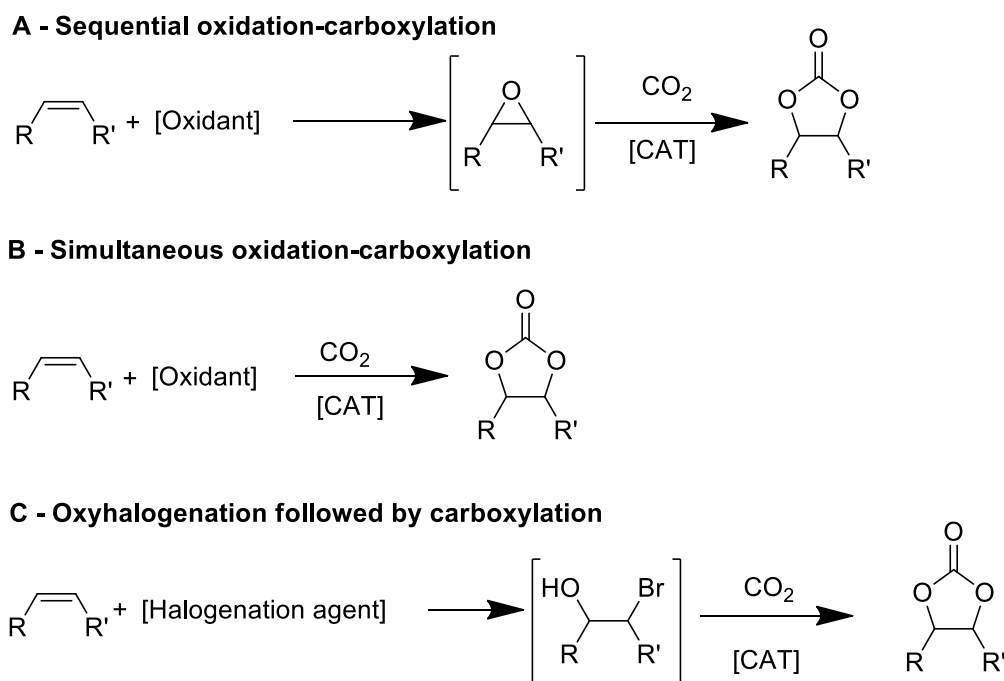


Figure 1.5. Graphical explanation of a sequential reaction.

Sequential reactions that proceed in automatic continuous flow processes involving precise space and time addition of reagents are particularly interesting.¹⁰⁴ Over the past 5 years, a series of publications in high-impact international journals, related to sequential reactions under continuous flow conditions were reported.¹⁰⁵⁻¹¹⁰

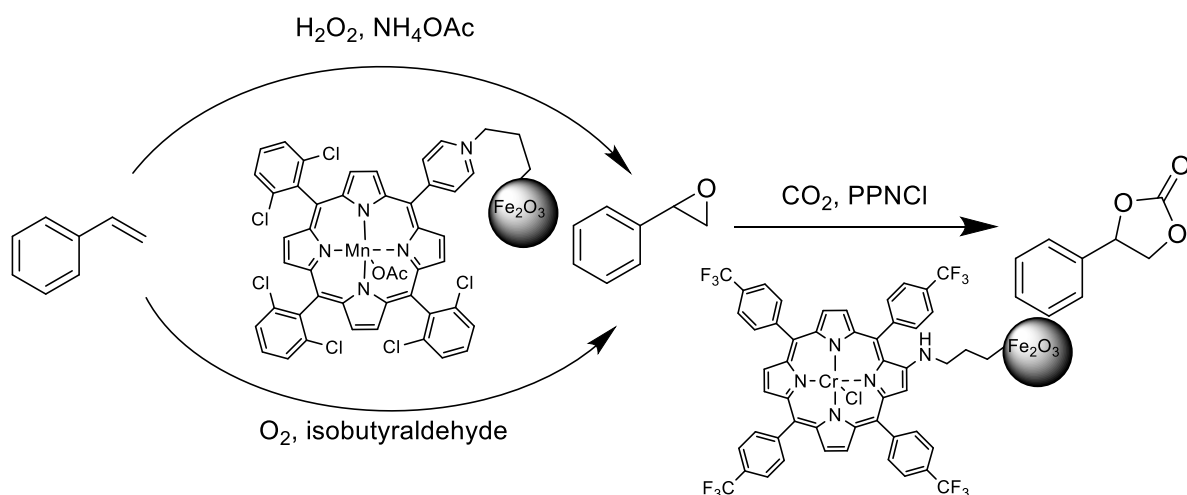
Among them we highlight the sequential flow reaction based on epoxidation of olefins followed by CO₂ cycloaddition, without isolation of the epoxide. This reaction is also known as oxidative carboxylation. There are different pathways to obtain the cyclic carbonate: i) sequential oxidation followed by carboxylation, ii) simultaneous oxidation and carboxylation, and iii) carboxylation via oxyhalogenation (Scheme 1.12). The main difficulty to implement these sequential oxidative carboxylations is related to the

incompatibility between the catalysts and the reaction conditions, as the epoxidation requires an oxidant that frequently is incompatible with the catalytic system used in the CO₂ cycloaddition step.¹⁰⁴



Scheme 1.12. Different reaction pathways for oxidative carboxylation reactions.

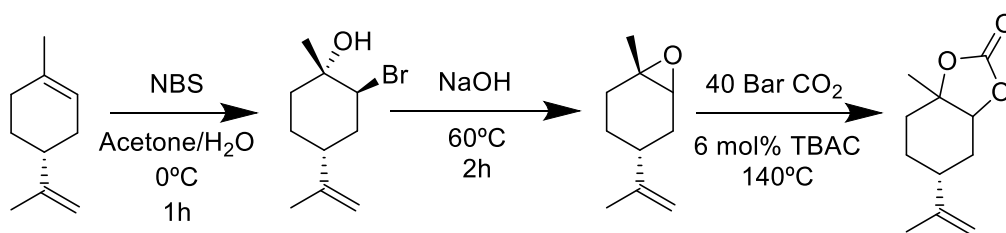
Among the most significant sequential approaches, we highlight the work developed by Coimbra Catalysis & Fine Chemistry group in which a metalloporphyrin immobilized onto magnetic nanoparticles was efficiently used for sequential epoxidation/CO₂ cycloaddition reactions, using green oxidants, such as molecular oxygen or H₂O₂ (Table 1.3, Entry 1, Scheme 1.13).¹¹¹ Both oxidants gave high conversions and selectivity toward epoxide. Without epoxide isolation, the catalyst was removed using a magnet, and a chromium porphyrin was added to promote the CO₂ cycloaddition, yielding 70% of isolated styrene carbonate, when H₂O₂ was used as oxidant. It should be noted that when oxygen was used, a complex mixture of products was obtained without any evidence for the formation of cyclic carbonates. The authors suggested that this result may be attributed to the epoxide ring-opening reaction initiated by the isobutyric acid produced in the epoxidation step. To overcome this problem the epoxide solution was neutralized with a basic aqueous solution before proceeding to the CO₂ cycloaddition step. Under these conditions the authors obtained up to 52% yield for cyclic carbonates.



Scheme 1.13. Sequential oxidative carboxylation described by Pereira.¹¹¹

Another less explored pathway is the simultaneous oxidation-carboxylation approach. Among the few examples reported so far, we highlight the work developed by Jing, where a ruthenium porphyrin was able to promote the epoxidation of styrene with molecular oxygen without any co-reductor, followed by *in situ* CO₂ cycloaddition, yielding 79% of styrene cyclic carbonate in 48 h. This is a promising sustainable approach since there is no need for a co-reductant, and the cyclic carbonate can be directly obtained from olefins with a 100% atom economy (Table 1.3, Entry 3).¹¹²

Regarding the oxidative carboxylation of natural compounds with potential application as fragrance, Harvey reported a limonene epoxidation using the bromohydrine methodology, followed by CO₂ cycloaddition (Table 1.3, entry 8, Scheme 1.14).¹¹³ First, the bromination of the olefin was carried out, using 2 equivalents of N-bromosuccinimide (NBS) and water as solvent. Then, in the presence of NaOH, the intramolecular reaction led to the formation of the desired epoxide with 97% yield in 5 minutes. This method has high diastereoselectivity with a *cis/trans* ratio of 4.3 to 95.7. For the cycloaddition step, the authors used 6 mol% tetrabutylammonium bromide as catalyst and CO₂ as a renewable reagent (30 bar) at 120 °C, obtaining 87% yield for the 1,2-limonene cyclic carbonate in 20 h.



Scheme 1.14. oxidative carboxylation described by Harvey.¹¹³

Table 1.3. Sequential epoxidation-CO₂ cycloaddition reactions described in the literature.

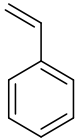
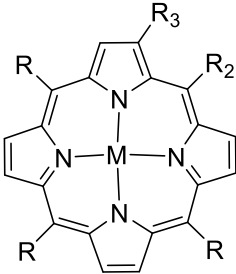
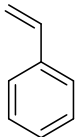
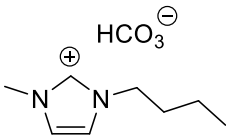
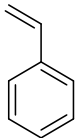
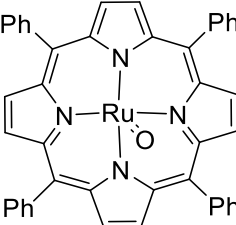
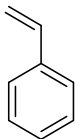
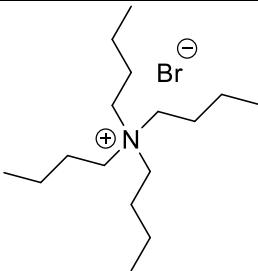
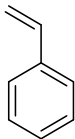
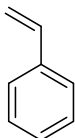
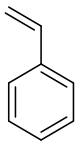
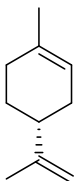
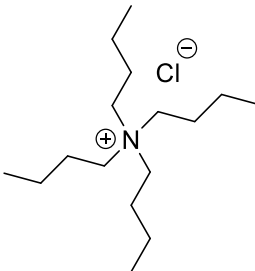
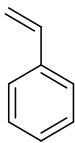
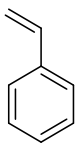
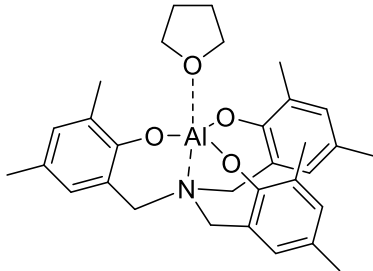
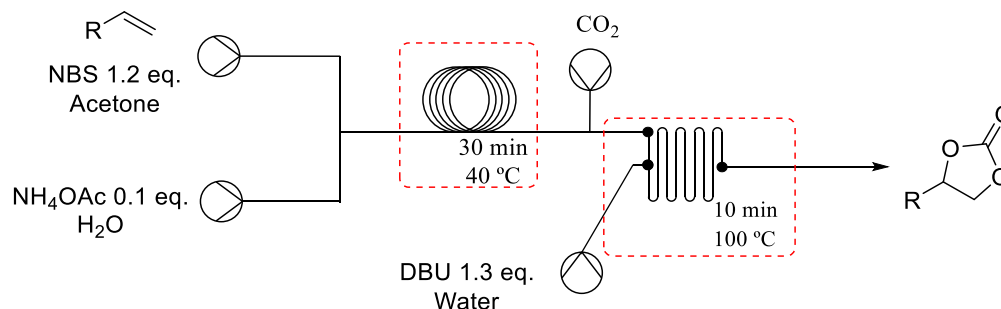
Entry	Substrate	Catalyst	Reaction Conditions	Results
1 ¹¹¹		 Oxidation: M=MnOac; R= <i>o</i> -Cl ₂ Ph; R ₂ =Py C ₃ H ₆ @SiO ₂ ; R ₃ =H CO₂ Cycloaddition: M=CrCl; R=R ₂ = <i>p</i> - CF ₃ Ph R ₃ =NHC ₃ H ₆ @SiO ₂	Oxidation with O₂: CH ₂ Cl ₂ as solvent, 25 °C, 140 min, 5 eq. Isobutyraldehyde, 0.07 mol% catalyst. Oxidation with H₂O₂: CH ₃ CN as solvent, 25 °C, 45 min, 0.5 eq. NH ₄ OAc, 0.07 mol% catalyst. CO₂ cycloaddition: 0.07 mol% PPNCI as co- cat., 80 °C, 10 bar, 24 h, 0.07 mol% catalyst.	70% yield while using H ₂ O ₂ as oxidant 52% yield while using O ₂ as oxidant
2 ¹¹⁴			6 mol% of cat., 4 eq of TBHP, 20 bar CO ₂ , 30 h, 65 °C	91.2% conversion with 82.3% selectivity
3 ¹¹²			0.05 mol% catalyst, 2 eq. of TBAI, 5 bar of O ₂ , 11 bar of CO ₂ , CH ₂ Cl ₂ , 30 °C, 48 h.	79% yield,
4 ¹¹⁵			11 mol% of TBAB, 1.5 eq of TBHP, 150 bar of CO ₂ , 80 °C and 6 h	33% yield
5 ¹¹⁶		Gold nanoparticles	0.01 wt% of gold nanoparticles, 1.5 eq of TBHP, 80 °C, 3 h and 40 bar of CO ₂	50.6% of yield
6 ¹¹⁷		ImBr-MOF-545(Mn)	5 wt% of cat., 2 eq. of isobutyraldehyde, 5 bar of O ₂ , 5 bar of CO ₂ , 10 h, 70 °C	88.2% yield

Table 1.3. Sequential epoxidation-CO₂ cycloaddition reactions described in the literature.

Entry	Substrate	Catalyst	Reaction Conditions	Results
7 ¹¹⁸		Oxidation: Au/SiO ₂ CO₂ cycloaddition: ZnBr ₂	Oxidation: 5 wt% Au/SiO ₂ (2.5 mol%), 1.5 eq. of TBHP, 80 °C, 4 h CO₂ cycloaddition: 2.5 mol% ZnBr ₂ , 5% of TBAB, 80 bar of CO ₂ , 80 °C and 4 h	42% yield
8 ¹¹³			Oxidation: 2 eq. of NBS, H ₂ O and acetone as solvent, NaOH, 2 h, 60 °C CO₂ cycloaddition: 6 mol% TBAC, 120 °C, 30 bar CO ₂ , 20 h	87% yield for the 1,2-limonene carbonate
9 ¹¹⁹		-----	Continuous flow: Oxidation: water and acetone as solvent, 1.2 eq. of NBS, 0.1 eq. of NH ₄ OAc, 30 min, 40 °C CO₂ cycloaddition: 9 bar of CO ₂ , 1.3 eq. of DBU, 10 minutes, 100 °C.	75% yield
10 ¹⁰⁴		Oxidation: Methylrhodium trioxide CO₂ cycloaddition: 	Continuous flow: Oxidation: CH ₂ Cl ₂ as solvent, 1 mol% of catalyst, 24 mol% 3-Methylpyrazole, 5 eq. of H ₂ O ₂ , 40 °C, 60 min CO₂ cycloaddition: 7.5 bar of CO ₂ , 2 mol% of catalyst, 10 mol% of TBAI, 100 °C, 75 min	98% yield

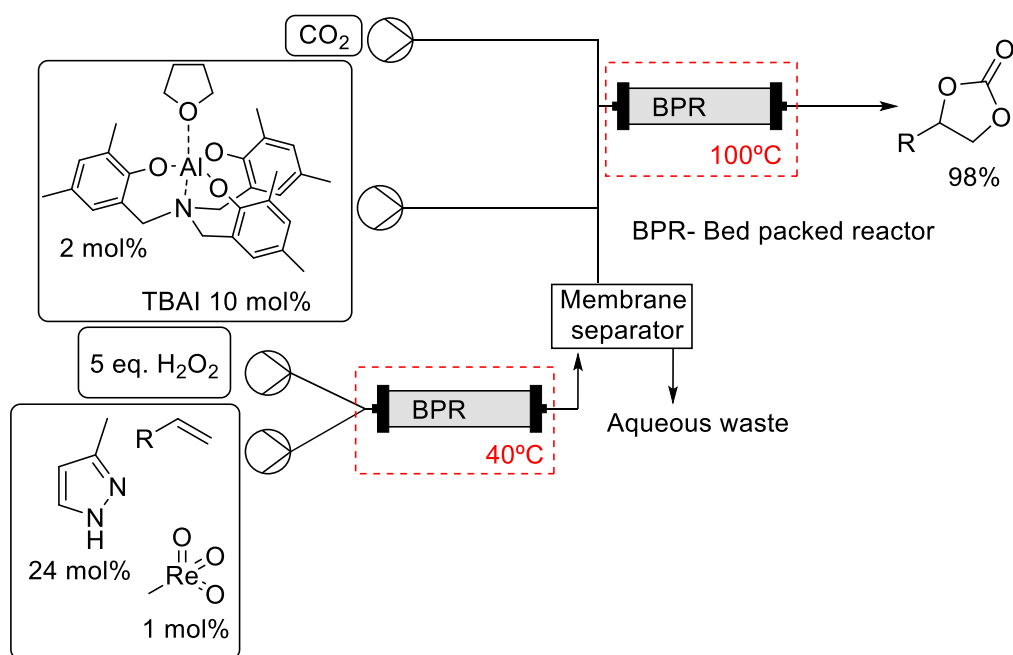
Continuous flow sequential carboxylation processes

Regarding continuous flow oxidative carboxylation processes, an oxyhalogenation carboxylation approach was described by Jamison in 2014, using also NBS as a bromination agent and DBU as a base (Table 1.3. entry 9, Scheme 1.15).¹¹⁹ However, the oxyhalogenation pathway presents a major disadvantage related to the use of stoichiometric amounts of halogenation agent.



Scheme 1.15. Oxyhalogenation carboxylation process, described by Jamison.¹¹⁹

A more sustainable approach is the sequential oxidative-carboxylation pathway described by Rioux (Table 1.3. entry 10, Scheme 1.16).¹⁰⁴ The authors describe the oxidation of styrene using methylrhenium trioxide as catalysts and H₂O₂ as oxidant, followed by CO₂ cycloaddition, using a homogenous aluminum amino trisphenolate catalyst and tetrabutylammonium iodide (TBAI) as co-catalyst. The two reactions, epoxidation and cycloaddition, were first optimized apart before putting them in a single sequence. For the epoxidation the optimal conditions were 1 mol% methylrhenium trioxide of catalyst, 24 mol% 3-methylpyrazole and 5 equivalents of hydrogen peroxide, with 30 minutes residence time at 40 °C, yielding 97% conversion. For the CO₂ cycloaddition, the optimal conditions were 2 mol% of aluminum amino trisphenolate catalyst, 10 mol% of TBAI, 7.5 bar of CO₂, 75 minutes of residence time and 100 °C temperature, giving 100% conversion and selectivity. After optimization of the individual reactions, the reaction was performed consecutively, separating the aqueous phase resulting from the epoxidation with a membrane, before adding the aluminum catalyst. Using this approach, 98% yield for the styrene carbonate was achieved.



Scheme 1.16. Sequential oxidative-carboxylation reaction described by R. Rioux.¹⁰⁴

Despite the latest achievements, there is still work to be done regarding the optimization of sustainable oxidative carboxylation sequential processes to turn this strategy into a real synthetic tool for the implementation of large-scale preparation of value-added products. Particularly the scope of the reaction is yet to be extended to natural/sustainable compounds and the use of heterogeneous catalysts is also lacking. It is also necessary to design reusable, selective and active catalysts. Therefore, in this work, we intended to develop sustainable sequential epoxidation/CO₂ addition processes via flow chemistry for the synthesis of natural-based fragrances.

1.6. Thesis Goals

Considering the state-of-the-art, the main goal of this work is the synthesis of natural-based eugenol derivatives as potential fragrances, using Green Chemistry principles and flow chemistry processes (Figure 1.7). The synthetic approaches include the protection of the eugenol hydroxyl group, followed by epoxidation of the C=C double bond, and epoxide ring expansion through CO₂ cycloaddition reactions. Furthermore, the characterization and toxicity studies of the new natural-based molecules, performed *in vitro* on human breast cells are intended to evaluate the potential of the new molecules as new fragrances.

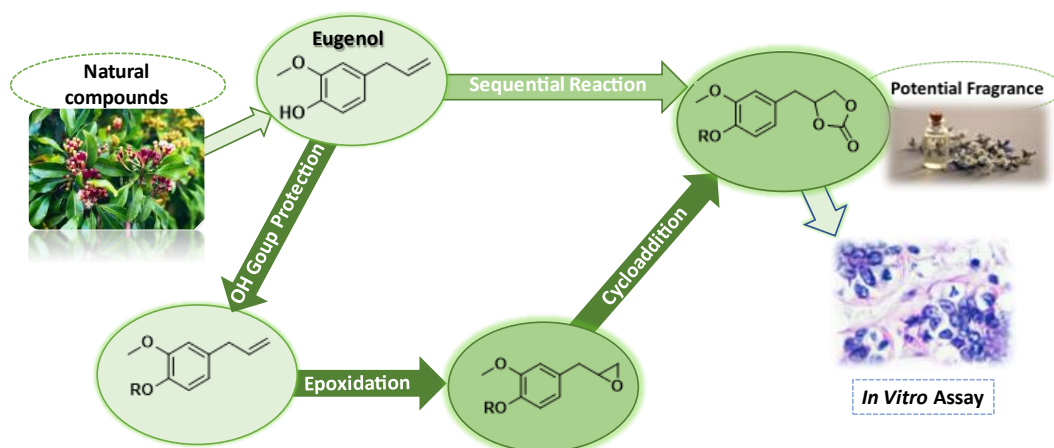


Figure 1.6. Thesis graphical abstract

1.7. References

1. Doaa Ragab Fadel, History of the Perfume Industry in Greco-Roman Egypt. *International Journal of History and Cultural Studies* **2020**, 6 (4), 26-45.
2. Pybus, D. H., The History of Aroma Chemistry and Perfume. In *The Chemistry Of Fragrances: From Perfumer to Consumer (2)*, Sell, C. S., Ed. The Royal Society of Chemistry: 2006, 3-23.
3. Zohar, A.; Lev, E., Trends in the Use of Perfumes and Incense in the Near East after the Muslim Conquests. *Journal of the Royal Asiatic Society* **2013**, 23 (1), 11-30.
4. Frangié-Joly, D., Perfumes, Aromatics, and Purple Dye: Phoenician Trade and Production in the Greco-Roman Period. *Journal of Eastern Mediterranean Archaeology and Heritage Studies* **2016**, 4 (1), 36-56.
5. Herman, S., Chapter 18 - Fragrance. In *Cosmetic Science and Technology*, Sakamoto, K.; Lochhead, R. Y.; Maibach, H. I.; Yamashita, Y., Eds. Elsevier: Amsterdam, 2017; pp 267-283.
6. Flavors And Fragrances Market Size, Share & Trends Analysis Report By Product (Natural, Aroma Chemicals), By Application (Flavors, Fragrances), By Region, And Segment Forecasts, 2022 - 2030, retrieved from <https://www.grandviewresearch.com/industry-analysis/flavors-fragrances-market>
7. Elisabetta, B.; Claudio, F., Recent Advances in the Synthesis of Fragrances. *Current Organic Chemistry* **2011**, 15 (7), 987-1005.
8. Masyita, A.; Mustika Sari, R.; Dwi Astuti, A.; Yasir, B.; Rahma Rumata, N.; Emran, T. B.; Nainu, F.; Simal-Gandara, J., Terpenes And Terpenoids As Main Bioactive Compounds Of Essential Oils, Their Roles In Human Health And Potential Application As Natural Food Preservatives. *Food Chemistry: X* **2022**, 13, 100217.
9. Steinemann, A., Fragranced Consumer Products: Effects On Asthmatics. *Air Quality, Atmosphere & Health* **2018**, 11 (1), 3-9.
10. Patel, S.; Homaei, A.; Sharifian, S., Need Of The Hour: To Raise Awareness On Vicious Fragrances And Synthetic Musks. *Environment, Development and Sustainability* **2021**, 23 (4), 4764-4781.
11. Weinberg, J. L.; Flattery, J.; Harrison, R., Fragrances And Work-Related Asthma—California Surveillance Data, 1993–2012. *Journal of Asthma* **2017**, 54 (10), 1041-1050.
12. Kim, S.; Hong, S.-H.; Bong, C.-K.; Cho, M.-H., Characterization Of Air Freshener Emission: The Potential Health Effects. *The Journal of Toxicological Sciences* **2015**, 40 (5), 535-550.

13. Klaschka, U., "This Perfume Makes Me Sick, But I Like It." Representative Survey On Health Effects Associated With Fragrances. *Environmental Sciences Europe* **2020**, *32* (1), 30.
14. Bagasra, O.; Golkar, Z.; Garcia, M.; Rice, L. N.; Pace, D. G., Role Of Perfumes In Pathogenesis Of Autism. *Medical Hypotheses* **2013**, *80* (6), 795-803.
15. regulation (ec) no 1223/2009 of the european parliament and of the council of 30 November 2009. Retrieved from <https://eur-lex.europa.eu/legal-content/EN/TXT/?uri=CELEX%3A02009R1223-20220301>.
16. Sarantis, H., Naidenko OV, Gray S, et al. Not So Sexy: The Health Risks Of Secretchemicals In Fragrance. Breast Cancer Fund, *Commonweal and Environmental Working Group*: **2010**;1-48.
17. Patel, S., Fragrance Compounds: The Wolves In Sheep's Clothings. *Medical Hypotheses* **2017**, *102*, 106-111.
18. Jaganathan, S. K.; Supriyanto, E., Antiproliferative And Molecular Mechanism Of Eugenol-Induced Apoptosis In Cancer Cells. *Molecules* **2012**, *17* (6), 6290-6304 .
19. Taleuzzaman, M.; Jain, P.; Verma, R.; Iqbal, Z.; Mirza, M. A., Eugenol As A Potential Drug Candidate: A Review. *Current topics in medicinal chemistry* **2021**, *21* (20), 1804-1815.
20. Pramod, K.; Ansari, S. H.; Ali, J., Eugenol: a Natural Compound With Versatile Pharmacological Actions. *Natural product communications* **2010**, *5* (12), 1999-2006.
21. Mohammadi Nejad, S.; Özgüneş, H.; Başaran, N., Pharmacological And Toxicological Properties Of Eugenol. *Turkish journal of pharmaceutical sciences* **2017**, *14* (2), 201-206.
22. Barboza, J. N.; da Silva Maia Bezerra Filho, C.; Silva, R. O.; Medeiros, J. V. R.; de Sousa, D. P., An Overview On The Anti-Inflammatory Potential And Antioxidant Profile Of Eugenol. *Oxidative medicine and cellular longevity* **2018**, *2018*, 3957262.
23. Zari, A. T.; Zari, T. A.; Hakeem, K. R., Anticancer Properties of Eugenol: A Review. **2021**, *26* (23), 7407.
24. Carvalho, R. P. R.; Lima, G. D. d. A.; Machado-Neves, M., Effect Of Eugenol Treatment In Hyperglycemic Murine Models: A Meta-Analysis. *Pharmacological Research* **2021**, *165*, 105315.
25. Aburel, O. M.; Pavel, I. Z.; Dănilă, M. D.; Lelcu, T.; Roi, A.; Lighezan, R.; Muntean, D. M.; Rusu, L. C., Pleiotropic Effects of Eugenol: The Good, The Bad, And The Unknown. *Oxidative medicine and cellular longevity* **2021**, *2021*, 3165159.

26. Api, A. M.; Belsito, D.; Biserta, S.; Botelho, D.; Bruze, M.; Burton, G. A.; Buschmann, J.; Cancellieri, M. A.; Dagli, M. L.; Date, M.; Dekant, W.; Deodhar, C.; Fryer, A. D.; Gadhia, S.; Jones, L.; Joshi, K.; Lapczynski, A.; Lavelle, M.; Liebler, D. C.; Na, M.; O'Brien, D.; Patel, A.; Penning, T. M.; Ritacco, G.; Rodriguez-Roperro, F.; Romine, J.; Sadekar, N.; Salvito, D.; Schultz, T. W.; Siddiqi, F.; Sipes, I. G.; Sullivan, G.; Thakkar, Y.; Tokura, Y.; Tsang, S., RIFM Fragrance Ingredient Safety Assessment, 2-methoxy-4-propylphenol, CAS Registry Number 2785-87-7. *Food and Chemical Toxicology* **2021**, *149*, 111853.
27. Zari, A. T.; Zari, T. A.; Hakeem, K. R., Anticancer Properties Of Eugenol: A Review. *Molecules* **2021**, *26* (23).
28. Rusu, M. L.; Marutoiu, C.; Sandu, I.; Tita, D.; Gogoasa, I.; Barbu, C. H.; Popescu, A., HPTLC and GC-MS for Separation And Identification Of Eugenol In Plants. *Jpc-journal of planar chromatography-modern tlc* **2007**, *20* (2), 139-140.
29. Kamatou, G. P.; Vermaak, I.; Viljoen, A. M., Eugenol—From The Remote Maluku Islands To The International Market Place: A Review Of A Remarkable And Versatile Molecule. **2012**, *17* (6), 6953-6981.
30. Baricelli, P. J.; Rodriguez, M.; Melean, L. G.; Alonso, M. M.; Borusiak, M.; Rosales, M.; Gonzalez, B.; de Oliveira, K. C. B.; Gusevskaya, E. V.; dos Santos, E. N., Rhodium Catalyzed Aqueous Biphasic Hydroformylation Of Naturally Occurring Allylbenzenes In The Presence Of Water-Soluble Phosphorus Ligands. *Applied Catalysis A: General* **2015**, *490*, 163-169.
31. Carvalho, G. A.; Gusevskaya, E. V.; Santos, E. N. d., An Electrostatically-Anchored Rhodium(I) Catalyst For The Hydroformylation And Tandem Hydroformylation/Acetalization Of Biorenewable Allyl Benzenes, *Journal of the Brazilian Chemical Society*. **2014**, *25*, 2370-2377.
32. Delolo, F. G.; Vieira, G. M.; Villarreal, J. A. A.; Santos, E. N.; Gusevskaya, E. V., One-Pot Hydroformylation/O-Acylation Of Propenylbenzenes For The Synthesis Of Polyfunctionalized Fragrances. *Catalysis Today* **2021**, *381*, 272-279.
33. Pinto, N. F. S.; Pereira, D. M.; Pereira, R. B.; Fortes, A. G.; Fernandes, M. J. G.; Castanheira, E. M. S.; Gonçalves, M. S. T., Synthesis Of Amino Alcohols From Eugenol And Their Insecticidal Activity Against Sf9 Cell Line. *Chemistry Proceedings* **2021**, *3* (1), 62.
34. Mahboub, R.; Memmou, F., Antimicrobial Properties Of 6-Bromoeugenol And Eugenol. *International Letters of Natural Sciences* **2016**, *53*, 57-64.

35. da Silva, F. F. M.; Monte, F. J. Q.; de Lemos, T. L. G.; do Nascimento, P. G. G.; de Medeiros Costa, A. K.; de Paiva, L. M. M., Eugenol Derivatives: Synthesis, Characterization, And Evaluation Of Antibacterial And Antioxidant Activities. *Chemistry Central Journal* **2018**, *12* (1), 34.
36. Rahayu, R.; Aziz, M. A.; Holil, M.; Santoso, M., Synthesis Of New Vanillin Derivatives From Natural Eugenol. *AIP Conference Proceedings* **2021**, *2349* (1), 020015.
37. Anastas, P.; Eghbali, N., Green Chemistry: Principles And Practice. *Chemical Society Reviews* **2010**, *39* (1), 301-312.
38. Lovato, K.; Fier, P. S.; Maloney, K. M., The Application Of Modern Reactions In Large-Scale Synthesis. *Nature Reviews Chemistry* **2021**, *5* (8), 546-563.
39. Guidi, M.; Seeberger, P. H.; Gilmore, K., How To Approach Flow Chemistry. *Chemical Society Reviews* **2020**, *49* (24), 8910-8932.
40. Sambigiato, C.; Noël, T., Flow Photochemistry: Shine Some Light On Those Tubes! *Trends in Chemistry* **2020**, *2* (2), 92-106.
41. Hafner, A.; Mancino, V.; Meisenbach, M.; Schenkel, B.; Sedelmeier, J., Dichloromethylithium: Synthesis And Application In Continuous Flow Mode. *Organic Letters* **2017**, *19* (4), 786-789.
42. Brandão, P.; Pineiro, M.; Pinho e Melo, T. M. V. D., Flow Chemistry: Towards A More Sustainable Heterocyclic Synthesis. **2019**, *2019* (43), 7188-7217.
43. Hartman, R. L., Flow Chemistry Remains An Opportunity For Chemists And Chemical Engineers. *Current Opinion in Chemical Engineering* **2020**, *29*, 42-50.
44. May, S. A.; Johnson, M. D.; Buser, J. Y.; Campbell, A. N.; Frank, S. A.; Haeberle, B. D.; Hoffman, P. C.; Lambertus, G. R.; McFarland, A. D.; Moher, E. D.; White, T. D.; Hurley, D. D.; Corrigan, A. P.; Gowran, O.; Kerrigan, N. G.; Kissane, M. G.; Lynch, R. R.; Sheehan, P.; Spencer, R. D.; Pulley, S. R.; Stout, J. R., Development and Manufacturing GMP Scale-Up of a Continuous Ir-Catalyzed Homogeneous Reductive Amination Reaction. *Organic Process Research & Development* **2016**, *20* (11), 1870-1898.
45. Vaccaro, L.; Lanari, D.; Marrocchi, A.; Strappaveccia, G., Flow Approaches Towards Sustainability. *Green Chemistry* **2014**, *16* (8), 3680-3704.
46. Dallinger, D.; Kappe, C. O., Why Flow Means Green – Evaluating The Merits Of Continuous Processing In The Context Of Sustainability. *Current Opinion in Green and Sustainable Chemistry* **2017**, *7*, 6-12.
47. Vieira, T.; Stevens, A. C.; Chtchemelinine, A.; Gao, D.; Badalov, P.; Heumann, L., Development Of A Large-Scale Cyanation Process Using Continuous Flow Chemistry

En Route To The Synthesis Of Remdesivir. *Organic Process Research & Development* **2020**, *24* (10), 2113-2121.

48. Tenchov, R.; Bird, R.; Curtze, A. E.; Zhou, Q., Lipid Nanoparticles-From Liposomes To Mrna Vaccine Delivery, A Landscape Of Research Diversity And Advancement. *ACS nano* **2021**, *15* (11), 16982–17015.

49. Gambacorta, G.; Sharley, J. S.; Baxendale, I. R., A Comprehensive Review Of Flow Chemistry Techniques Tailored To The Flavours And Fragrances Industries. *Beilstein Journal of Organic Chemistry* **2021**, *17*, 1181-1312.

50. Akwi, F. M.; Watts, P., Continuous Flow Chemistry: Where Are We Now? Recent Applications, Challenges And Limitations. *Chemical Communications* **2018**, *54* (99), 13894-13928.

51. A. Kundra, M.; Grall, T.; Ng, D.; Xie, Z.; Hornung, C. H., Continuous Flow Hydrogenation Of Flavorings And Fragrances Using 3D-Printed Catalytic Static Mixers. *Industrial & Engineering Chemistry Research* **2021**, *60* (5), 1989-2002.

B. Therre, J., Kaibel, G., Aquila, W., Wegner, G., Fuchs, H. (1999, September 24). Preparation of citral (US6175044B1). BASF SE.

52. A. Vajglová, Z.; Navas, M.; Mäki-Arvela, P.; Eränen, K.; Kumar, N.; Peurla, M.; Murzin, D. Y., Transformations Of Citral Over Bifunctional Ru-H-Y-80 Extrudates In A Continuous Reactor. *Chemical Engineering Journal* **2022**, *429*, 132190.

B. Johannes, E., Ebel, K., Johann, T., Löber, O. (2008, June 12). Method for the production of menthol (US7709688B2). BASF SE.

53. Tentori, F.; Brenna, E.; Crotti, M.; Pedrocchi-Fantoni, G.; Ghezzi, M. C.; Tessaro, D., Continuous-Flow Biocatalytic Process For The Synthesis Of The Best Stereoisomers Of The Commercial Fragrances Leather Cyclohexanol (4-Isopropylcyclohexanol) And Woody Acetate (4-(Tert-Butyl)Cyclohexyl Acetate). *Catalysts* **2020**, *10* (1), 102.

54. Lanteri, D.; Quattrosoldi, S.; Soccio, M.; Basso, A.; Cavallo, D.; Munari, A.; Riva, R.; Lotti, N.; Moni, L., Regioselective Photooxidation Of Citronellol: A Way To Monomers For Functionalized Bio-Polyesters. *Frontiers in Chemistry* **2020**, *8*, 85.

55. Wau, J. S.; Robertson, M. J.; Oelgemöller, M., Solar Photooxygenations For The Manufacturing Of Fine Chemicals—Technologies And Applications. **2021**, *26* (6), 1685.

56. Hamami, Z. E.; Vanoye, L.; Fongarland, P.; de Bellefon, C.; Favre-Réguillon, A., Improved Reactor Productivity For The Safe Photo-Oxidation Of Citronellol Under Visible Light LED Irradiation. *ChemPhotoChem* **2019**, *3* (3), 122-128.

57. Seemann, A.; Panten, J.; Kirschning, A., Flow Chemistry Under Extreme Conditions: Synthesis Of Macrocycles With Musklike Olfactoric Properties. *The Journal of Organic Chemistry* **2021**, *86* (20), 13924-13933.
58. de Oliveira, M. P.; Delolo, F. G.; Villarreal, J. A. A.; dos Santos, E. N.; Gusevskaya, E. V., Hydroformylation And One-Pot Hydroformylation/Epoxy Ring Cleavage Of Limonene Oxide: A Sustainable Access To Biomass-Based Multi-Functional Fragrances. *Applied Catalysis A: General* **2021**, *616*, 118082.
59. Moschona, F.; Savvopoulou, I.; Tsitopoulou, M.; Tataraki, D.; Rassias, G., Epoxide Syntheses And Ring-Opening Reactions In Drug Development. *Catalysts* **2020**, *10* (10), 1117.
60. Fogassy, G.; Ke, P.; Figueras, F.; Cassagnau, P.; Rouzeau, S.; Courault, V.; Gelbard, G.; Pinel, C., Catalyzed Ring Opening Of Epoxides: Application To Bioplasticizers Synthesis. *Applied Catalysis A: General* **2011**, *393* (1), 1-8.
61. Jinshuai, Z.; Yun, H.; Fei, Z.; Jianyu, L.; Jia, H.; Chengguo, L.; Puyou, J.; Lihong, H.; Rongrong, A.; Yonghong, Z., Recent Progress In Microwave-Assisted Modification Of Vegetable Oils Or Their Derivatives. *Current Organic Chemistry* **2020**, *24* (8), 870-884.
62. Hosney, H.; Nadiem, B.; Ashour, I.; Mustafa, I.; El-Shibiny, A., Epoxidized Vegetable Oil And Bio-Based Materials As PVC Plasticizer. *Journal of Applied Polymer Science* **2018**, *135* (20), 46270.
63. Cecilia, J. A.; Ballesteros Plata, D.; Alves Saboya, R. M.; Tavares de Luna, F. M.; Cavalcante, C. L.; Rodríguez-Castellón, E., An Overview Of The Biolubricant Production Process: Challenges And Future Perspectives. *Processes* **2020**, *8* (3), 257.
64. Fraile, J. M.; García, J. I.; Herrerías, C. I.; Pires, E., Synthetic Transformations For The Valorization Of Fatty Acid Derivatives. *Synthesis* **2017**, *49* (07), 1444-1460.
65. Meng, Y.; Taddeo, F.; Aguilera, A. F.; Cai, X.; Russo, V.; Tolvanen, P.; Leveneur, S., The Lord Of The Chemical Rings: Catalytic Synthesis Of Important Industrial Epoxide Compounds. *Catalysts* **2021**, *11* (7), 765.
66. Wai, P. T.; Jiang, P.; Shen, Y.; Zhang, P.; Gu, Q.; Leng, Y., Catalytic Developments In The Epoxidation Of Vegetable Oils And The Analysis Methods Of Epoxidized Products. *RSC Advances* **2019**, *9* (65), 38119-38136.
67. Grzegorz, L.; Marlina, M.; Kornelia, M.-M.; Łukasz, S.; Eugeniusz, M., Epoxidation Of Vegetable Oils, Unsaturated Fatty Acids And Fatty Acid Esters: A Review. *Mini-Reviews in Organic Chemistry* **2020**, *17* (4), 412-422.

68. Mahamat Ahmat, Y.; Madadi, S.; Charbonneau, L.; Kaliaguine, S., Epoxidation of Terpenes. *Catalysts* **2021**, *11* (7), 847.
69. Denicourt-Nowicki, A.; Rauchdi, M.; Ait Ali, M.; Roucoux, A., Catalytic Oxidation Processes For The Upgrading Of Terpenes: State-Of-The-Art And Future Trends. *Catalysts* **2019**, *9* (11), 893.
70. Della Monica, F.; Kleij, A. W., From Terpenes To Sustainable And Functional Polymers. *Polymer Chemistry* **2020**, *11* (32), 5109-5127.
71. Renata, H., Synthetic Utility Of Oxygenases In Site-Selective Terpenoid Functionalization. *Journal of Industrial Microbiology and Biotechnology* **2021**, *48*, 3-4.
72. Piccolo, D.; Vianello, C.; Lorenzetti, A.; Maschio, G., Epoxidation Of Soybean Oil Enhanced By Microwave Radiation. *Chemical Engineering Journal* **2019**, *377*, 120113.
73. Chen, J.; de Liedekerke Beaufort, M.; Gyurik, L.; Dorresteyn, J.; Otte, M.; Klein Gebbink, R. J. M., Highly Efficient Epoxidation Of Vegetable Oils Catalyzed By A Manganese Complex With Hydrogen Peroxide And Acetic Acid. *Green Chemistry* **2019**, *21* (9), 2436-2447.
74. Dorado, V.; Gil, L.; Mayoral, J. A.; Herrerías, C. I.; Fraile, J. M., Synthesis Of Fatty Ketoesters By Tandem Epoxidation–Rearrangement With Heterogeneous Catalysis. *Catalysis Science & Technology* **2020**, *10* (6), 1789-1795.
75. Gottuso, A.; Köckritz, A.; Saladino, M. L.; Armetta, F.; De Pasquale, C.; Nasillo, G.; Parrino, F., Catalytic And Photocatalytic Epoxidation Of Limonene: Using Mesoporous Silica Nanoparticles As Functional Support For A Janus-Like Approach. *Journal of Catalysis* **2020**, *391*, 202-211.
76. Abram, P. H.; Burns, R. C.; Li, L., Three- And Two-Site Heteropolyoxotungstate Anions As Catalysts For The Epoxidation Of Allylic Alcohols By H₂O₂ Under Biphasic Conditions: Reactivity And Kinetic Studies Of The [Ni₃(OH)₂]₃(B-PW₉O₃₄){WO₅(H₂O)}⁷⁻, [Co₃(OH)₂]₆(A-PW₉O₃₄)₂¹²⁻, and [M₄(OH)₂]₂(B-PW₉O₃₄)₂¹⁰⁻ Anions, Where M = Mn(II), Co(II), Ni(II), Cu(II) and Zn(II). *Inorganica Chimica Acta* **2020**, *499*, 119178.
77. Vilanculo, C. B.; da Silva, M. J., Can Brønsted Acids Catalyze The Epoxidation Of Allylic Alcohols With H₂O₂? With A Little Help From The Proton, the H₃PMo₁₂O₄₀ Acid Did It And Well. *Molecular Catalysis* **2021**, *512*, 111780.
78. Aldhayan, D.; Kalíková, K.; Shaik, M. R.; Siddiqui, M. R. H.; Přeck, J., Selective Oxidation Of Citronellol Over Titanosilicate Catalysts. *Catalysts* **2020**, *10* (11).

79. Shi, L.; Mao, W.; Zhang, L.; Zhao, Y.; Huang, H.; Xiao, Y.; Mao, L.; Fu, Z.; Yu, N.; Yin, D., An Ultrathin Amino-Acid Based Copper(II) Coordination Polymer Nanosheet For Efficient Epoxidation Of β -caryophyllene. *Molecular Catalysis* **2021**, *511*, 111754.
80. Fernandes, M. J. G.; Pereira, R. B.; Pereira, D. M.; Fortes, A. G.; Castanheira, E. M. S.; Gonçalves, M. S. T., New Eugenol Derivatives With Enhanced Insecticidal Activity. *International Journal of Molecular Sciences* **2020**, *21* (23), 9257.
81. Okopi, S. A., LM, Synthesis And Olfactory Characteristics Of Hydroxyether Derivatives Of Methyl Eugenol. *Journal of Applied Sciences and Environmental Management* **2020**, *24* (9), 1503-1507.
82. Tibbetts, J. D.; Cunningham, W. B.; Vezzoli, M.; Plucinski, P.; Bull, S. D., Sustainable Catalytic Epoxidation Of Biorenewable Terpene Feedstocks Using H₂O₂ As An Oxidant In Flow Microreactors. *Green Chemistry* **2021**, *23* (15), 5449-5455.
83. Yan, Z.; Tian, J.; Wang, K.; Nigam, K. D. P.; Luo, G., Microreaction Processes For Synthesis And Utilization Of Epoxides: A Review. *Chemical Engineering Science* **2021**, *229*, 116071.
84. Sulley, G. S.; Gregory, G. L.; Chen, T. T. D.; Peña Carrodegas, L.; Trott, G.; Santmarti, A.; Lee, K.-Y.; Terrill, N. J.; Williams, C. K., Switchable Catalysis Improves The Properties Of CO₂-Derived Polymers: Poly(Cyclohexene Carbonate-B-E-Decalactone-B-Cyclohexene Carbonate) Adhesives, Elastomers, And Toughened Plastics. *Journal of the American Chemical Society* **2020**, *142* (9), 4367-4378.
85. Kamada, K.; Jung, J.; Wakabayashi, T.; Sekizawa, K.; Sato, S.; Morikawa, T.; Fukuzumi, S.; Saito, S., Photocatalytic CO₂ Reduction Using A Robust Multifunctional Iridium Complex Toward The Selective Formation Of Formic Acid. *Journal of the American Chemical Society* **2020**, *142* (23), 10261-10266.
86. Sun, S.; Sun, H.; Williams, P. T.; Wu, C., Recent Advances In Integrated CO₂ Capture And Utilization: A Review. *Sustainable Energy & Fuels* **2021**, *5* (18), 4546-4559.
87. Rollin, P.; Soares, L. K.; Barcellos, A. M.; Araujo, D. R.; Lenardão, E. J.; Jacob, R. G.; Perin, G., Five-Membered Cyclic Carbonates: Versatility For Applications In Organic Synthesis, Pharmaceutical, And Materials Sciences. *Applied Sciences* **2021**, *11* (11), 5024.
88. Luo, R.; Chen, M.; Liu, X.; Xu, W.; Li, J.; Liu, B.; Fang, Y., Recent Advances In CO₂ Capture And Simultaneous Conversion Into Cyclic Carbonates Over Porous

Organic Polymers Having Accessible Metal Sites. *Journal of Materials Chemistry A* **2020**, 8 (36), 18408-18424.

89. Lian, S.; Song, C.; Liu, Q.; Duan, E.; Ren, H.; Kitamura, Y., Recent Advances In Ionic Liquids-Based Hybrid Processes For CO₂ Capture And Utilization. *Journal of Environmental Sciences* **2021**, 99, 281-295.

90. Luo, R.; Yang, Y.; Chen, K.; Liu, X.; Chen, M.; Xu, W.; Liu, B.; Ji, H.; Fang, Y., Tailored Covalent Organic Frameworks For Simultaneously Capturing And Converting CO₂ Into Cyclic Carbonates. *Journal of Materials Chemistry A* **2021**, 9 (37), 20941-20956.

91. Claver, C.; Yeamin, M. B.; Reguero, M.; Masdeu-Bultó, A. M., Recent Advances In The Use Of Catalysts Based On Natural Products For The Conversion Of CO₂ Into Cyclic Carbonates. *Green Chemistry* **2020**, 22 (22), 7665-7706.

92. Liao, J.; Zeng, W.; Zheng, B.; Cao, X.; Wang, Z.; Wang, G.; Yang, Q., Highly Efficient CO₂ Capture And Conversion Of A Microporous Acylamide Functionalized Rht-Type Metal–Organic Framework. *Inorganic Chemistry Frontiers* **2020**, 7 (9), 1939-1948.

93. Liu, M.; Wang, X.; Jiang, Y.; Sun, J.; Arai, M., Hydrogen Bond Activation Strategy For Cyclic Carbonates Synthesis From Epoxides And CO₂: Current State-Of-The Art Of Catalyst Development And Reaction Analysis. *Catalysis Reviews* **2019**, 61 (2), 214-269.

94. Jin, X.; Ding, J.; Xia, Q.; Zhang, G.; Yang, C.; Shen, J.; Subramaniam, B.; Chaudhari, R. V., Catalytic Conversion Of CO₂ And Shale Gas-Derived Substrates Into Saturated Carbonates And Derivatives: Catalyst Design, Performances And Reaction Mechanism. *Journal of CO₂ Utilization* **2019**, 34, 115-148.

95. Lan, D.-H.; Fan, N.; Wang, Y.; Gao, X.; Zhang, P.; Chen, L.; Au, C.-T.; Yin, S.-F., Recent Advances In Metal-Free Catalysts For The Synthesis Of Cyclic Carbonates From CO₂ And Epoxides. *Chinese Journal of Catalysis* **2016**, 37 (6), 826-845.

96. Molina-Gutiérrez, S.; Manseri, A.; Ladmiral, V.; Bongiovanni, R.; Caillol, S.; Lacroix-Desmazes, P., Eugenol: A Promising Building Block For Synthesis Of Radically Polymerizable Monomers. *Macromolecular Chemistry and Physics* **2019**, 220 (14), 1900179.

97. Rehman, A.; López Fernández, A. M.; Gunam Resul, M. F. M.; Harvey, A., Highly Selective, Sustainable Synthesis Of Limonene Cyclic Carbonate From Bio-Based Limonene Oxide And CO₂: A Kinetic Study. *Journal of CO₂ Utilization* **2019**, 29, 126-133.

98. Cruz-Martínez, F.; Martínez de Sarasa Buchaca, M.; Martínez, J.; Fernández-Baeza, J.; Sánchez-Barba, L. F.; Rodríguez-Diéguez, A.; Castro-Osma, J. A.; Lara-Sánchez, A., Synthesis Of Bio-Derived Cyclic Carbonates From Renewable Resources. *ACS Sustainable Chemistry & Engineering* **2019**, *7* (24), 20126-20138.
99. Navarro, M.; Sánchez-Barba, L. F.; Garcés, A.; Fernández-Baeza, J.; Fernández, I.; Lara-Sánchez, A.; Rodríguez, A. M., Bimetallic Scorpionate-Based Helical Organoaluminum Complexes For Efficient Carbon Dioxide Fixation Into A Variety Of Cyclic Carbonates. *Catalysis Science & Technology* **2020**, *10* (10), 3265-3278.
100. Paninho, A. B.; Mustapa, A. N.; Mahmudov, K. T.; Pombeiro, A. J. L.; Guedes da Silva, M. F. C.; Bermejo, M. D.; Martín, Á.; Cocero, M. J.; Nunes, A. V. M., A Bio-Based Alginate Aerogel As An Ionic Liquid Support For The Efficient Synthesis Of Cyclic Carbonates From CO₂ And Epoxides. *Catalysts* **2021**, *11* (8), 872.
101. Pescarmona, P. P., Cyclic carbonates synthesised from CO₂: Applications, Challenges And Recent Research Trends. *Current Opinion in Green and Sustainable Chemistry* **2021**, *29*, 100457.
102. Zeng, X., Recent Advances in Catalytic Sequential Reactions Involving Hydroelement Addition To Carbon–Carbon Multiple Bonds. *Chemical Reviews* **2013**, *113* (8), 6864-6900.
103. Miranda, L. S. d. M.; de Souza, R. O. M. A.; Leão, R. A. C.; Carneiro, P. F.; Pedraza, S. F.; de Carvalho, O. V.; de Souza, S. P.; Neves, R. V., Continuous-Flow Sequential Schotten–Baumann Carbamoylation and Acetate Hydrolysis in the Synthesis of Capecitabine. *Organic Process Research & Development* **2019**, *23* (11), 2516-2520.
104. Sathe, A. A.; Nambiar, A. M. K.; Rioux, R. M., Synthesis Of Cyclic Organic Carbonates Via Catalytic Oxidative Carboxylation Of Olefins In Flow Reactors. *Catalysis Science & Technology* **2017**, *7* (1), 84-89.
105. Gagnon, C.; Godin, É.; Minozzi, C.; Sosoe, J.; Pochet, C.; Collins Shawn, K., Biocatalytic Synthesis Of Planar Chiral Macrocycles. *Science* **2020**, *367* (6480), 917-921.
106. Yu, Y.-J.; Zhang, F.-L.; Peng, T.-Y.; Wang, C.-L.; Cheng, J.; Chen, C.; Houk Kendall, N.; Wang, Y.-F., Sequential C–F Bond Functionalizations Of Trifluoroacetamides And Acetates Via Spin-Center Shifts. *Science* **2021**, *371* (6535), 1232-1240.
107. Xia, L.; Zhang, Z.; You, Y.-Z., Synthesis Of Sequence-Controlled Polymers Via Sequential Multicomponent Reactions And Interconvertible Hybrid Copolymerizations. *Polymer Journal* **2020**, *52* (1), 33-43.

108. Xia, X.; Suzuki, R.; Gao, T.; Isono, T.; Satoh, T., One-Step Synthesis Of Sequence-Controlled Multiblock Polymers With Up To 11 Segments From Monomer Mixture. *Nature Communications* **2022**, *13* (1), 163.
109. Sun, Y.; Guo, J.; Shen, X.; Lu, Z., Ligand Relay Catalysis For Cobalt-Catalyzed Sequential Hydrosilylation And Hydrohydrazidation Of Terminal Alkynes. *Nature Communications* **2022**, *13* (1), 650.
110. Zhang, X.; Yang, F.; Cui, S.; Wei, W.; Chen, W.; Mi, L., Consecutive Reaction To Construct Hierarchical Nanocrystalline Cus “Branch” With Tunable Catalysis Properties. *Scientific Reports* **2016**, *6* (1), 30604.
111. Dias, L. D.; Carrilho, R. M. B.; Henriques, C. A.; Calvete, M. J. F.; Masdeu-Bultó, A. M.; Claver, C.; Rossi, L. M.; Pereira, M. M., Hybrid Metalloporphyrin Magnetic Nanoparticles As Catalysts For Sequential Transformation Of Alkenes And CO₂ Into Cyclic Carbonates. *ChemCatChem* **2018**, *10* (13), 2792-2803.
112. Bai, D.; Jing, H., Aerobic Oxidative Carboxylation Of Olefins With Metalloporphyrin Catalysts. *Green Chemistry* **2010**, *12* (1), 39-41.
113. Rehman, A.; Russell, E.; Saleem, F.; Javed, F.; Ahmad, S.; Eze, V. C.; Harvey, A., Synthesis Of Trans-Limonene Bis-Epoxy By Stereoselective Epoxidation of (R)-(+)-Limonene. *Journal of Environmental Chemical Engineering* **2021**, *9* (1), 104680.
114. Liu, J.; Yang, G.; Liu, Y.; Wu, D.; Hu, X.; Zhang, Z., Metal-Free Imidazolium Hydrogen Carbonate Ionic Liquids As Bifunctional Catalysts For The One-Pot Synthesis Of Cyclic Carbonates From Olefins And CO₂. *Green Chemistry* **2019**, *21* (14), 3834-3838.
115. Sun, J.; Fujita, S.-i.; Bhanage, B. M.; Arai, M., Direct Oxidative Carboxylation Of Styrene To Styrene Carbonate In The Presence Of Ionic Liquids. *Catalysis Communications* **2004**, *5* (2), 83-87.
116. Xiang, D.; Liu, X.; Sun, J.; Xiao, F.-S.; Sun, J., A Novel Route For Synthesis Of Styrene Carbonate Using Styrene And CO₂ As Substrates Over Basic Resin R201 Supported Au Catalyst. *Catalysis Today* **2009**, *148* (3), 383-388.
117. Yu, K.; Puthiaraj, P.; Ahn, W.-S., One-Pot Catalytic Transformation Of Olefins Into Cyclic Carbonates Over An Imidazolium Bromide-Functionalized Mn(III)-Porphyrin Metal–Organic Framework. *Applied Catalysis B: Environmental* **2020**, *273*, 119059.
118. Sun, J.; Fujita, S.-i.; Zhao, F.; Hasegawa, M.; Arai, M., A Direct Synthesis Of Styrene Carbonate From Styrene With The Au/SiO₂–ZnBr₂/Bu₄NBr Catalyst System. *Journal of Catalysis* **2005**, *230* (2), 398-405.

119. Wu, J.; Kozak, J. A.; Simeon, F.; Hatton, T. A.; Jamison, T. F., Mechanism-Guided Design Of Flow Systems For Multicomponent Reactions: Conversion Of CO₂ And Olefins To Cyclic Carbonates. *Chemical Science* **2014**, 5 (3), 1227-1231.

Chemical Transformations of Eugenol

Eugenol (4-allyl-2-methoxyphenol) is a natural volatile compound with fragrant properties, found in different plants, such as cinnamon, nutmeg, tea, and clove.¹ Its structure is composed by a phenol group and a terminal olefin, which makes it a great building block for the preparation of value-added compounds (Figure 2.1).

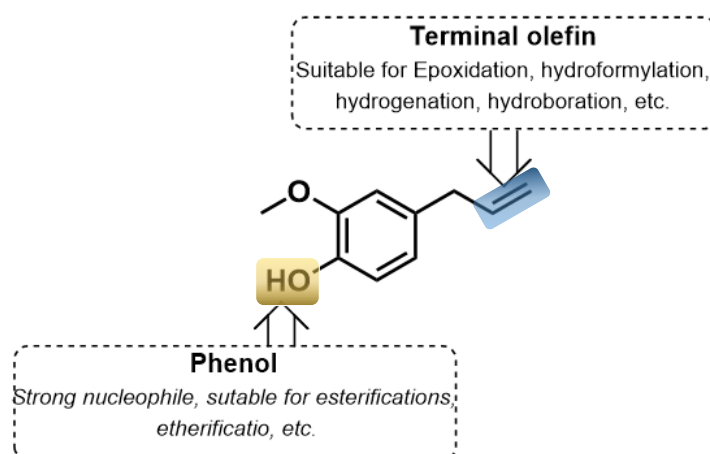


Figure 2.1 Eugenol structure.

Eugenol is widely known for its application in the flavor and fragrance industries.² Recently, eugenol has also received a lot of attention due to its pharmacological potential. Several reviews were published on eugenol biological activities.³⁻¹⁰ Clove oil, which is almost fully consisted of eugenol (90-95%), was used in traditional Chinese medicine for more than 1500 years due to its antimicrobial, antispasmodic, antiparasitic and was commonly used to treat dyspepsia, gastritis and diarrhea.¹¹ In Europe, eugenol was used since the 17th century to treat toothaches. Today, eugenol is still used in dentary medicine in form of a thick mixture with zinc oxide to fill tooth roots and cavities.¹² More recently,

eugenol has been used in oral care products created by Solvay, not only as a fragrance and flavor ingredient but as an anti-bacterial and anti-inflammatory agent.¹³

Considering the global interest of the catalysis and fine chemistry (C&FC) research group in the development of sustainable synthetic processes, this work was guided towards the transposition of batch processes to continuous flow systems for the sustainable development of eugenol transformations *via* epoxidation and CO₂ cycloaddition reactions.

This chapter is divided into two sections: in the first, we present the synthesis of metalloporphyrins, developed for application as catalysts in epoxidation and CO₂ cycloaddition reactions. In the second section, we present the studies of eugenol modifications using both batch methodology and its transposition to continuous flow systems, namely epoxidation reaction followed by CO₂ cycloaddition reaction. The main purpose was to prepare eugenol derivatives containing cyclic carbonates functionalities, which can be considered potential candidates for the development of new fragrances.

2.1. Synthesis of metalloporphyrin-based catalysts

Porphyrins play a key role in diverse biological systems and are essential for many living beings including humans. Their application in catalysis is widely known for being an efficient and versatile organic ligand. Observing the cytochrome P-450 high activity and selectivity for monooxygenation reactions, Groves and co-workers presented the first oxygenation reaction using a bioinspired synthetic metalloporphyrin.¹⁴ Since then, porphyrins and metalloporphyrins have been widely used as effective ligands and catalysts in a number of reactions, namely in epoxidations, CO₂ cycloadditions, C-H hydroxylations, hydroxyl group oxidations and many others.¹⁵⁻¹⁸

Porphyrins have two modulable positions, the *meso* and β positions, which can be modified to enhance the catalytic properties (Figure 2.2). In the center of the porphyrin are located four nitrogen atoms capable of coordinating with diverse metals, such as iron, chromium or manganese. Two of these nitrogen atoms act as electron dative donors while the other two create coordinating bonds. The conjunction of dative and coordinating bonds stabilizes the metal, preventing its leaching during the catalytic process.

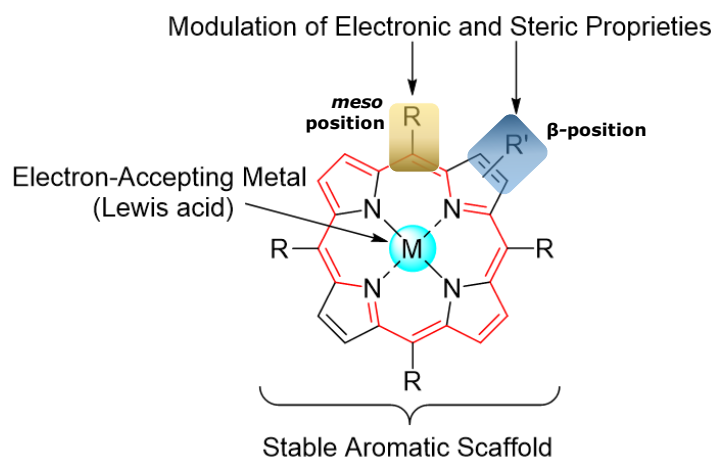


Figure 2.2. General structure of a metalloporphyrin catalyst showing its versatility.

It is well-established that halogen atoms at the *ortho* positions of the *meso*-phenyl groups are known to increase the stability and activity of metalloporphyrin catalysts, due to steric hindrance and through the withdrawing of electrons from the metal, making it more acidic, and consequently more active in the designed catalytic reactions.¹⁹ Therefore, our studies started with the synthesis of halogenated porphyrins, namely MnOAc-TDCPP (**CAT1**) intended to be used as catalyst for epoxidation reactions and CrCl-*p*-CF₃TPP (**CAT2**) intended to be evaluated as catalyst for CO₂ cycloaddition reactions to epoxides (Figure 2.3).

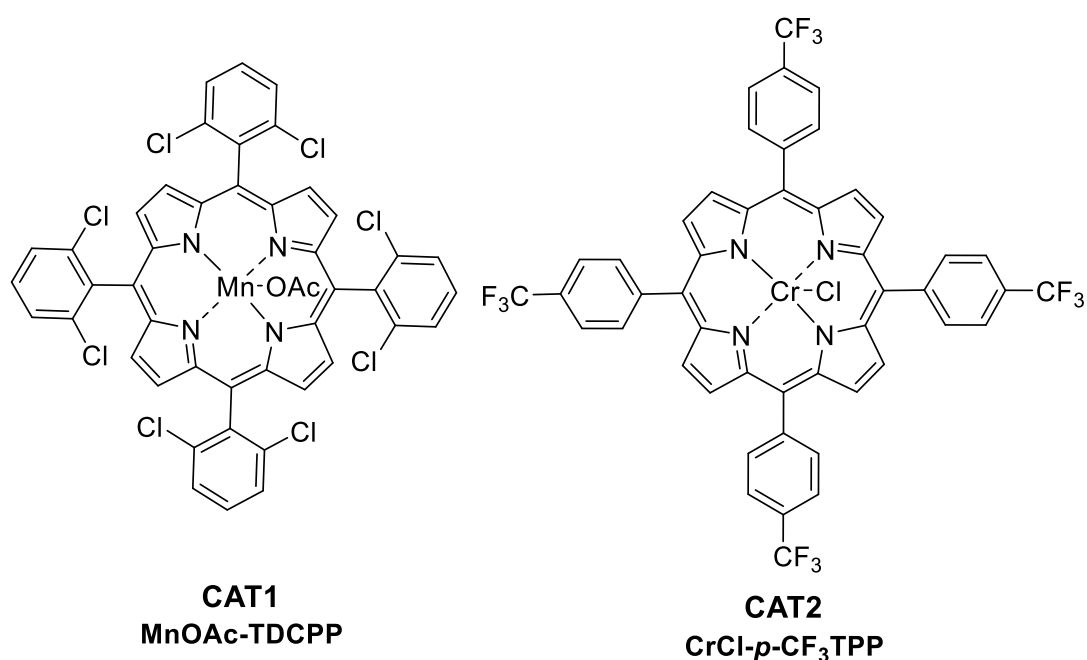
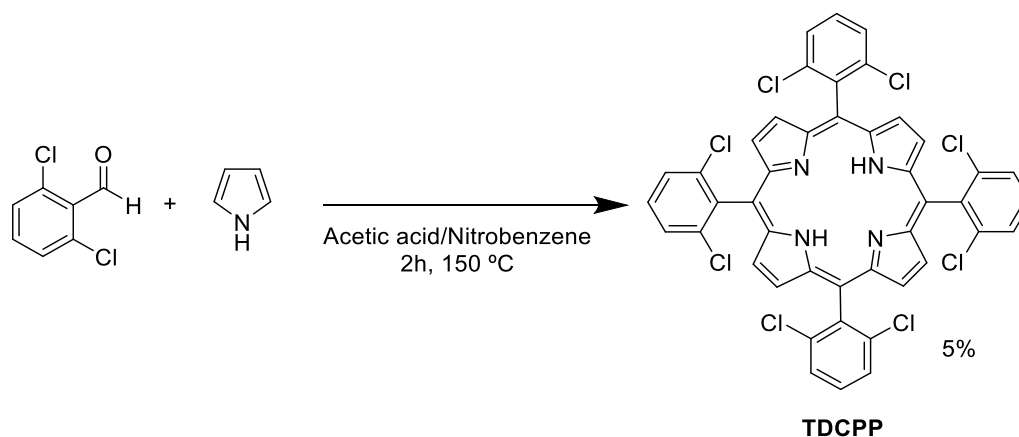


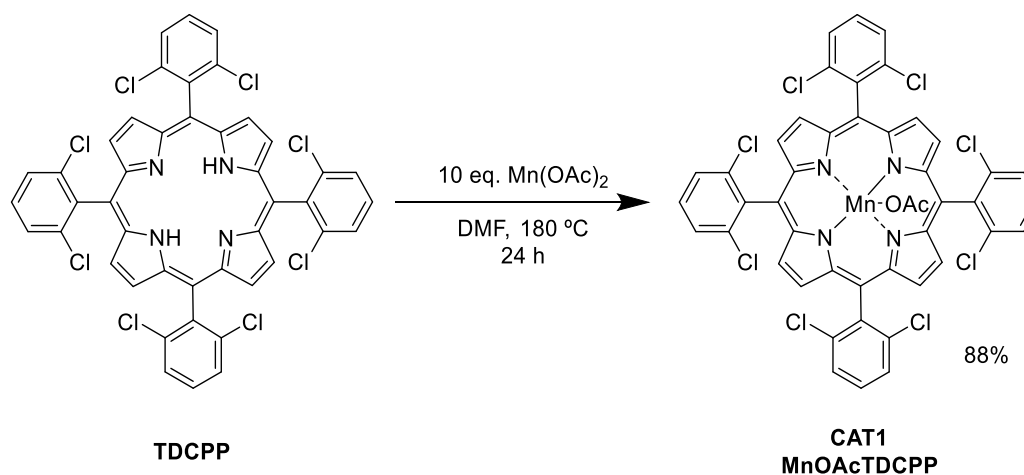
Figure 2.3. Structure of homogeneous metalloporphyrin-based catalysts synthesized in this work.

First, in order to synthesize **CAT1**, the 5,10,15,20-tetra(2,6-dichlorophenyl)porphyrin (**TDCPP**) was prepared through the nitrobenzene method, developed by Pereira and Gonsalves^{20,21} and recently optimized in the C&FC research group.²² In a typical reaction, pyrrole was slowly added to a boiling solution of 1 equivalent 2,6-dichlorobenzaldehyde dissolved in nitrobenzene and glacial acetic acid (1:2) and the mixture was left for 2 hours under constant stirring at 150 °C (Scheme 2.1). After 2 hours, the reaction was stopped and cooled to 25 °C, then ice-cold methanol was added to promote the precipitation of the porphyrin and the mixture was kept at 5 °C overnight. After filtration, the solid was washed with ice-cold methanol and the resulting compound was dried in an oven at 70 °C for 2 hours, obtaining a purple solid with a 5% yield. The yield and characterization data are in good agreement with those reported in the literature.^{20,21}



Scheme 2.1. Synthesis of 5,10,15,20-tetra(2,6-dichlorophenyl)porphyrin (**TDCPP**) by the nitrobenzene method.

The second step of the catalyst synthesis was the preparation of the corresponding manganese (III) porphyrin complex. Following a previously optimized methodology,²³ **TDCPP** was dissolved in dimethylformamide (DMF) and then 7 equivalents of manganese (II) acetate was added (Scheme 2.2). The solution was kept at 180 °C for 24 hours, during which the reaction progress was followed by UV-Vis. Afterwards, the reaction crude was diluted in CH₂Cl₂ and washed several times with water to remove the remaining manganese salts and DMF. The organic phase was then dried with anhydrous sodium sulfate and finally the solvent, CH₂Cl₂, was evaporated, resulting in a greenish solid (**CAT1**) with 88% isolated yield. This complex was characterized by mass spectrometry and UV-Vis and the data are in agreement with the literature.²⁴



Scheme 2.2. Synthesis of 5,10,15,20-tetra(2,6-dichlorophenyl)porphyrinatomanganese acetate (**CAT1**)

The comparative normalized spectra of free-base porphyrin **TDCPP** and MnOAcTDCPP (**CAT1**) are shown in Figure 2.4. As previously reported, significant differences in the spectra are observed, the base porphyrin presenting a Soret band at 417.5 nm followed by 4 Q bands, while for the manganese complex, the Soret band suffers a redshift of *ca.* 59 nm, appearing at 476.5 nm and 2 Q bands. Overmore, the spectrum of manganese complex MnOAcTDCPP (**CAT1**) shows additional broad bands at 370 and 400 nm, resultant of metal to ligand charge transfer events. It should be noted that, during this reaction, the metal is oxidized by the porphyrin ligand, changing its oxidation state from Mn(II) to Mn(III).

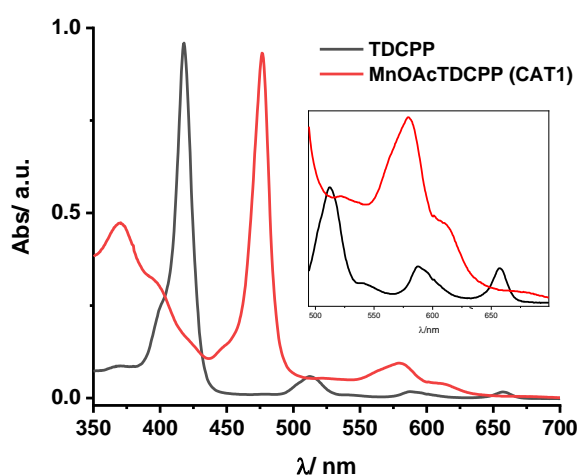
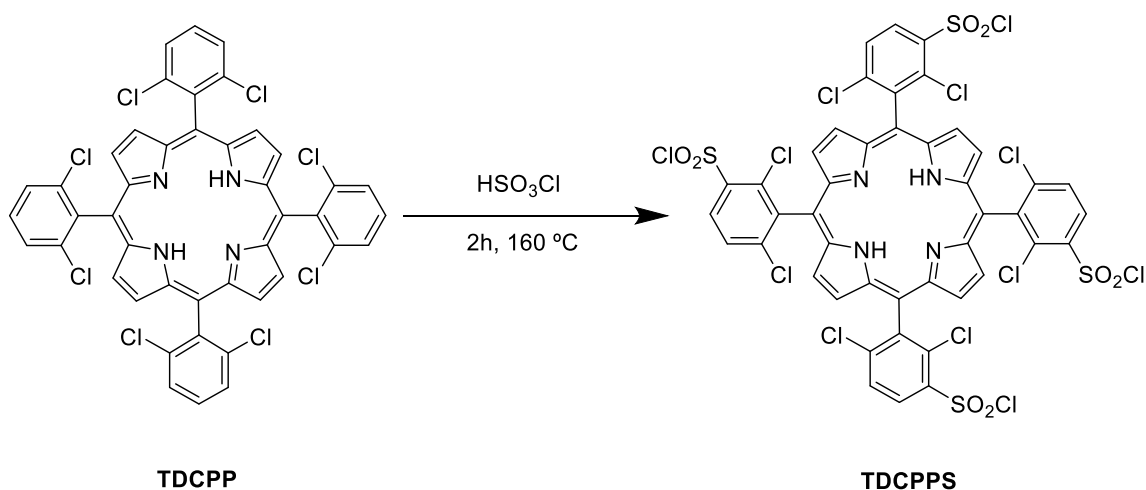


Figure 2.4. Normalized UV-Vis spectra of **TDCPP** and MnOAcTDCPP (**CAT1**) taken at 25 °C using CH₃CN as solvent.

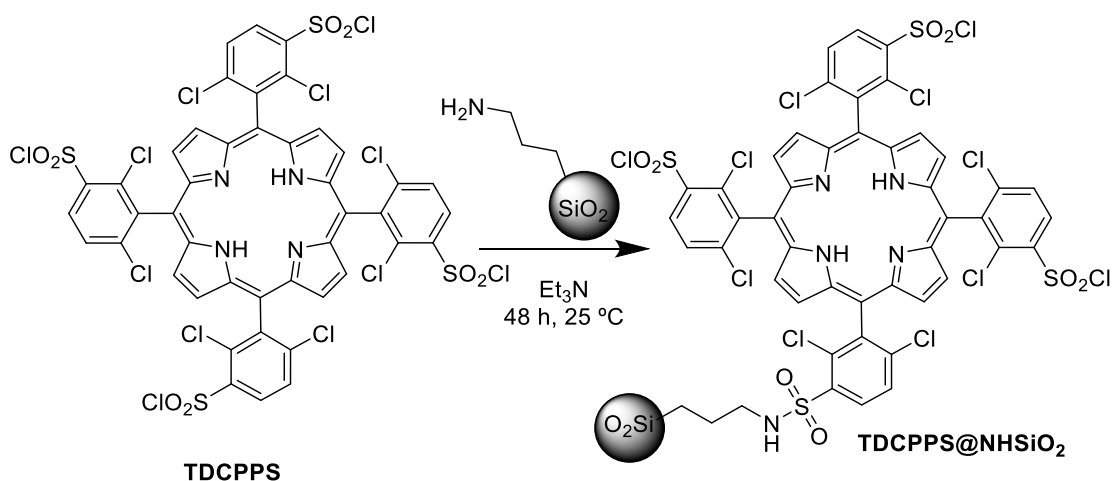
In order to obtain a reusable heterogeneous catalyst, we pursued the studies with the immobilization of **CAT1** onto functionalized silica particles, using a methodology developed by the C&FC group.²⁵ To achieve this goal, the chlorosulfonation of **TDCPP** followed by immobilization onto aminated (aminopropyl groups) silica particles and complexation with manganese acetate was performed.²⁶⁻²⁸ Firstly, in a round bottom flask, **TDCPP** was dissolved in chlorosulfonic acid and left with stirring at 160 °C for 2 hours (Scheme 2.3). Then, the reaction crude was diluted in chloroform and continuously washed with cold water, using an appropriate homemade apparatus, specifically developed in the group. The organic phase was then washed with a concentrated solution of sodium bicarbonate followed by distilled water. After ensuring the neutralization of

the solution by pH control, the organic phase was dried with sodium sulfate and evaporated under reduced pressure. The desired 5,10,15,20-tetra(2,4-dichlorobenzenesulfonyl chloride)porphyrin (**TDCPPS**) was obtained as a purple solid and used in the next step without further purification.



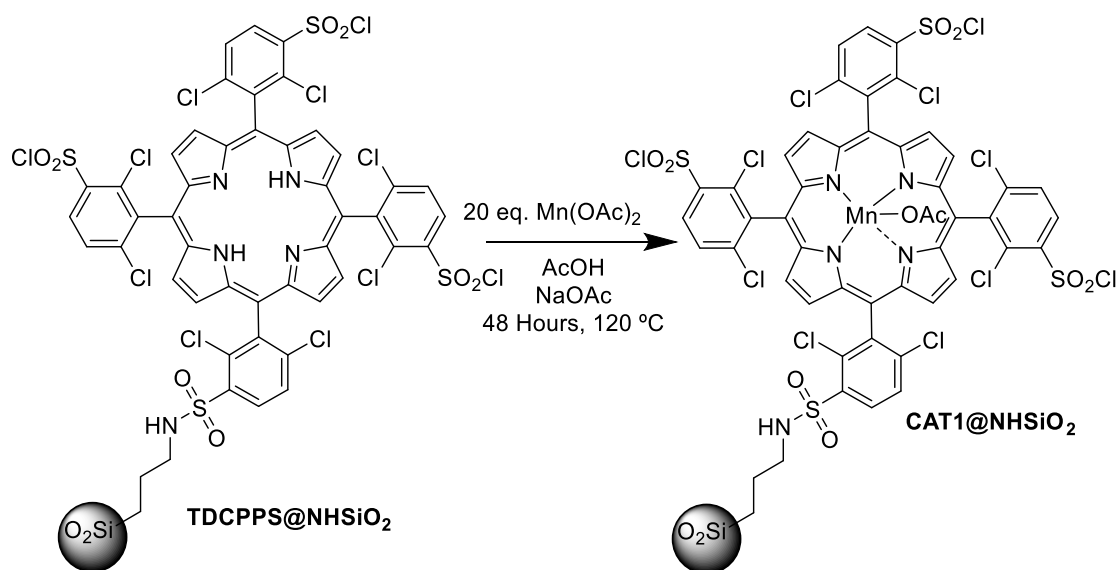
Scheme 2.3. Synthesis of 5,10,15,20-tetra(2,6-dichloro-3-chlorosulfonylphenyl)porphyrin (**TDCPPS**).

The next step was the immobilization of the chlorosulfonated porphyrin **TDCPPS** onto amino functionalized silica particles (Scheme 2.4), which occurs through a $\text{S}_{\text{N}}2$ mechanism in which the amine group of the silica support acts as a nucleophile. The reaction was carried out at $25\text{ }^\circ\text{C}$ using triethylamine as solvent, for 48 hours, under constant stirring, after which the reaction crude was centrifuged, and the supernatant was carefully removed. Then CH_2Cl_2 was added, stirred, centrifuged, and the supernatant was removed three more times, to wash any adsorbed porphyrin. The silica was also washed twice with ethanol and twice with acetone and finally, the solid was dried under vacuum, for 24 hours to obtain **TDCPPS@NHSiO₂**.



Scheme 2.4. Immobilization of **TDCPPS** onto aminated silica particles.

Finally, we proceeded with the preparation of the immobilized metal complex through the reaction between **TDCPPS@NHSiO₂** and manganese (II) acetate. In a typical procedure, the silica-immobilized porphyrin and 20 molar equivalents of manganese (II) acetate, were dissolved in acetic acid in the presence of a sodium acetate buffer (Scheme 2.5). The reaction was vigorously stirred, ensuring silica dispersion. Then, the reaction was left at 120 °C for 48 hours. After this time, the reaction was cooled to 25 °C, and the crude was centrifuged to facilitate the material isolation. Then, to remove the excess of manganese salts and acetic acid, methanol was added to the solid and stirred for a couple of minutes followed by centrifugation. This procedure was repeated several times. Finally, the solid material was washed twice with acetone and dried under reduced pressure for 24 hours at 25 °C, taking the necessary precaution to protect the immobilized catalyst from light, in order to prevent its degradation due to photosensitive properties.



Scheme 2.5. Synthesis of Mn(III) complex of **TDCPPS** porphyrin immobilized onto silica particles.

The resulting dark brown silica was characterized by solid-state UV (Figure 2.5). Comparing the UV–Vis spectra profiles of the **CAT1@NHSiO₂** with the **CAT1**, we concluded that the metalloporphyrin was effectively immobilized onto the silica support since the material exhibits the expected **CAT1** spectrum profile with broad bands and blue shift, as already described.²⁵

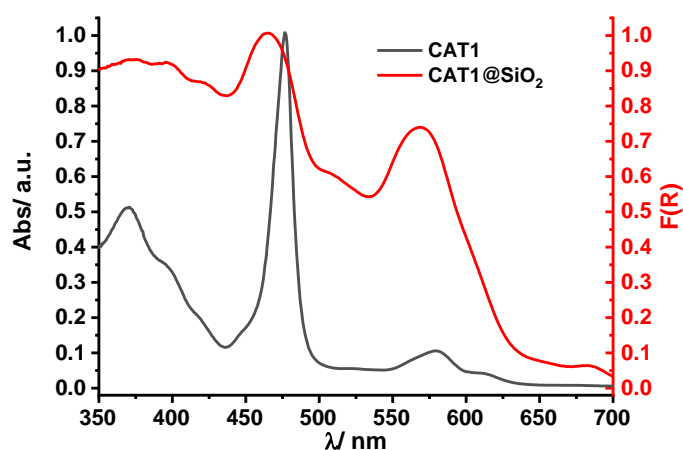


Figure 2.5. Normalized spectra of **CAT1** UV-Vis in chloroform (Black) and **CAT2** solid state UV-Vis (Red).

In addition, to quantify the amount of immobilized **CAT1** onto the silica support, thermogravimetric analysis was carried out at a temperature range of 25–800 °C (Figure 2.6).

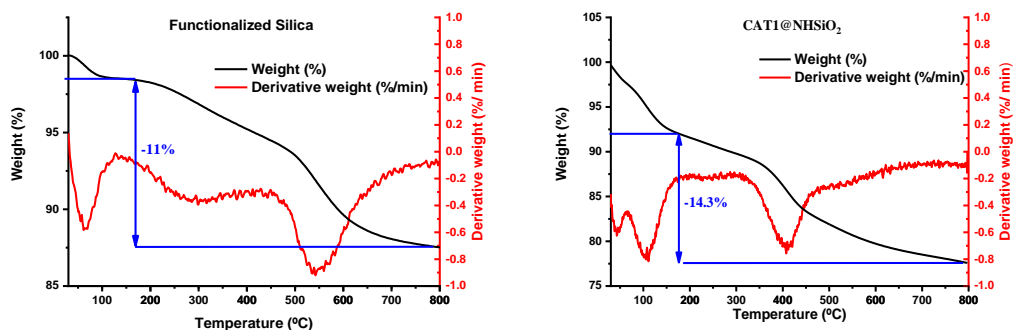
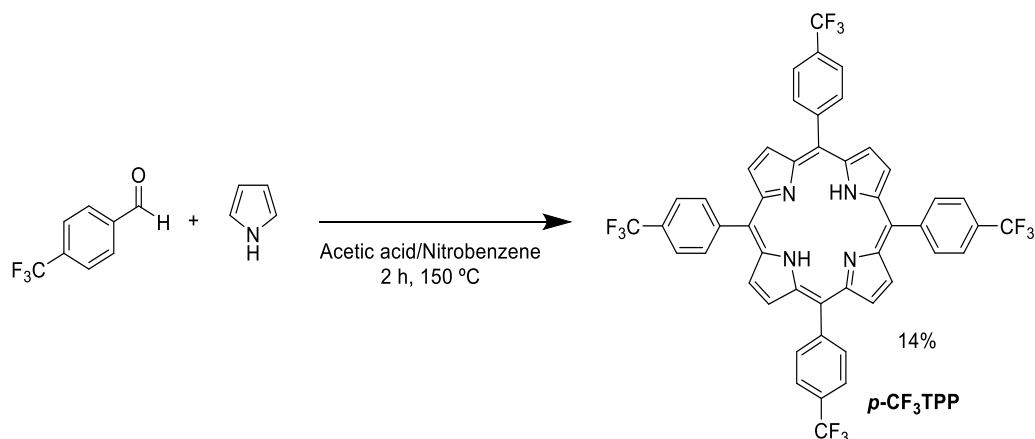


Figure 2.6. Thermogravimetric analysis of functionalized silica (Left) and **CAT1@NHSiO₂** (Right).

From the figure, we clearly observed that both 3-aminopropyl functionalized silica support and **CAT1@NHSiO₂** present mass losses between 25 °C and 175 °C, which are due to the presence of solvent or adsorbed water in the materials. For the pristine functionalized silica, a weight loss of 11% is observed at the 175 to 800 °C range, with a most intense step between 500–700 °C. As for the **CAT1@NHSiO₂**, a total of 14.3%

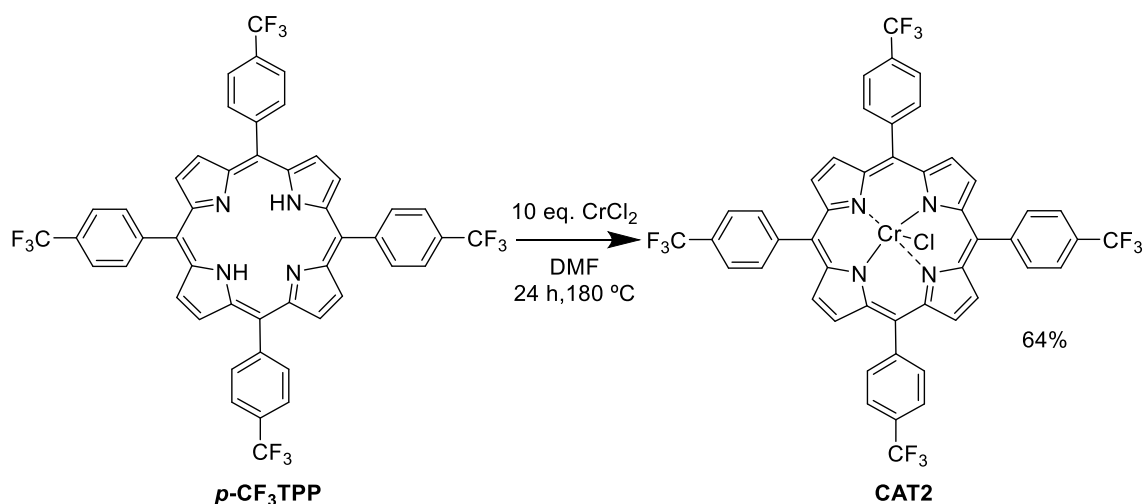
weight was lost between 175 and 800 °C. Thus, we obtained 3.3% difference in mass loss between standard aminated silica and **CAT1@NHSiO₂**. This difference is attributed to the thermic decomposition of the organic part of the immobilized metalloporphyrin, using the porphyrin molecular weight we obtain 2.75×10^{-5} mol of **CAT1** per gram of material corresponding to a 22% yield of immobilization. Additionally, the amount of manganese present in the solid material was quantified through inductively coupled plasma optical emission spectrometry (ICP-OES), which revealed a 0.2% wt/wt of manganese (2 mg Mn/g material) demonstrating the successful preparation of the heterogeneous immobilized manganese metalloporphyrin. The reaction yield and catalyst characterization are in accordance with the previously reported literature.²⁵

Next, the studies proceeded with the synthesis of CrCl-*p*-CF₃TPP (**CAT2**), intended to be used as catalyst for CO₂ cycloaddition to epoxides. It was recently reported, by previous works in the group,^{28, 29} that electron attracting groups in the periphery of the porphyrin increase the Lewis acidity of the central metal, leading to higher catalytic activities. Furthermore, it is well-established that chromium(III)-porphyrins are among the most active and selective catalysts for CO₂ cycloaddition reactions.^{28, 29} Therefore, this metalloporphyrin catalyst was chosen due to the known high activity and selectivity toward cyclic carbonates when terminal epoxides are used as substrates.²⁹ The synthesis of 5,10,15,20-tetra(4-trifluoromethylphenyl)porphyrin (*p*-CF₃TPP) was performed using the nitrobenzene method, previously described for **TDCPP**. In this case, pyrrole was slowly added to a boiling mixture of 4-(trifluoromethyl)benzaldehyde, dissolved in acetic acid/ nitrobenzene in a 2 to 1 ratio (Scheme 2.6). After 2 hours at 150 °C, the reaction was cooled, and then cold methanol was added to precipitate the porphyrin. The resulting *p*-CF₃TPP was filtered and washed several times with cold methanol. The purple solid was left in an oven for 2 hours to dry, yielding 14%. Similar to the previous porphyrin, the compound was characterized through UV-Vis and NMR, and the results were in accordance with the literature.²⁹



Scheme 2.6. Synthesis of 5,10,15,20-tetra(4-trifluoromethylphenyl)porphyrin (*p*-CF₃TPP)

For the synthesis of the corresponding chromium(III) complex, *p*-CF₃TPP and 7 equivalents of chromium (III) chloride were dissolved in the minimum amount of DMF and heated to 180 °C (Scheme 2.7). After 2 hours an UV-Vis spectrum was done, concluding that the conversion was not complete, as the Soret band of free-base porphyrin at 417 nm was still present. Therefore, 3 more equivalents of chromium chloride were added and the reaction was left under stirring for 24 hours. Then, another spectrum was obtained, still showing the band at 417 nm, meaning that there was still free-base porphyrin. The reaction was stopped and dissolved in CH₂Cl₂. The reaction crude was washed with water to remove the chromium salt excesses. After drying and evaporating the organic phase, a silica gel column chromatography was performed to purify the catalyst. The chromatography started with CH₂Cl₂/*n*-hexane 1:1, slowly decreasing the amount of *n*-hexane until the free-base porphyrin was fully removed, while the chromium porphyrin remained in the application point. Then, the eluent was slowly changed to acetyl acetate to remove the pure CAT2. The organic solvent was then evaporated under reduced pressure and the resulting green solid was dried in an oven at 70 °C for 2 hours.



Scheme 2.7. Synthesis of chromium porphyrin complex (**CAT2**).

The **CAT2** was analysed by UV-Vis spectroscopy (Figure 2.7), and when compared to the free-base porphyrin, a redshift of the Soret band is observed of ca. 29 nm and, as expected, the four Q bands degenerate into two Q bands. The Cr (III) porphyrin complex also presents one new band at near UV region, corresponding to the metal to ligand charge transfer. This metal complex was characterized by mass spectrometry and the data is in agreement to that previously reported.³⁰ Transformation of this porphyrin aiming its further immobilization onto a solid support is currently underway.

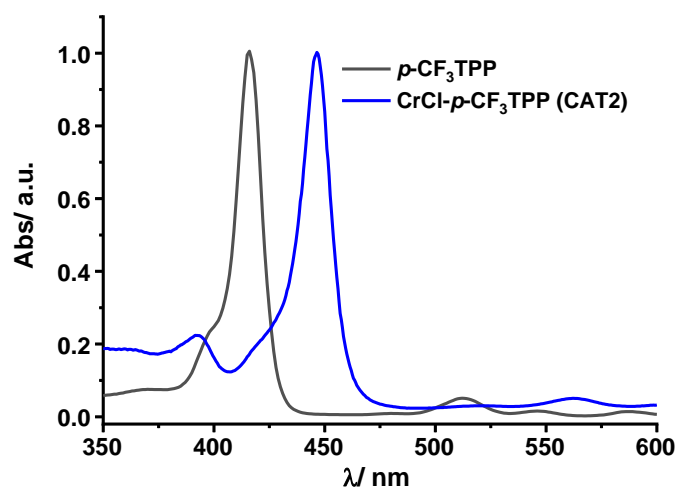


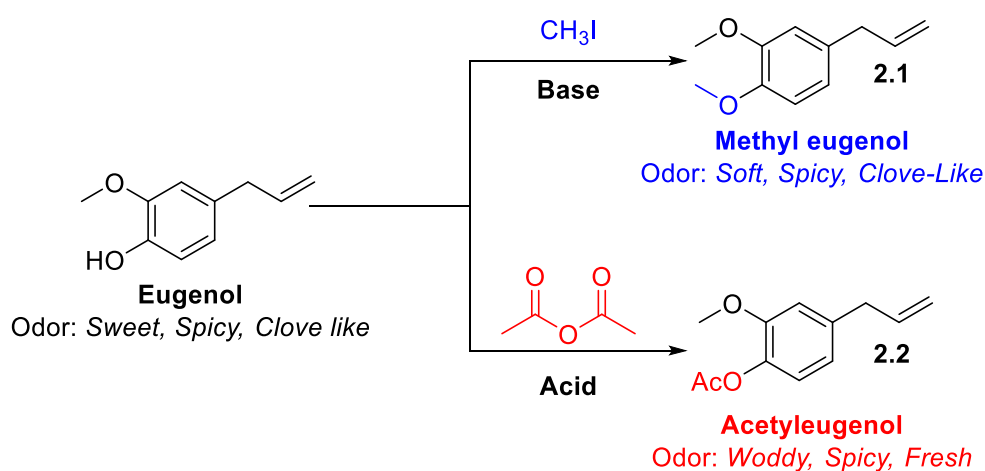
Figure 2.7. Normalised UV-Vis spectra of 5,10,15,20-tetra(4-trifluoromethylphenyl)porphyrin (**p-CF₃TPP**) and 5,10,15,20-tetra(4-trifluoromethylphenyl)porphyrinatochromium(III) Chloride (**CAT2**) at $25\text{ }^\circ\text{C}$ using CH_3CN as solvent.

2.2. Eugenol hydroxyl group protection

The studies started with the protection of the eugenol hydroxyl group to prevent intermolecular reactions with the epoxide ring in acidic medium, which would lead to the formation of hydroxyether species, with subsequent oligomerization/polymerization reactions.³¹

Therefore, two different approaches were followed to prepare the protected eugenol derivatives. The first one was a typical S_N2 reaction of eugenol with iodomethane in a basic medium, yielding methyl eugenol (**2.1**). The second approach was acetylation reaction of eugenol with acetic anhydride in acidic medium to obtain acetyleugenol (**2.2**) (Scheme 2.8). The latter was prepared using 2 different methodologies: a classic system, under batch conditions and an alternative continuous flow apparatus, with two different catalysts (K10 and sulfuric acid).

These compounds are present in nature and their uses in the fragrance and flavor industry are well reported.³²

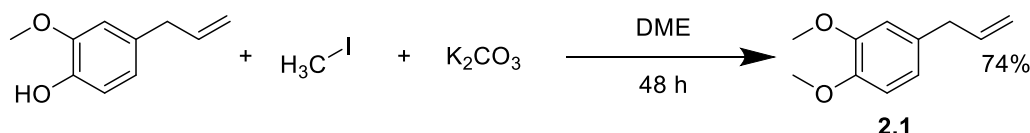


Scheme 2.8. Two different approaches for eugenol protection.

2.2.1. Eugenol methylation

The methylation of eugenol was done using 5 equivalents of iodomethane and 5 equivalents of potassium carbonate in dimethoxyethane (DME) as solvent (Scheme 2.9). The reaction was carried out at 25 °C along 24 hours. Then, a sample was taken and analyzed by GC and 83% conversion was observed. The reaction was left for an extra 24 hours, after which full conversion with 99% selectivity was reached. At this point, the

reaction was stopped and the reaction crude was evaporated under reduced pressure. Then, DME was added to dissolve methyl eugenol (**2.1**) and several extractions with distilled water were performed to remove the remaining salts. After drying the organic phase with anhydrous sodium sulfate and evaporation of the solvent under reduced pressure, the product methyl eugenol (**2.1**) was isolated with 74% isolated yield. The product was characterized by $^1\text{H NMR}$ and $^{13}\text{C NMR}$ (See Chapter 3, section 4), and the spectroscopic data were in agreement with those previously reported.³³

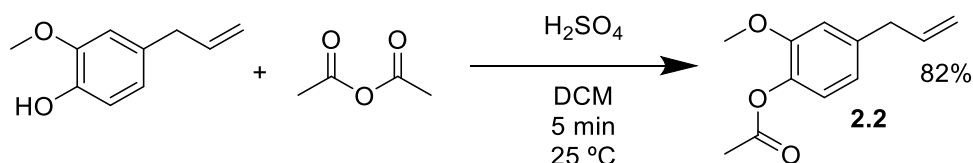


Scheme 2.9. Eugenol methylation reaction.

2.2.2. Eugenol Acetylation

Batch

We started by using 1.2 eq. of acetic anhydride, a drop of sulfuric acid and eugenol in CH_2Cl_2 (Scheme 2.10). After five minutes the reaction was complete. As demonstrated by TLC and further confirmed by GC analysis. Then, the mixture was diluted with CH_2Cl_2 and washed with a solution of sodium hydrogen carbonate to remove the sulfuric acid used as catalyst and the excess acetic anhydride. The organic phase was dried with sodium sulfate and passed through a small silica plug. Finally, the organic solvent was evaporated under reduced pressure, obtaining a colorless oil. The desired product **2.2** was isolated with high purity in 82% yield, without the need of further purification procedures.

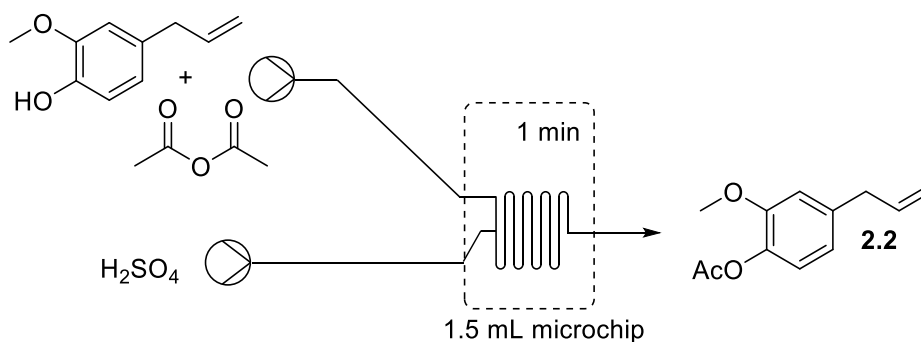


Scheme 2.10. Eugenol acetylation reaction.

Continuous-flow

Aiming for the development of highly sustainable processes and the scale-up of the reaction, eugenol acetylation process was then transposed to flow chemistry. First, we carried out a reaction under conditions previously described for batch. In a typical flow chemistry experiment, we prepared a solution of acetic anhydride and eugenol in CH_2Cl_2 , with 1.2 equivalents of acetic anhydride, and another solution with sulfuric acid. Afterwards, the two solutions were pumped into a microreactor, this type of reactor ensures efficient mixing and high heat exchange. Samples of each flow experiment were taken and analyzed by GC. The effects of the temperature and acid concentration were evaluated and the results are presented in Table 2.1.

Table 2.1. Effect of the concentration of sulfuric acid as catalyst in eugenol protection at 25 and 50 °C.

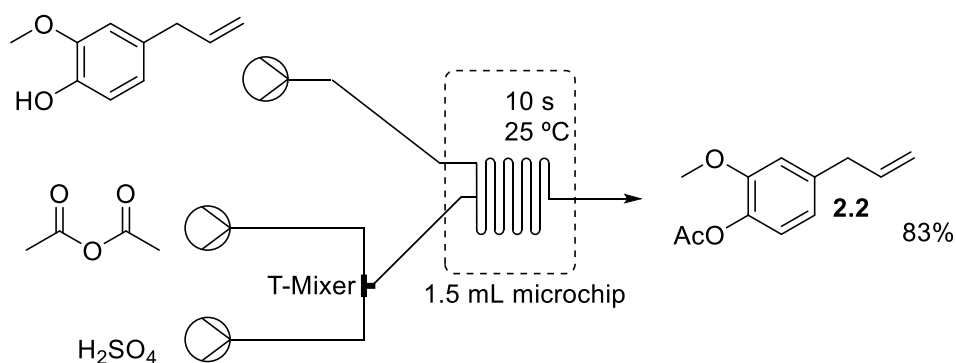


Entry	[Acid] (M)	Temperature (°C)	Conversion (%)
1	0.091	25	3
2	0.091	50	2
3	0.18	25	3
4	0.18	50	4
5	0.92	25	6
6	0.92	50	12
7	1.84	25	52
8	1.84	50	55

Reaction conditions: 1.2 molar equivalents acetic anhydride, 1 min residence time, Eugenol concentration 0.23 M in CH_2Cl_2 . Acetic anhydride concentration 0.27 M in CH_2Cl_2 .

The sulfuric acid concentration between 0.09 and 0.18 M, leads to low conversion values (2-4%), at both 25 °C and 50 °C (Table 2.1, entries 1-4). When the acid concentration was increased to 0.92 M, a slight increase in conversion was observed, particularly at 50 °C for which *ca.* 12% conversion was obtained (Table 2.1, entries 5-6). The acid concentration was then increased to 1.9 M and, at this concentration, the conversion of eugenol was 52% (Table 2.1, entry 7). This transformation was accompanied by a color change of the solution to a deep red color, as previously observed in the batch process. The increase in temperature from 25 to 50 °C only raised the conversion by 3% (Table 2.1, entry 8). Therefore, we concluded that the use of sulfuric acid as catalyst under flow chemistry conditions is less efficient than in the batch process. These results may be attributed to difficulty of mixing sulfuric acid with the solution reaction.

To avoid this problem, a different experimental approach for the reaction was followed, which consisted in the mixture between acetic anhydride and sulfuric acid, previous to their addition to eugenol. The acetic anhydride and concentrated sulfuric acid were mixed for ~1 second, in a proportion of 1 to 10, using a T-mixer, before adding to the eugenol solution in a microchip for 10 seconds.. With this method, a conversion of 83% was achieved (Scheme 2.11). The space-time yield (STY) was calculated for this process. The STY is used to measure the volumetric productivity of a reactive system, which can be simplified to measure the overall productivity of a process in function of the reactor's volume.^{34, 35} In this case the STY was of 20 g min⁻¹ dm⁻³. It should be mentioned that under the equivalent batch conditions, a 2.5 L reactor would be required to have a similar output of acetyleneugenol per minute. These values clearly demonstrate the potentiality of performing this reaction in flow conditions, particularly using microchip reactor over round-bottom flask.



Scheme 2.11. Acetylation reaction of eugenol using three pumps.

This strategy not only prevents the solubility problems, but also pre-activated the acetic anhydride, through the protonation of the oxygen atoms, causing an increase in the electrophilicity of the adjacent carbon atoms, making them more vulnerable to the nucleophilic attack of the eugenol hydroxyl group.

With these results in hand, we decided to search for a more sustainable alternative to sulfuric acid, which is known as a dangerous, corrosive and toxic reagent. Such alternative are heterogenous catalysts, which are a reusable, eco-friendly and not harmful.

2.2.3. Heterogenous eugenol acetylation

First, we tested as heterogeneous acid catalyst the commercially available Amberlite 120 (IRA-120H), a strongly acidic cation exchange resin, prepared from sulfonation of polystyrene (Figure 2.8).^{36, 37} Before using it, the resin was activated following a standard procedure.³⁸ The catalyst was washed with 1 molar solution of hydrochloric acid and then with distilled water. Then, the resin catalyst was washed twice with ethanol and acetone. After that, the resin was left to dry for 24 hours in open air, after which the catalyst was ready to be used. This step was necessary to ensure that all the sulfonic groups are protonated which increases the number of active catalytic sites.

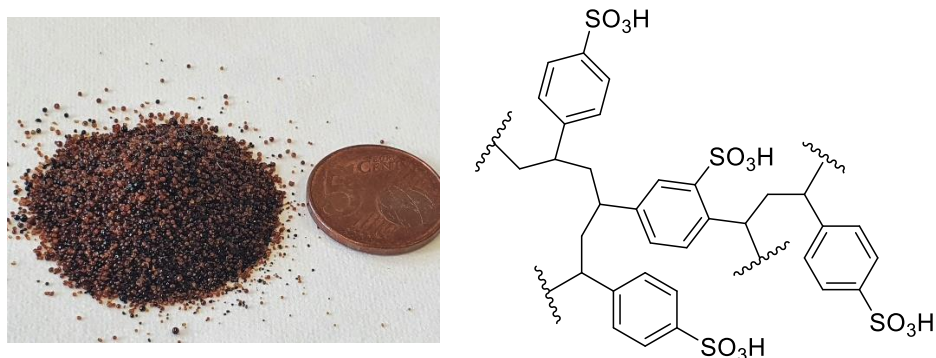


Figure 2.8. Commercially available resin Amberlite 120 and representation of its chemical structure. Figure adapted from the literature.³⁹

Another heterogeneous acid catalyst was also tested, the commercially available K10 montmorillonite (Figure 2.9). This clay is an abundant, natural aluminosilicate mineral, widely used as an affordable and eco-friendly catalyst.⁴⁰

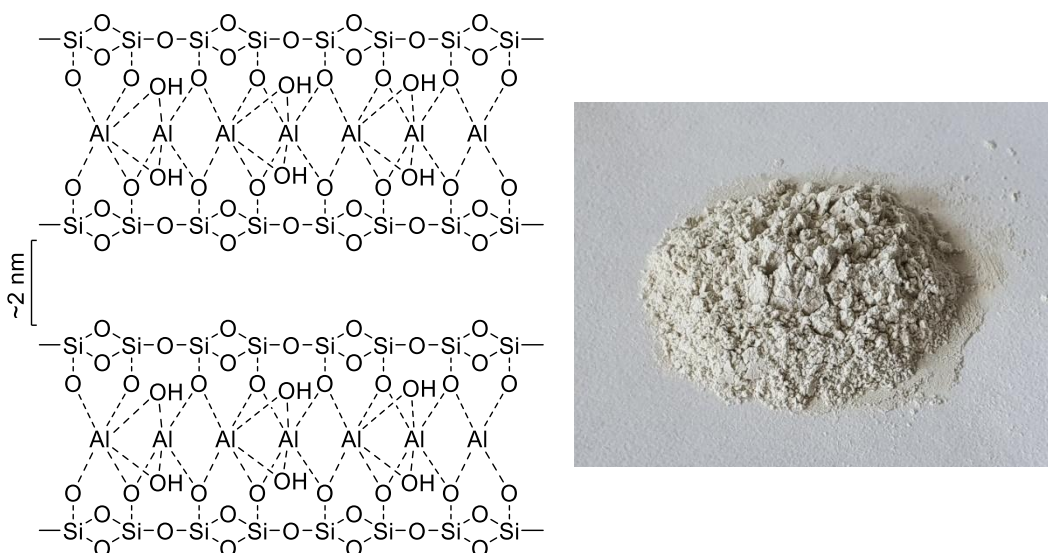
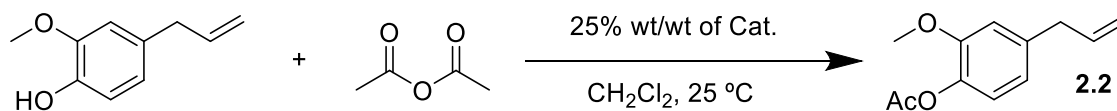


Figure 2.9. Image of commercially available K10 Montmorillonite clay and representation of its chemical structure.⁴¹

Batch

The evaluation of the heterogeneous catalysts in the acid-catalyzed acetylation of eugenol was first tested in batch. In a typical procedure, the heterogeneous acetylation reaction was carried out, using 10 equivalents of acetic anhydride with 25% wt/wt catalyst loading. The higher number of acetic anhydride equivalents is required, as the use of 2 equivalents was not enough, resulting in no conversion being observed. After 4 hours a sample was taken and analyzed to GC using chlorobenzene as internal standard. The results are presented in Table 2.2.

Table 2.2. Optimization of the acetylation reaction using heterogeneous catalysts.



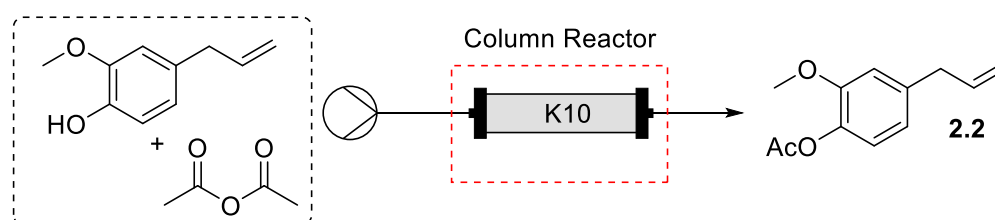
Entry	Catalyst	Conversion (%)
1	IRA-120H	19
2	K10	>99

Reaction conditions: 25% wt/wt solid catalyst, 6.5 mmol eugenol, 10 mL CH₂Cl₂, 25 °C, 0.065 mol of acetic anhydride, 4 hours, 3.6 mol of chlorobenzene, conversion calculated using GC-FID.

From the analysis of the results reported on table 2.2, it was possible to conclude that under similar reaction conditions K10 shows significantly higher activity than IRA-120H, achieving full conversions, while IRA-120H only achieved 19% conversion for acetyleneugenol. This may be attributed to the number and type of acidic sites in each catalyst. For this reason, the heterogenous catalysts K10 was selected to be evaluated under continuous-flow conditions.

Continuous-flow

The studies were performed using a column reactor, also known as packed bed reactor, since these are the most suitable continuous-flow reactors for the use of solid materials in flow chemistry systems (Scheme 2.12).



Scheme 2.12. Continuous-flow heterogeneous Acetylation of eugenol using K10.

First, it was necessary to calculate the column's dead volume (the free space between the solid catalyst particles, which, during the reaction, will be occupied by the solution), to know for how long the reactants will be in contact with the catalyst.

Therefore, the reactor was first filled with catalyst and weighted. Then, the reactor was connected to the continuous flow system and the solvent was pumped through the reactor. Finally, the reactor was disconnected and weighted with the solid and solvent inside. Using the difference in weights and the density of the solvent we obtained a dead volume of 2.0 mL.

After the column's dead volume calculation, the reactor was once again connected to the system and a solution of acetic anhydride and eugenol were pumped through the reactor, and the reaction was conducted at variable temperatures (40 and 70 °C) and residence times (10 and 20 min). The results are presented in Table 2.3.

Table 2.3. Acetylation of eugenol under continuous flow conditions using K10.

Entry	Temperature (°C)	Residence time (min)	Conversion (%)	STY (g min ⁻¹ dm ⁻³)
1	40	10	29	1.16
2	40	20	83	1.66
2	70	20	98	1.96

Reaction conditions: 0.23 M eugenol, 2.3 M acetic anhydride, CH₂Cl₂, 1.78 g K10 clay, 3.6 mmol chlorobenzene, 2 mL dead volume.

To optimize the reaction parameters, the temperature and residence time were evaluated. First, we used only 10 minutes of residence time and a temperature of 40 °C and 29% conversion was observed (Table 2.3, entry 1). Then, the residence time was increased to 20 minutes and the conversion reached 83% (Table 2.3, entry 2). Finally, using the same residence time (20 min) but increasing the temperature to 70 °C, 98% conversion was obtained (Table 2.3, entry 3). Under these conditions we obtained a STY of 1.96 g min⁻¹ dm⁻³. For comparison, a reaction under batch conditions would require a 7 L reactor to have a similar output of material per minute. Therefore, we conclude that continuous flow processes allow higher outputs of material, while having a small ecological footprint, which is crucial for scale up.

2.3. Epoxidation of Eugenol derivatives

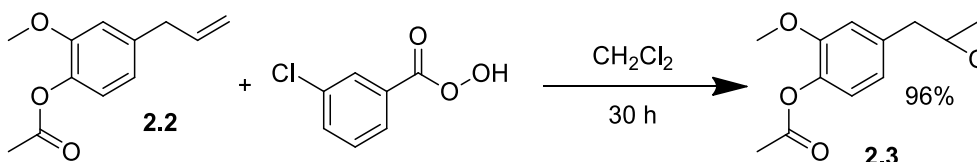
As previously stated, there are different pathways to obtain epoxide rings. We highlight the use of peroxy acids and alternative oxidants, namely molecular oxygen and peroxides. In this section we describe the epoxidation of eugenol derivatives using chloroperoxybenzoic acid (mCPBA) in batch and flow conditions, followed by epoxidations using high valent manganese-oxo porphyrins generated through the use of molecular oxygen and hydrogen peroxide.

2.3.1. Prilejaev epoxidation of eugenol

We started with the standard Prilejaev epoxidation reaction, using *meta*-chloroperoxybenzoic acid (mCPBA) as the oxidant. The studies were first performed in batch systems followed by their transposition to continuous flow.

Batch system

In a typical batch epoxidation procedure, the acetyleneugenol derivative **2.2** was placed in a round-bottom flask with 1.2 eq. of mCPBA, using CH₂Cl₂ as solvent, and the reaction was conducted at 25 °C (Scheme 2.13). After 30 h, the excess of peroxyacid was neutralized with sodium bisulfite aqueous solution, and then the resulting acid was removed by washing with a bicarbonate solution. The organic phase was then dried with anhydrous sodium sulfate and analyzed by GC, which indicated a 96% conversion with >99% selectivity.



Scheme 2.13. Prilejaev epoxidation reaction of acetyleneugenol (**2.2**) under batch conditions.

The solvent was then evaporated and the desired epoxide **2.3** was obtained as a yellow oil, without any further purification, in 91% yield. Finally, the eugenol epoxide product **2.3** was characterized by ^1H and ^{13}C NMR (Figure 2.10 and 2.11), and by HRMS (ESI), which confirmed the structure and high purity of the obtained product.

The ^1H -NMR spectrum of **2.3** in CDCl_3 , shows the three signals at the typical aromatic region, a doublet at $\delta = 6.96$ ppm ($J = 8.0$ Hz) assigned to proton H6, followed by another doublet at $\delta = 6.86$ ppm ($J = 1.9$ Hz) assigned to H3, and then a double doublet at $\delta = 6.82$ ppm ($J = 8.0, 1.9$ Hz) assigned to the last aromatic proton H5. At $\delta = 3.82$ ppm a singlet signal assigned to the methoxy group proton H1'' is located. Next, a multiplet signal at $\delta = 3.17 - 3.12$ ppm is present, assigned to the H2''' proton of the epoxide ring group. At $\delta = 2.83$ ppm ($J = 5.5$ Hz) a doublet signal assigned to the H1''' protons is observed. A double doublet at $\delta = 2.79$ ppm ($J = 4.8, 4.0$ Hz), assigned to one of protons of the H3''' position is present, at $\delta = 2.55$ ppm (4.9, 2.6 Hz) another double doublets is observed, and assigned to the other H3''' proton. Finally, at $\delta = 2.30$ ppm is located a singlet signal assigned to the acetyl group H2' protons.

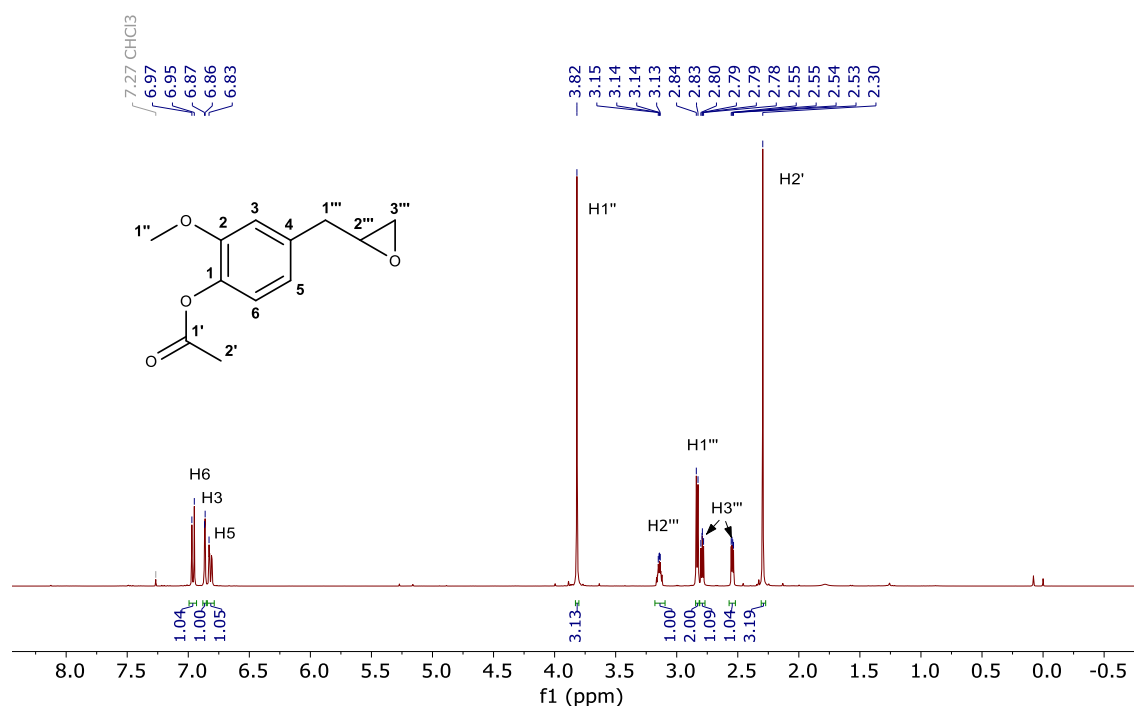


Figure 2.10. ^1H NMR of acetyleugenol epoxide (**2.3**) in CDCl_3 , at 25 °C.

Regarding the ^{13}C NMR, at $\delta = 169.1$ ppm we can observe a signal assigned to acetyl carbon $\text{C1}'$, followed by the signals assigned to the six aromatic carbons (C1-C6), at $\delta = 113.2-151.0$ ppm. At $\delta = 55.8$ ppm we observed a signal corresponding to the methoxy $\text{C1}''$ carbon, the signal present at $\delta = 52.3$ and $\delta = 46.8$ ppm were assigned to the epoxide ring carbons ($\text{C2}'''$ and $\text{C3}'''$). Finally, the last two signals are assigned to the alkyl carbon $\text{C1}'''$ found at $\delta = 38.7$ ppm and the acetyl group $\text{C2}'$ carbon found at $\delta = 20.7$ ppm respectively.

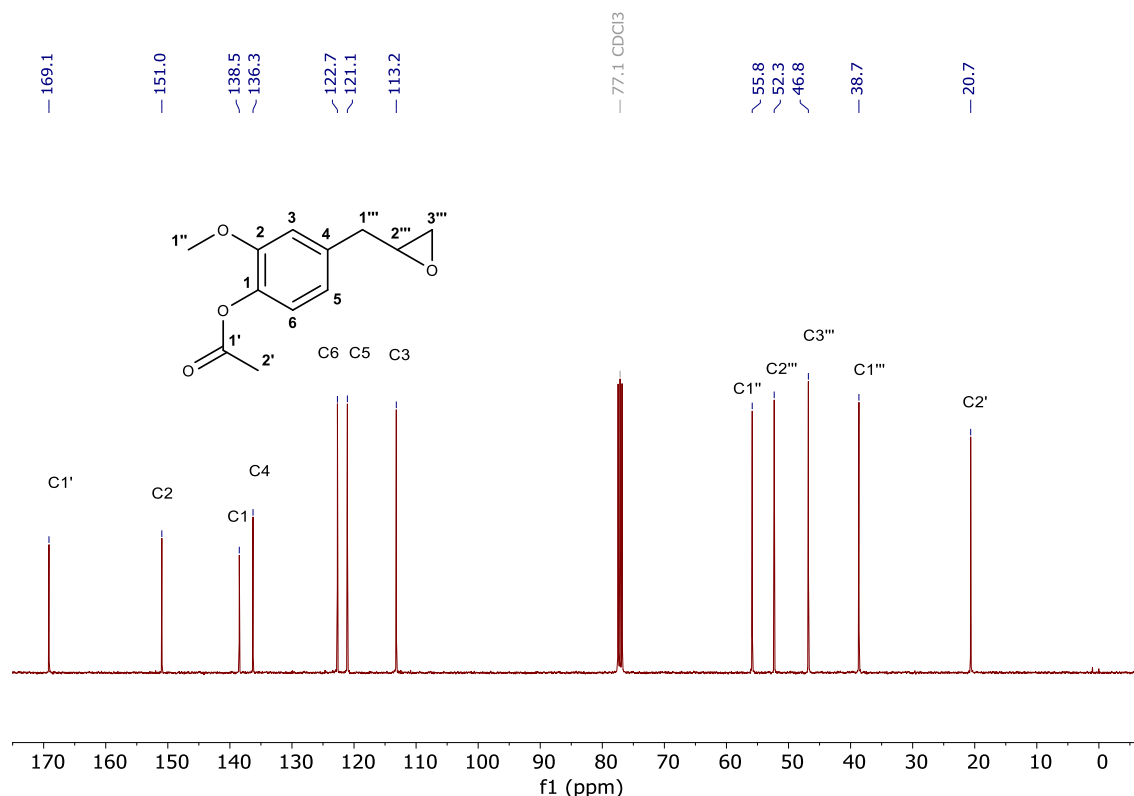


Figure 2.11. ^{13}C NMR of acetylenol epoxide (**2.3**) in CDCl_3 , at 25°C .

Additionally, **2.3** was also analyzed through electron spray ionization (ESI) high resolution mass spectrometry (HRMS), showing a peak at $m/z = 245.0784$, while the theoretical value for $[\text{M}+\text{Na}]^+$ ($\text{C}_{12}\text{H}_{14}\text{O}_4\text{Na}^+$) is $m/z = 245.0785$. (Figure 2.12)

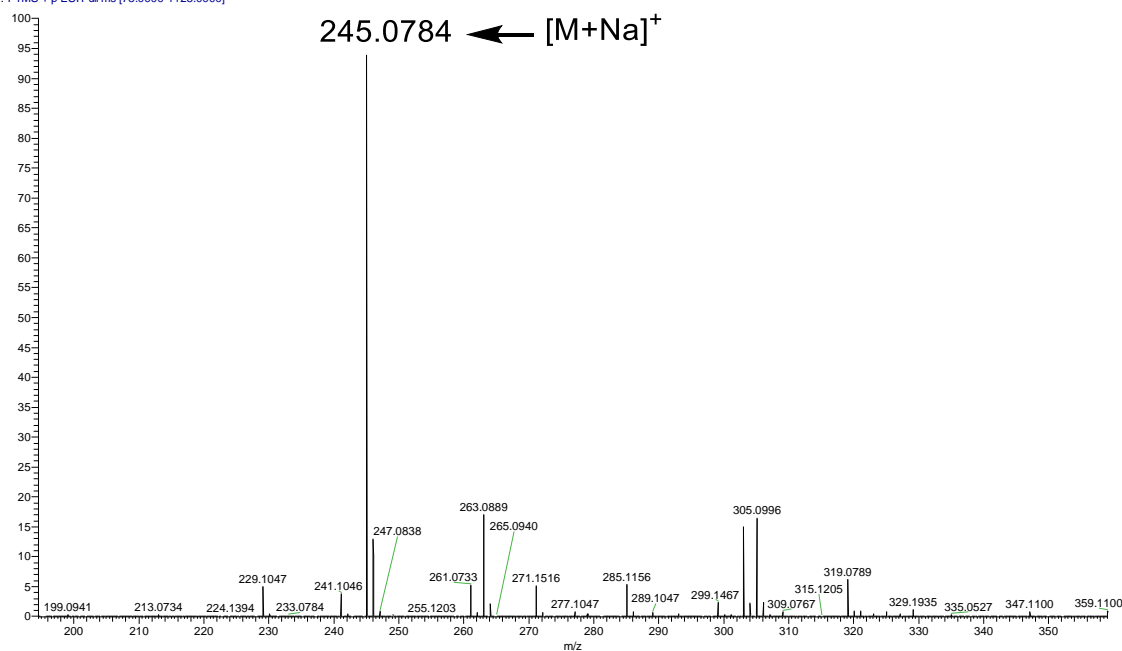


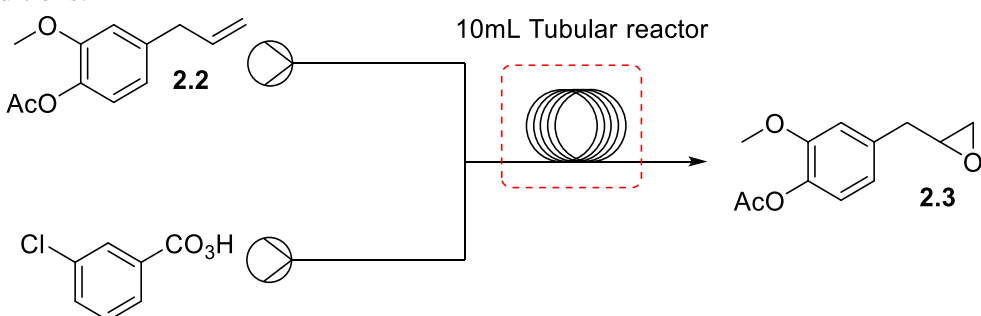
Figure 2.12. HRMS (ESI) spectrum of **2.3**.

After full characterization of compound **2.3**, the studies proceeded with the transposition of the Prilejaev epoxidation of eugenol to continuous-flow system.

Continuous-flow

In a typical flow epoxidation procedure, two solutions were prepared, one with acetyleneugenol (**2.2**), and the other with mCPBA in CH₂Cl₂ and pumped through a 10 mL tubular reactor. This tubular reactor was used to maximize the residence time. The solutions were pumped using a 1:1.2 (eugenol acetate/mCPBA) volumetric ratio to keep an excess of mCPBA. The residence time and reaction temperature were the two studied parameters for the reaction optimization and the results are summarized in table 2.4.

Table 2.4. Optimization of acetylugenol (**2.2**) epoxidation under continuous flow conditions.



Entry	Residence time (min)	Temperature (°C)	Conversion (%)	STY (g min ⁻¹ dm ⁻³)
1	10	25	14	0.30
2	10	40	31	0.67
3	40	40	40	0.22
4	40	60	59	0.32
5	40	80	77	0.42
6	40	100	83	0.45

Reaction conditions: 0.23 M acetylugenol(**2.2**), 0.23 M mCPBA, CH₂CL₂, volumetric ratio 1:1.2; selectivity for epoxide **2.3** was >99% in all cases.

First, we tested the reaction at 25 °C with 10 minutes residence time, resulting in a 14% conversion and 100% selectivity for the acetylugenol epoxide (Table 2.4, entry 1). Then, we tried to increase the temperature to 40 °C and the conversion increased to 31% (Table 2.4, entry 2). Then, using the same reaction temperature of 40 °C, the residence time was increased to 40 minutes, which produced a 40% conversion (Table 2.4, entry 3). The internal flow system pressure was increased to 9 bar, which allowed us to further increase the reaction temperature to 60 °C, without causing the solvent to boil. Under these conditions, and with a 40 minutes residence time, 59% conversion was achieved (Table 2.4, entry 4). Finally, the reaction was conducted at 80 °C and 100 °C, achieving 77% and 83% conversion, respectively (Table 2.4, entries 5 and 6).

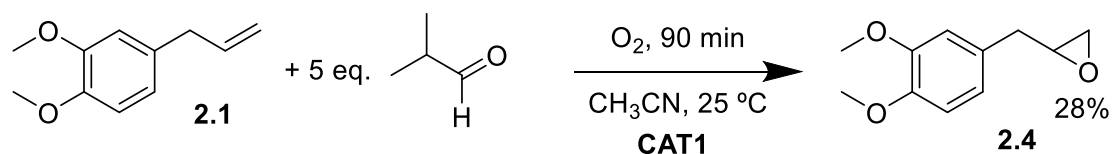
This process' best STY was 0.67 g min⁻¹ dm⁻³, to obtain a similar output in batch a 40 L reactor would be required, although it should be mentioned that the batch reaction could be optimized to decrease the reactor's volume.

As previously mentioned in chapter 1, organic peracids are not considered green reagents due to high waste production, low atom economy, high toxicity and security issues, and so, more sustainable approaches must be developed. Therefore, the use of green oxidants such as molecular oxygen and hydrogen peroxide appeared as more sustainable alternatives for epoxidation reactions. In both cases, manganese porphyrins have shown to be remarkably efficient and selective epoxidation catalysts.^{23, 42-46}

2.3.2. Catalytic epoxidation using oxygen as oxidant

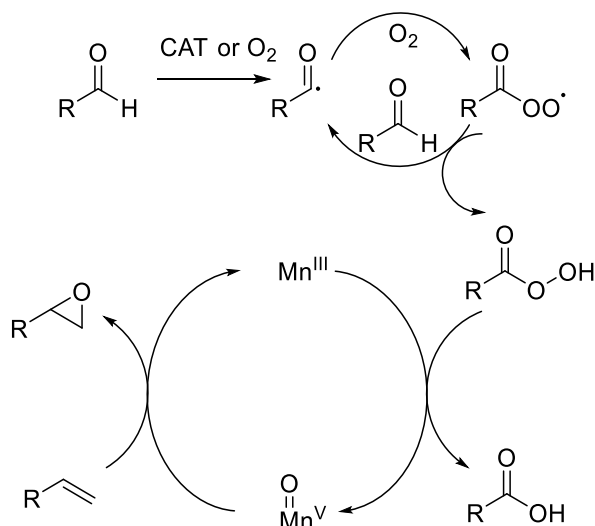
The studies continued with the catalytic epoxidation of methyl eugenol (**2.1**) using molecular oxygen as the oxidant (Mukaiyama epoxidation). Manganese (III) 5,10,15,20-tetra(2,6-dichlorophenyl)porphyrin (**CAT1**) was used as the model catalyst based on our previous experience regarding its high activity and stability towards oxidation.⁴⁷

This reaction requires the use of a sacrificial co-reductant, which is usually an alkyl aldehyde prone to be easily oxidized during the reaction. The most commonly used sacrificial co-reductant are isobutyraldehyde or 2-ethylhexanal.^{48, 49} In our studies, we selected the first one – isobutyraldehyde. In a typical reaction, in a glass vial, methyl eugenol **2.1**, 5 equivalents of isobutyraldehyde and 2 mol% of **CAT1** were dissolved in 2 mL of CH₃CN. Then, pure molecular oxygen was bubbled through the solution for over 90 minutes at 25 °C (Scheme 2.14). After GC analysis 60% conversion was obtained, with 47% selectivity for the formation of the desired epoxide **2.4**, whose structure was confirmed by GC-MS, in a complex mixture of products and side-products.



Scheme 2.14. Mukaiyama epoxidation reaction of methyl eugenol (**2.1**) under batch conditions.

The catalytic cycle for the oxygen-based epoxidation (Scheme 2.15) is widely known. It was well described by Feiters and coworkers,⁵⁰ that a peroxyacid species, formed in the presence of molecular oxygen and the aldehyde, is assumed to act as an oxygen donor to generate the high-valent Mn(V)-oxo intermediate, which operates as the catalytically active epoxidation species.⁵¹⁻⁵³



Scheme 2.15. Epoxidation catalytic cycle for manganese-based catalysts using oxygen as oxidant and an aldehyde as co-reductant.

The presence of the Mn(V) porphyrin oxo-species was demonstrated by a UV-Vis spectroscopy experiment, in which we dissolved the porphyrin MnOAcTDCPP (**CAT1**) in CH₂Cl₂, and added a few droplets of isobutyraldehyde. Then, oxygen was bubbled into the solution and the UV-Vis spectra were taken for each step (Figure 2.13). As we can clearly observe, when isobutyraldehyde is added, the UV-Vis spectrum of the metalloporphyrin MnOAcTDCPP (**CAT1**) remains unchanged. However, after bubbling molecular oxygen, the spectrum presents a blue-shifted Soret band at 425.5 nm, characteristic of Mn(V)porphyrin oxo-species.^{54, 55}

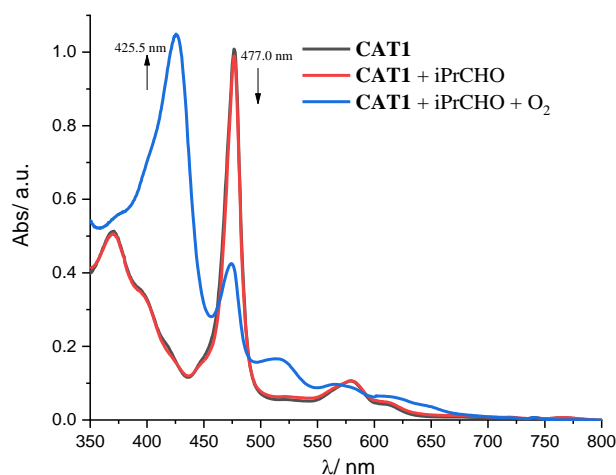


Figure 2.13. Spectra of **CAT1** (Black), **CAT** and isobutyraldehyde before bubbling oxygen (Red) and after bubbling oxygen through the solution (Blue), all spectra were taken at 25 °C using CH_2Cl_2 .

2.3.3. Catalytic epoxidations using hydrogen peroxide as oxidant

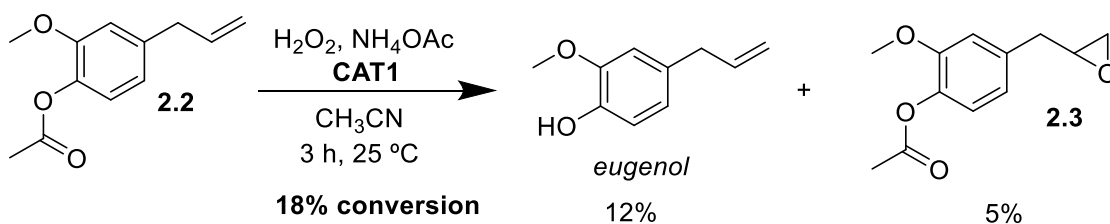
We then decided to use hydrogen peroxide as an alternative green oxidant. This type of system requires a co-catalyst instead of a co-reductant. The co-catalyst is necessary for the dehydration of hydrogen peroxide bound to the manganese to produce the active oxo-species. In our studies, we use ammonium acetate or imidazole as co-catalysts since these are the most commonly used co-catalysts reported so far.

Batch system

In a typical batch reaction, in a round-bottom flask, 0.5 mol of methyl eugenol **2.1**, 2 mol% of catalyst and 0.5 equivalents of co-catalyst were dissolved in acetonitrile. Then, 4 equivalents of 35% hydrogen peroxide diluted 1:10 in acetonitrile, were loaded into a syringe pump, this solution was slowly injected in to the reaction mixture over 30 minutes. After 3 hours, we took a sample from the reaction, neutralized it with sodium bisulfate and removed the water with anhydrous sodium sulfate, filtered the solution, and injected it into a gas chromatograph. Once again, the catalytic system **CAT1** was first validated in the catalytic epoxidation of model olefin substrates such as styrene and 1-octene, using imidazole as co-catalyst. In these reactions, close to full conversions were obtained after

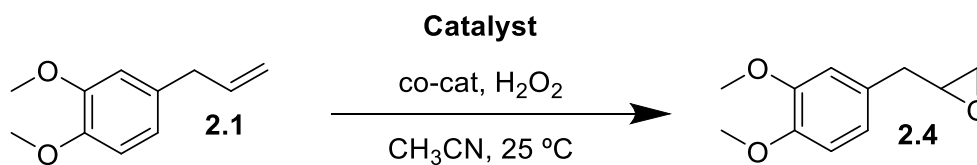
1 h and 3 h, respectively, in both cases with >95 % selectivity for the formation of the corresponding epoxides.

Following our goals, we proceeded with the catalytic epoxidation of eugenol acetate **2.2**, using **CAT1** as catalyst and ammonium acetate as co-catalyst. However, a conversion of 18 % was obtained in 3 h, and the desired epoxide product was formed in just 5%, with the main product formed being eugenol (12%), resultant from hydrolysis of the acetyl group under these acidic conditions (Scheme 2.16).



Scheme 2.16. Epoxidation of acetyleugenol using **CAT1** and hydrogen peroxide as oxidant.

To avoid this problem, the methyl eugenol derivative **2.1**, having a more stable methyl ether substituent, was used as model substrate in the following reactions to evaluate the catalytic activity and the effect of the co-catalyst in the reaction activity and selectivity. The results are summarized in the table 2.5.

Table 2.5. Olefin epoxidation using hydrogen peroxide.

Entry	Catalyst	Co-catalyst	Oxidant (Eq.)	Time (h)	Conversion (%)
1	CAT1	NH ₄ OAc	2	3	27
2		NH ₄ OAc	4	3	34
3		imidazole	2	3	53
4		imidazole	4	3	83
5	CAT1@NH-SiO₂	imidazole	4	24	13

Reaction conditions: 0.5 mmol of **2.1**, **CAT1** (1 μmol) or **CAT1@NH-SiO₂** (100 mg), 0.25 mmol co-catalyst, 2 mL CH₃CN, 35% hydrogen peroxide diluted in 1:10 in CH₃CN (slowly added over 30 minutes), conversion calculated using GC-FID.

Selectivity for epoxides was > 94% in all cases.

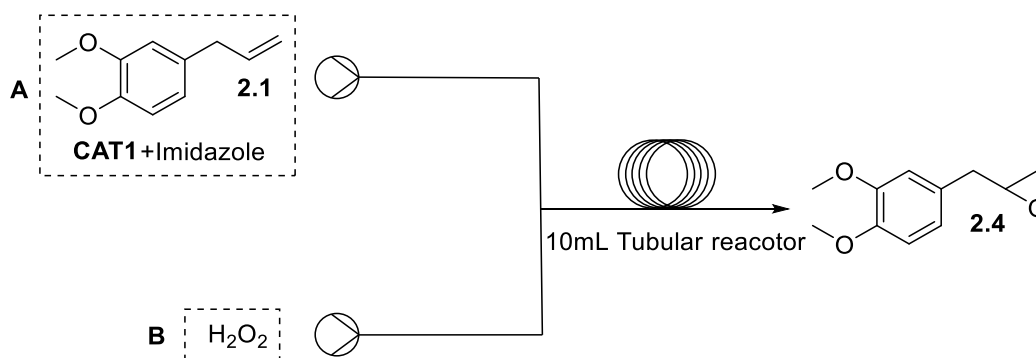
The epoxidation of methyl eugenol (**2.1**) was first carried out using the MnOAcTDCPP (**CAT1**) as catalyst, ammonium acetate as co-catalyst (0.5 eq) and 2 equivalent of H₂O₂. In this reaction, 27% conversion was obtained in 3 h, with full selectivity for the epoxide formation (Table 2.5, Entry 1). Another reaction was done, under the same conditions but using 4 equivalents of oxidant, which resulted in 36% conversion after 3 hours (Table 2.5, Entry 2). The reaction was extended for two additional hours but no further conversion was observed. Then, we studied the effect of changing the co-catalyst from ammonium acetate to imidazole. Under the conditions previously described, but using 0.5 equivalents of imidazole and 2 equivalent of H₂O₂, 53% conversion was achieved in 3 hours, which is twice the value of the conversion obtained using ammonium acetate as the co-catalyst under similar conditions (Table 2.5, Entries 1 and 3). Finally, using 4 equivalents of peroxide, we achieved 83% conversion within 3 hours (Table 2.5, Entry 4) demonstrating the need an excess of H₂O₂. We also evaluated the heterogeneous **CAT1@NH-SiO₂** as catalyst, using 4 equivalents of peroxide and imidazole as co-catalyst, but at the end of 24 hours, only 13% conversion was observed through GC-FID. The catalyst was easily recovered after the reaction by centrifugation but reutilization studies have not been carried out, since the conversion

was low. Optimization studies to improve the catalyst activity and perform the reutilization of the catalyst are currently underway.

Continuous-flow system

After optimizing this reaction in batch, we have then transposed the best conditions (Table 2.5, Entry 4) to a continuous-flow methodology. For that, two solutions were prepared, the first one was methyl eugenol (**2.1**) with 2 mol% of **CAT1** and 0.5 eq. of imidazole in CH₃CN (Solution A), and another solution of hydrogen peroxide dissolved in CH₃CN in concentrations ranging from 1.75% to 35% (Solution B). The results are presented in table 2.6.

Table 2.6. Epoxidation of methyl eugenol (**2.2**) with **CAT1** and imidazole.

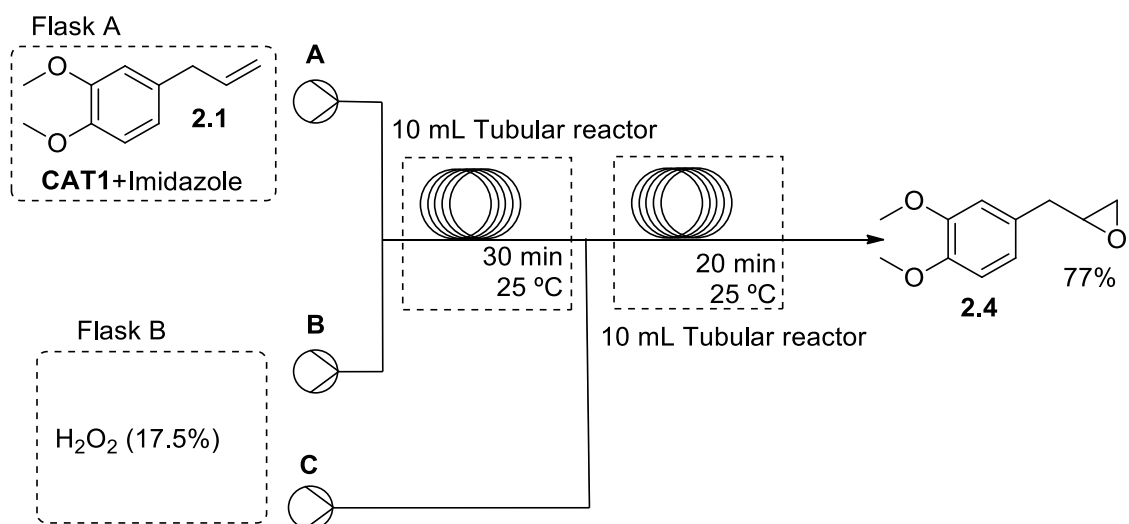


Entry	Residence time (min)	Stock solution H ₂ O ₂ (%)	Volumetric ratio (A:B)	H ₂ O ₂ equivalents	Conversion (%)	STY (g min ⁻¹ dm ⁻³)
1	5	1.75	1:1	2	7	0.28
2	25	1.75	1:1	2	20	0.16
3	50	1.75	1:1	2	21	0.08
4	50	3.5	1:1	4	30	0.12
5	30	3.5	1:1.5	6	27	0.11
6	30	17.5	1:0.5	10	40	0.32
7	30	17.5	1:1	20	35	0.14

Reaction conditions: 0.23 M methyleugenol (**2.1**), CH₃CN as solvent, 2 mol% **CAT1**, 50 mol% imidazole, T = 25 °C. Selectivity forepoxides was higher than 94% for **2.4** in all cases.

First, we used a 1.75% stock solution of hydrogen peroxide in CH₃CN. With a volumetric ratio of 1:1, the molar ratio of this solution is of 2 equivalents of peroxide. We used 5 minutes residence time at 25 °C, which was analyzed *via* GC, obtaining 7% conversion for epoxide (Table 2.6, entry 1). Next, we increased the residence time to 25 minutes, which resulted in *ca.* 20% conversion towards the epoxide (Table 2.6 entry 2). Even using a residence time of 50 min, under the same conditions, a similar conversion value (21%) was obtained (Table 2.6 entry 3), which led us to conclude that the 2 equivalents of peroxide were fully consumed after 25 min. Therefore, we increased the peroxide stock solution concentration to 3.5% and performed a 50 minute reaction with 4 equivalents peroxide, which resulted in 30% conversion (Table 2.6 entry 4). Before increasing the peroxide concentration, we decided to increase the volumetric ratio of the peroxide, using 1:1.5 ratio of olefin solution to hydrogen peroxide solution. In the previous experiments, we used the minimal flow rate for both reagents to maximize the residence time, which was 50 minutes. Due to the equipment limitation of operating with a minimum flow rate of 100 μL/min, the increment of the stock solutions volumetric ratio leads to a decrease in residence time. With a volumetric ratio of 1:1.5 the maximum residence time for a 10 mL reactor is approximately 30 minutes. Therefore, a volumetric ratio of 1:1.5 allowed us to use a higher amount of hydrogen peroxide (6 equivalents), but with 30 minutes residence time. However, in this experiment we only achieved 27% conversion (Table 2.6 entry 5). Then, we further increased the peroxide stock solution concentration to 17.5% using a 1:0.5 A/B volumetric ratio, which allows to use 10 equivalents of H₂O₂ with a residence time of 30 minutes, achieving 40% conversion (Table 2.6 entry 6). A final experiment was carried out by increasing the A/B volumetric ratio to 1:1, which allowed to use 20 equivalents of H₂O₂. However, using 30 minutes residence time, we achieved a slightly lower conversion of 35% (Table 2.6 entry 7).

To further increase the maximum residence time, we connected another 10 mL reactor (Scheme 2.17). In this experiment, we used the 17.5% peroxide stock solution that was added in two stages, at the start of the reaction with a volumetric ratio of A:B of 1:0.5 and then adding another A:C 1:0.5 volumetric ratio before entering the second reactor.



Scheme 2.17. Epoxidation reaction of **2.1** under flow condition using two 10 mL tubular reactors.

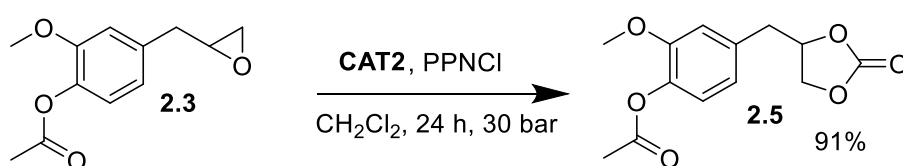
This system allowed to extend the residence time to 50 minutes (30 + 20), and a remarkable conversion of 77% was obtained. As two 10 ml reactors are required, the STY of this process is $0.31 \text{ g min}^{-1} \text{ dm}^{-3}$ despite having a 77% conversion. A similar output of **2.4** would be achieved under batch conditions with a reactor larger than 40 L.

2.4. Synthesis of acetyeugenol cyclic carbonate

In this subchapter are described the synthesis of acetyeugenol cyclic carbonates using CO₂ as a building block. Two different approaches were taken, first the cycloaddition of CO₂ to epoxides using a chromium porphyrin catalyst (**CAT2**), second is the use of a bromating agent for the creation bromohydrin intermediates from olefins and epoxides, capable of reacting with CO₂ for the cyclisation into a cyclic carbonate.

2.4.1. Cycloaddition of CO₂ to epoxides

After optimizing the epoxidation reaction, we proceeded the studies with the CO₂ cycloaddition to acetyeugenol epoxide **2.3** using **CAT2** as catalyst. In a high-pressure stainless steel reactor were introduced 0.2 mol% of **CAT2** (10 μmol) as catalyst and 0.2 mol% of PPNCI (10 μmol) as co-catalyst, CH₂Cl₂ as solvent and the respective epoxide **2.3** (4.6 mmol). The reactor was then closed and pressurized with 30 bar of high purity CO₂ gas, heated until 80 °C and left for 24 hours under stirring (Scheme 2.18). After that period the resulting liquid was analyzed by GC-FID, obtaining full conversion and >99% selectivity for the desired cyclic carbonate **2.5**. Silica-gel chromatography was done to remove the catalyst and co-catalyst, using CH₂Cl₂ as eluent. The solvent was then evaporated under reduced pressure, resulting in a pale-yellow powder in 91% isolated yield.



Scheme 2.18. Carbon dioxide cycloaddition to acetyeugenol epoxide.

After purification the obtained eugenol derivative cyclic carbonate **2.5** was characterized by ¹H NMR, ¹³C NMR and HRMS(ESI) (Figures 2.14, 2.15 and 2.16 respectively). Additionally, complete proton and carbon spectral assignment was performed using 2D NMR data (see annex) and described in the experimental chapter.

The ¹H NMR spectrum (Figure 2.14) presents three signals in the typical aromatic region, at δ = 6.99 ppm (J= 8.0 Hz), a doublet is observed and is attributed to the H6

proton. At $\delta = 6.83$ ppm ($J = 1.7$ Hz) another doublet is present, which was attributed to the H3 position, and a double doublet at $\delta = 6.78$ ($J = 8.0, 1.9$ Hz) was attributed to the last proton of the aromatic proton H5. Next, a pentet ($J = 6.5$ Hz) signal is observed at $\delta = 4.91$ ppm assigned to the H2''' proton. Right after at $\delta = 4.46$ ppm ($J = 8.2$ Hz) a triplet is presented, attributed to the proton H3''' from the cyclic carbonate group, followed by a signal $\delta = 4.15$ ppm with a double doublet multiplicity ($J = 8.6, 6.8$ Hz) assigned to a proton at the same position, H3'''. At $\delta = 3.82$ ppm is observed another singlet signal assigned to the methoxy group protons H1''. At $\delta = 3.11$ and 2.96 ppm, ($J = 14.4, 6.5$ Hz and $J = 14.3, 6.2$ Hz respectively) a pair of double doublets is observed, assigned to H1''' proton. Finally, at $\delta = 2.30$ ppm a singlet signal assigned CH₃ protons from the acetyl group H2' is located.

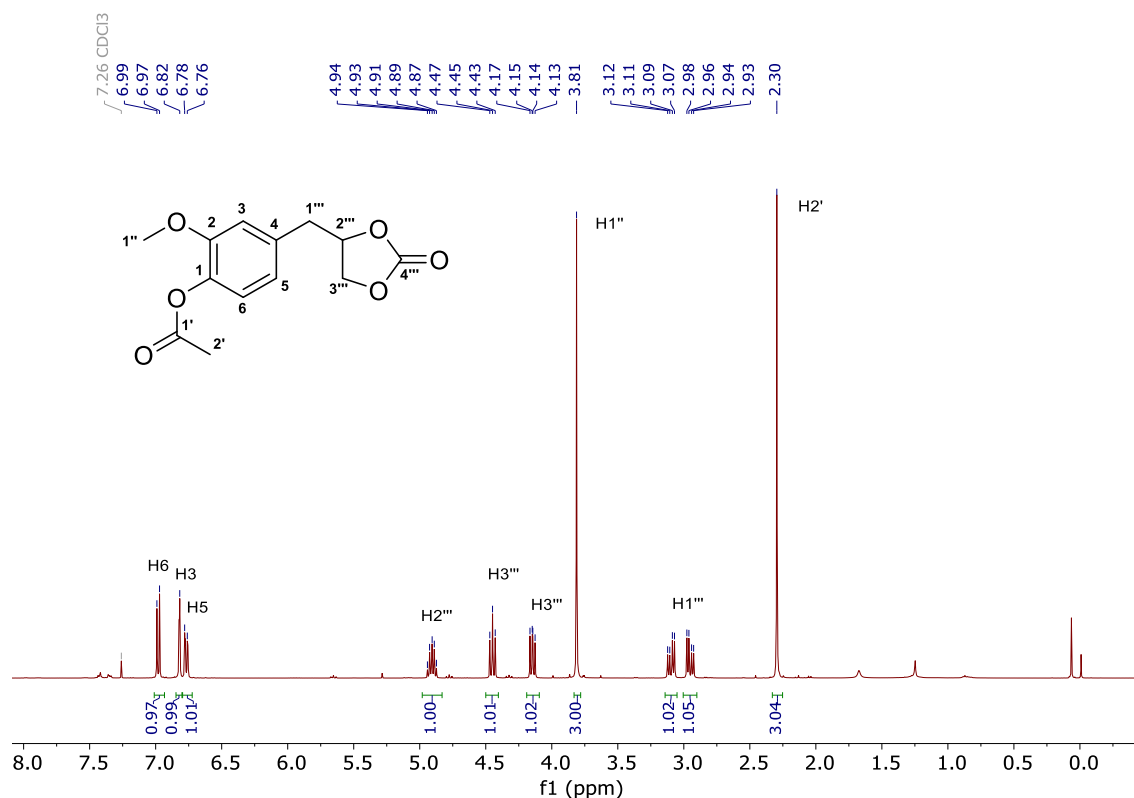


Figure 2.14. ¹H NMR of 2.5 done in CDCl₃ at 25 °C.

A similar analysis can be performed to the ¹³C NMR spectrum (Figure 2.15). Starting from the last signals at $\delta = 169.1$ and 154.8 ppm which were attributed to the C1' and C4''' carbons, as they are very typical signals for this kind of carbons. Next at $\delta =$

151.4 - 113.5 ppm are located all the signals assigned to the aromatic ring carbons C1-C6. At $\delta = 76.8$ ppm, overlapping with the chloroform signal, is a signal attributed to the C2''', followed by a signal at $\delta = 68.6$ ppm attributed to the neighbor carbon C3'''. At $\delta = 56.0$ ppm is a signal assigned to the methoxy group carbon C1'', followed, at $\delta = 39.5$ ppm is a signal assigned to the alkyl C1''' carbon. Finally, at $\delta = 20.7$ is the last signal assigned to the acetyl group C2' carbon.

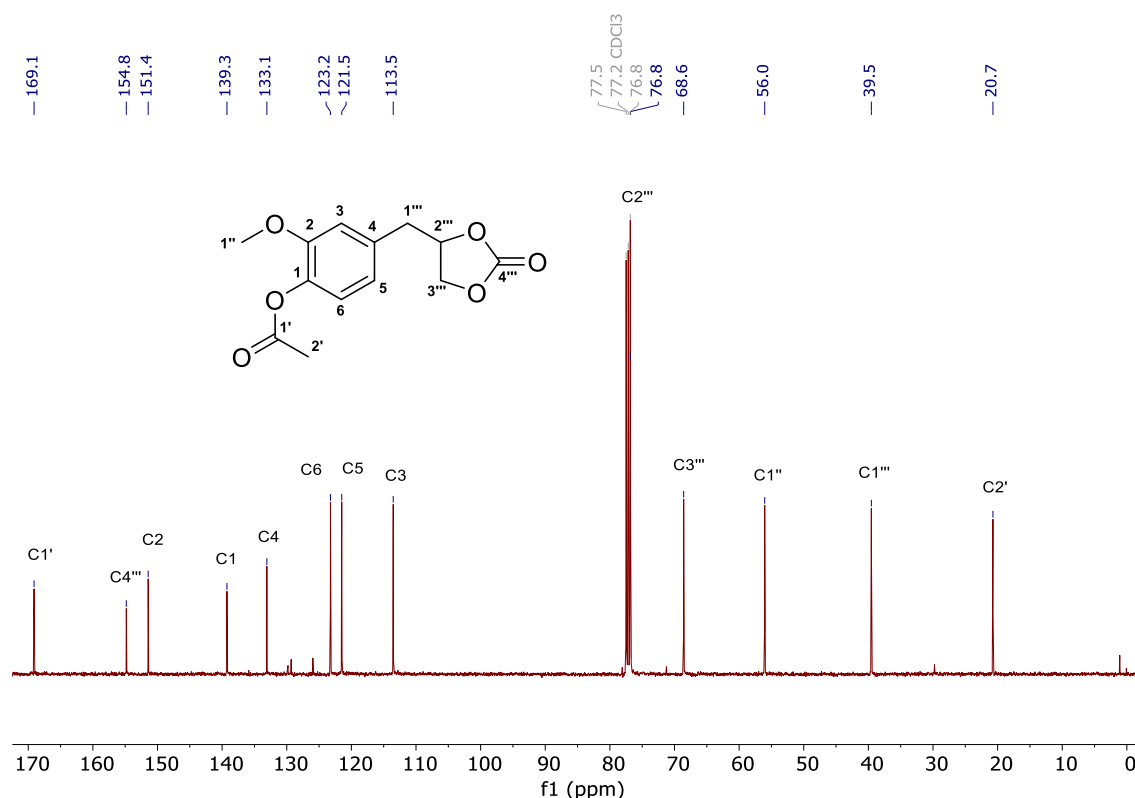


Figure 2.15. ^{13}C NMR of **2.5**, performed at 25 °C using CDCl_3 as solvent.

Additionally, **2.5** was also analyzed through electron spray ionization (ESI) high resolution mass spectrometry (HRMS), showing two major signals, one corresponding to the molecular ion and sodium $[\text{M}+\text{Na}]^+$ at $m/z = 289.0683$ (theoretical value calculated for $\text{C}_{13}\text{H}_{14}\text{O}_6\text{Na}^+$ is $m/z = 289.0688$), and the second signal at $m/z = 555.1473$ which we presume to correspond to the formation of a dimeric specie $[2\text{M}+\text{Na}]^+$ (theoretical value calculated for $\text{C}_{26}\text{H}_{28}\text{O}_{12}\text{Na}^+$ is $m/z = 555.1478$).

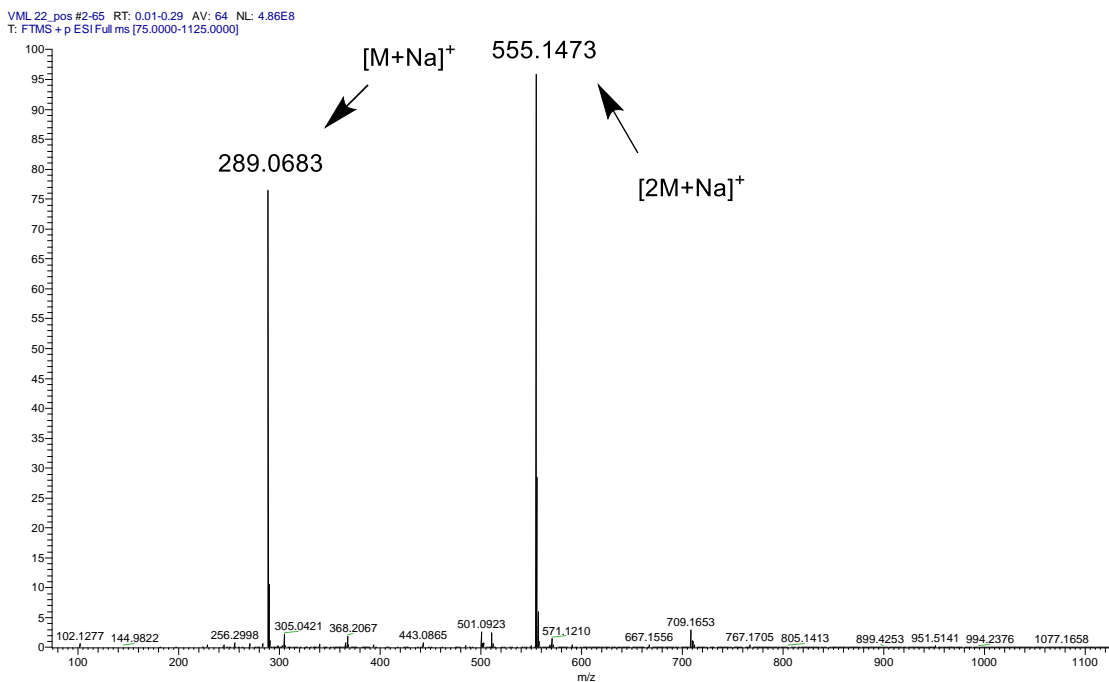


Figure 2.16. HRMS (ESI) spectrum of **2.5**.

As discussed in the introduction of this thesis (chapter 1), the evaluation of the toxicity of compounds to be applied in the fragrance and flavor industry is of high importance. Therefore, the studies continued with the evaluation of acetyeugenol carbonate (**2.5**) cytotoxicity.

This study was conducted using MCF-12A (normal healthy breast cells) and MTT (3-(4,5-dimethylthiazol-2-yl)-2,5-diphenyltetrazolium bromide) assay. For that we used an aqueous solution of **2.5** with 1% DMSO, and tested the toxicity at 3 different concentrations, 200 mM, 100 mM and 50 mM analyzing the results after adding the compound at 4 and 24 hours, in triplicate. All concentration were compared to a control group which had no acetyeugenol cyclic carbonate (**2.5**) and the results are presented in Figure 2.17.

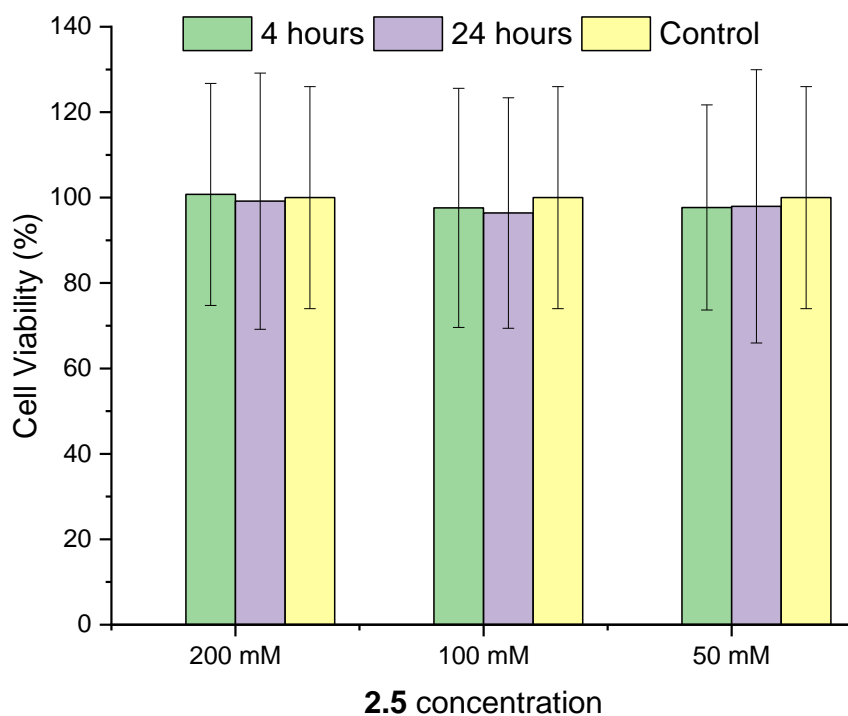


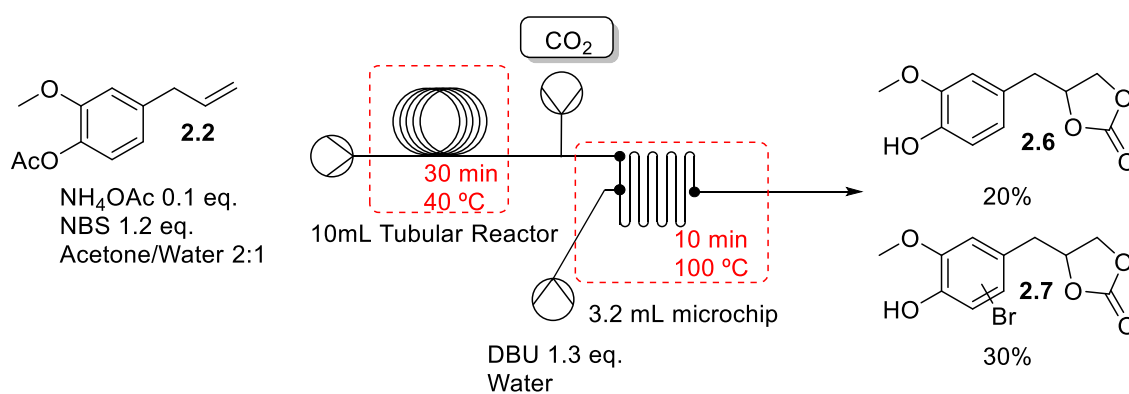
Figure 2.17. Toxicity assays of **2.5** in human breast cells using 200 mM, 100 mM and 50 mM.

From Figure 2.16, we conclude that acetylugenol cyclic carbonate (**2.5**) does not present toxicity in the selected concentration range, (200, 100 and 50 mM), as no statistical difference from the control group was observed. Through this experiment we can conclude that acetylugenol cyclic carbonate is not toxic, and so, fulfills the absence of toxicity requirement to be applied in fragrances.

2.4.2. Oxidative carboxylation

Pursuing the objective of synthesizing cyclic carbonates using sustainable methodologies we evaluated the possibility of the implementation of a sequential process involving the direct transformation of a protected eugenol derivative to the corresponding cyclic carbonate. After a careful inspection of the reported methodologies we selected a sustainable continuous flow oxidative carboxylation of olefins using a mixture of 2:1 acetone and water and stoichiometric amounts of NBS as bromination reagent described by Timothy Jamison.⁵⁶

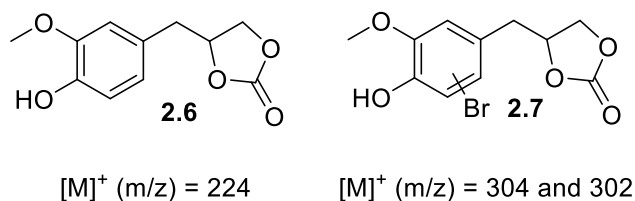
For that, two solutions were prepared: one with acetyleugenol (**2.2**) (0.33M), NBS (0.40M) and ammonium acetate (0.33M) in water and acetone 1:2 and another with DBU in water (0.43M). The reaction was carried out using two reactors, one 10 mL tubular reactor where the solution of **2.2**, NBS and ammonium acetate flows with a residence time of 30 min at 40 °C followed by addition of CO₂ and the solution of DBU in a second reactor, chip size (1.7 mL), with a residence time of 10 min at 100 °C. The flow stream was then collected and after solvent extraction with CH₂Cl₂ a sample of the reaction crude was analyzed by GC-FID and ¹H NMR. The results revealed a complex mixture of products, from which we can observe full consumption of the starting material (**2.2**) with 50% chemoselectivity for cyclic carbonates (Scheme 2.19).



Scheme 2.19. Bromohydration of **2.2** followed by CO₂ addition.

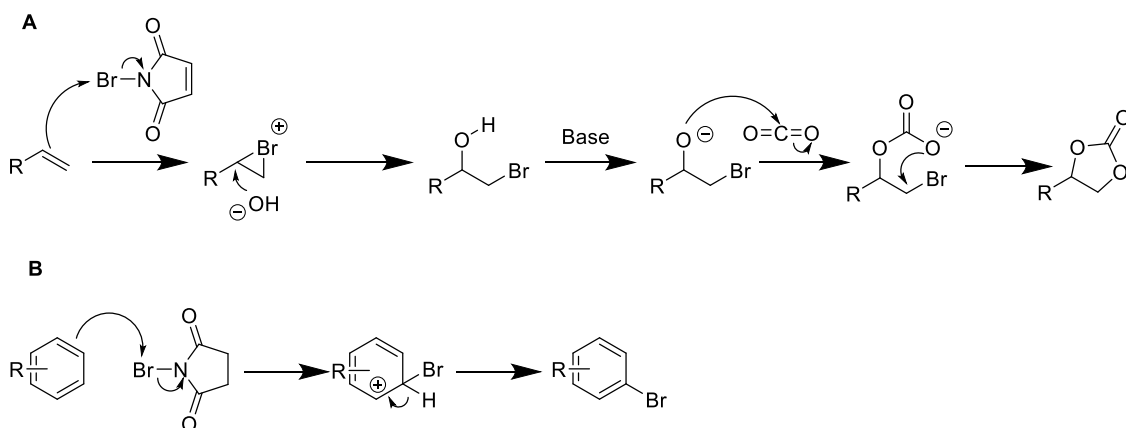
The major reaction products are **2.6** resulting from the expected CO₂ addition reaction with acetyl group hydrolysis and **2.7** resulting from de aromatic bromination of **2.6**. The structure of these molecules was disclosed using GC-MS analysis of the reaction crude. The obtained chromatogram revealed two major peaks, one with a mass spectrum showing a molecular ion corresponding to the **2.6** cyclic carbonate ($m/z = 224$) differing from the previously obtained acetyl-protected cyclic carbonate **2.5** ($m/z = 266$) by the acetyl group mass. Additionally, the presence of the base peak characteristic of the eugenol derivatives at $m/z = 137$ and respective fragments are observed. The analysis of the mass spectra of the other signal revealed a molecular ion with $m/z = 304$ followed by a characteristic peak at $m/z = 302$ with the same intensity, typical of bromide-containing molecules. Additionally, the spectrum shows a peak at $m/z = 217$ and 215 revealing the presence of the bromine atom in the aromatic fragment of the eugenol structure. These spectral data are in accordance with the proposed structure of **2.7** (Scheme 2.20). From

the combination of the ^1H NMR and GC-MS data we were able to identify the major reaction products as **2.6** and **2.7** obtained in 20% and 30% yield, respectively.



Scheme 2.20. Cyclic carbonate and bromohydrin species found through GC-MS analysis.

From the GC-MS analysis we also were able to identify some of the minor signal as the bromohydrin intermediates. This reaction mechanism follows a well-known mechanism, which starts from the bromonium ion generation, which is then attacked by a water molecule, creating the bromohydrin intermediate. Then, the intermediate reacts with the carbon dioxide through a nucleophilic attack of the bromohydrin oxygen activated by base, resulting in cyclization by eliminating the bromide to yield the cyclic carbonate (Scheme 2.21A).⁵⁷ Additionally, the formation of the aryl bromide eugenol derivative can be explained by the occurrence of the aromatic electrophilic substitution in the presence of the N-Bromosuccinimide (Scheme 2.21B).⁵⁸



Scheme 2.21. A) Oxybromination methodology mechanism for the synthesis of cyclic carbonates. B) Aromatic electrophilic substitution in the presence of the NBS.

These preliminary results present promising perspectives for the implementation of continuous flow processes for direct preparation of eugenol-derivative cyclic carbonates starting from eugenol. Optimization studies are currently underway.

2.5. Conclusion and future perspectives

The flavor and fragrance industry (F&F) is one of the biggest industries in the world being also one of the most regulated. There is a constant need to develop new molecules and sustainable synthetic processes as the regulations became strict and every year more and more molecules are banned from this market due to safety concerns. In this context, we were interested in developing new natural-based derivatives to be applied in this sector, using new sustainable approaches regarding their synthesis. Therefore, this work is focused on the synthesis of eugenol cyclic carbonate derivatives as a potential F&F compound, using green methodologies and continuous flow conditions.

The study started with the synthesis of the catalysts, which were used in the epoxidation reaction and the CO₂ cycloaddition. Two porphyrin-type ligands were selected and synthesized using the nitrobenzene methodology, the **TDCPP** and *p*-**CF₃TPP**, with 5% and 14% yields respectively. The **TDCPP** ligand was complexed with manganese (II) acetate, which resulted in **CAT1** with 88% yield, while *p*-**CF₃TPP** was complexed with chromium (II) chloride resulting in **CAT2** with 64% yield. Additionally, **CAT1** was immobilized onto amine-functionalized silica particles, using a methodology based on chlorosulfonation of **TDCPP** followed by nucleophilic substitution and preparation of the manganese metal complex, resulting in a solid material with 2.75×10^{-5} mol of manganese per gram of material (**CAT1@NHSiO₂**).

To prepare the desired eugenol cyclic carbonates we started the studies with the optimization of eugenol hydroxy group protection to prevent any possible reaction of the hydroxyl group in the further reaction steps. As protecting groups, we chose the methyl and the acetyl group, prepared under conventional batch and flow conditions. The methylation was performed using iodomethane and potassium carbonate, achieving 74% isolated yield. The acetylation reaction was done using sulfuric acid or K10 as catalysts. With sulfuric acid we achieved full conversion in batch conditions and 83% conversion under continuous flow conditions. When using K10 full conversion was achieved in both batch and continuous flow systems, being the use of continuous flow more efficient as it can produce more material per minute than the batch system under similar conditions.

Next, the resulting eugenol derivatives were used as starting material in the epoxidation of the olefin group. For that different methodologies were employed, one used organic peroxy acids, other uses hydrogen peroxide or molecular oxygen and the metalloporphyrins-based catalysts (**CAT1** and **CAT1@NHSiO₂**). In the first methodology, we used acetyeugenol as substrate and achieved 93% conversion under batch conditions and 83% under continuous flow. For the generation of high valent oxo-manganese species we used **CAT1** as catalyst, and two different oxygen donors, oxygen and hydrogen peroxide. The use of hydrogen peroxide showed to be more efficient so we proceeded with the studies using this oxidant as reagent. Using imidazole as co-catalyst, we achieved 83% conversion in batch and 77% conversion under optimized continuous flow conditions. This reaction was also done using **CAT1@NHSiO₂** as catalyst achieving only 13% conversion.

Finally, we prepared acetyeugenol cyclic carbonate (**2.5**) using acetyeugenol epoxide (**2.3**) as substrate and CO₂ as building block. For that we used **CAT2** catalyst, PPnCl as co-catalyst and 30 bar CO₂ pressure, which resulted in full conversion and >99% selectivity for the desired eugenol cyclic carbonate, which was then fully characterized using ¹H NMR, ¹³C NMR, 2D NMR and HRMS (ESI) analysis. The toxicity of this compound was characterized using MTT assay, which indicated that put compound **2.5** is not toxic at 200 mM after 4 and 24 hours of exposure. Additionally, in a tentative to improve the synthetic route sustainability, we also performed some preliminary studies on the sequential synthesis of cyclic carbonates from olefins, using the bromohydration methodology. We achieved 50% yield for cyclic carbonate under continuous flow conditions, although it should be mentioned that the system needs more optimization, as under the used condition the major product results from the aromatic ring bromination of the cyclic carbonate (30% yield).

In conclusion, we successfully synthesized and characterized the acetyeugenol cyclic carbonate in high yields, using green methodologies and continuous flow conditions, suitable for scale-up of the synthetic procedures. The preliminary biological studies showed promising results as the compound showed no toxicity at all.

As future perspectives, we intend to perform the hydroformylation reaction on eugenol derivatives under continuous flow conditions, as the aldehyde type compounds are well known in the F&F industry and can be further modified into useful groups such as acetals and carboxylic acids (Figure 2.18).

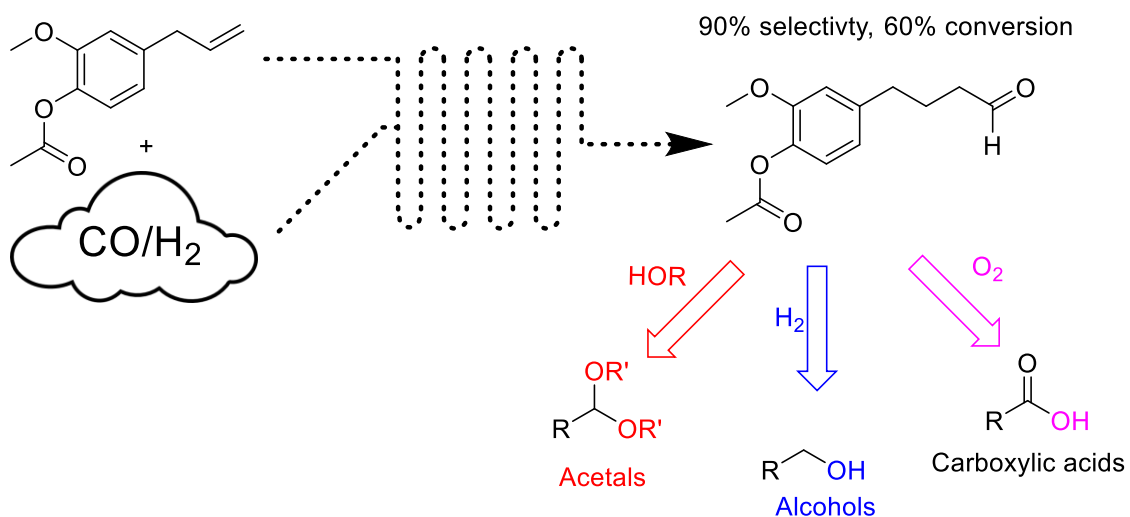


Figure 2.18. Future perspectives in eugenol modification.

2.7. References

1. Khalil, A. A.; Rahman, U. u.; Khan, M. R.; Sahar, A.; Mehmood, T.; Khan, M., Essential Oil Eugenol: Sources, Extraction Techniques And Nutraceutical Perspectives. *RSC Advances* **2017**, 7 (52), 32669-32681.
2. Kliszcz, A.; Danel, A.; Puła, J.; Barabasz-Krasny, B.; Możdżeń, K., Fleeting Beauty—The World Of Plant Fragrances And Their Application. *Molecules* **2021**, 26 (9), 2473.
3. Taleuzzaman, M.; Jain, P.; Verma, R.; Iqbal, Z.; Mirza, M. A., Eugenol As A Potential Drug Candidate: A Review. *Current topics in medicinal chemistry* **2021**, 21 (20), 1804-1815.
4. Pramod, K.; Ansari, S. H.; Ali, J., Eugenol: A Natural Compound With Versatile Pharmacological Actions. *Natural product communications* **2010**, 5 (12), 1999-2006.
5. Mohammadi Nejad, S.; Özgüneş, H.; Başaran, N., Pharmacological And Toxicological Properties Of Eugenol. *Turkish journal of pharmaceutical sciences* **2017**, 14 (2), 201-206.
6. Barboza, J. N.; da Silva Maia Bezerra Filho, C.; Silva, R. O.; Medeiros, J. V. R.; de Sousa, D. P., An Overview On The Anti-Inflammatory Potential And Antioxidant Profile Of Eugenol. *Oxidative medicine and cellular longevity* **2018**, 2018, 3957262.
7. Zari, A. T.; Zari, T. A.; Hakeem, K. R., Anticancer Properties Of Eugenol: A Review. **2021**, 26 (23), 7407.
8. Carvalho, R. P. R.; Lima, G. D. d. A.; Machado-Neves, M., Effect Of Eugenol Treatment In Hyperglycemic Murine Models: A Meta-Analysis. *Pharmacological Research* **2021**, 165, 105315.
9. Aburel, O. M.; Pavel, I. Z.; Dănilă, M. D.; Lelcu, T.; Roi, A.; Lighezan, R.; Muntean, D. M.; Rusu, L. C., Pleiotropic Effects of Eugenol: The Good, The Bad, And The Unknown. *Oxidative medicine and cellular longevity* **2021**, 2021, 3165159.
10. Api, A. M.; Belsito, D.; Biserta, S.; Botelho, D.; Bruze, M.; Burton, G. A.; Buschmann, J.; Cancellieri, M. A.; Dagli, M. L.; Date, M.; Dekant, W.; Deodhar, C.; Fryer, A. D.; Gadhia, S.; Jones, L.; Joshi, K.; Lapczynski, A.; Lavelle, M.; Liebler, D. C.; Na, M.; O'Brien, D.; Patel, A.; Penning, T. M.; Ritacco, G.; Rodriguez-Roper, F.; Romine, J.; Sadekar, N.; Salvito, D.; Schultz, T. W.; Siddiqi, F.; Sipes, I. G.; Sullivan, G.; Thakkar, Y.; Tokura, Y.; Tsang, S., RIFM Fragrance Ingredient Safety

Assessment, 2-Methoxy-4-Propylphenol, CAS Registry Number 2785-87-7. *Food and Chemical Toxicology* **2021**, *149*, 111853.

11. Mateen, S.; Rehman, M. T.; Shahzad, S.; Naeem, S. S.; Faizy, A. F.; Khan, A. Q.; Khan, M. S.; Husain, F. M.; Moin, S., Anti-Oxidant And Anti-Inflammatory Effects Of Cinnamaldehyde And Eugenol On Mononuclear Cells Of Rheumatoid Arthritis Patients. *European Journal of Pharmacology* **2019**, *852*, 14-24.
12. Rajput, J.; Bagul, S.; Karandikar, P., Outlooks On Medicinal Properties Of Eugenol And Its Synthetic Derivatives. *Natural Products Chemistry & Research* **2016**, *4*, 1-6.
13. Eugenol Synth. <https://www.solvay.com/en/brands/eugenol-synth> (accessed 05/08/2022).
14. Groves, J. T.; Nemo, T. E.; Myers, R. S., Hydroxylation And Epoxidation Catalyzed By Iron-Porphine Complexes. Oxygen Transfer From Iodosylbenzene. *Journal of the American Chemical Society* **1979**, *101* (4), 1032-1033.
15. Maux, P. L.; Srour, H. F.; Simonneaux, G., Enantioselective Water-Soluble Iron-Porphyrin-Catalyzed Epoxidation With Aqueous Hydrogen Peroxide And Hydroxylation With Iodobenzene Diacetate. *Tetrahedron* **2012**, *68* (29), 5824-5828.
16. Srour, H.; Maux, P. L.; Simonneaux, G., Enantioselective Manganese-Porphyrin-Catalyzed Epoxidation And C-H Hydroxylation With Hydrogen Peroxide In Water/Methanol Solutions. *Inorganic Chemistry* **2012**, *51* (10), 5850-5856.
17. Stephenson, N. A.; Bell, A. T., Mechanistic Insights Into Iron Porphyrin-Catalyzed Olefin Epoxidation By Hydrogen Peroxide: Factors Controlling Activity And Selectivity. *Journal of Molecular Catalysis A: Chemical* **2007**, *275* (1), 54-62.
18. Ren, Q.-G.; Chen, S.-Y.; Zhou, X.-T.; Ji, H.-B., Highly Efficient Controllable Oxidation Of Alcohols To Aldehydes And Acids With Sodium Periodate Catalyzed By Water-Soluble Metalloporphyrins As Biomimetic Catalyst. *Bioorganic & Medicinal Chemistry* **2010**, *18* (23), 8144-8149.
19. Meunier, B., Metalloporphyrins As Versatile Catalysts For Oxidation Reactions And Oxidative DNA Cleavage. *Chemical Reviews* **1992**, *92* (6), 1411-1456.
20. Gonsalves, A. M. d. A. R.; Varejão, J. M. T. B.; Pereira, M. M., Some New Aspects Related To The Synthesis Of Meso-Substituted Porphyrins. *Journal of Heterocyclic Chemistry* **1991**, *28* (3), 635-640.

21. Johnstone, R. A. W.; Nunes, M. L. P. G.; Pereira, M. M.; D'A. Rocha Gonsalves, A. M.; Serra, A. C., Improved Syntheses of 5,10,15,20-Tetrakisaryl- and Tetrakisalkylporphyrins. *ChemInform* **1996**, 27 (46), 1423-1437.
22. Cuesta-Aluja, L.; Castilla, J.; Masdeu-Bulto, A. M.; Henriques, C. A.; Calvete, M. J. F.; Pereira, M. M., Halogenated Meso-Phenyl Mn(III) Porphyrins As Highly Efficient Catalysts For The Synthesis Of Polycarbonates And Cyclic Carbonates Using Carbon Dioxide And Epoxides. *Journal of molecular catalysis a-chemical* **2016**, 423, 489-494.
23. Dias, L. D.; Carrilho, R. M. B.; Henriques, C. A.; Piccirillo, G.; Fernandes, A.; Rossi, L. M.; Filipa Ribeiro, M.; Calvete, M. J. F.; Pereira, M. M., A Recyclable Hybrid Manganese(III) Porphyrin Magnetic Catalyst For Selective Olefin Epoxidation Using Molecular Oxygen. *Journal of Porphyrins and Phthalocyanines* **2018**, 22 (04), 331-341.
24. Boaen, N. K.; Hillmyer, M. A., Selective And Mild Oxyfunctionalization Of Model Polyolefins. *Macromolecules* **2003**, 36 (19), 7027-7034.
25. Piccirillo, G.; Moreira-Santos, M.; Válega, M.; Eusébio, M. E. S.; Silva, A. M. S.; Ribeiro, R.; Freitas, H.; Pereira, M. M.; Calvete, M. J. F., Supported Metalloporphyrins As Reusable Catalysts For The Degradation Of Antibiotics: Synthesis, Characterization, Activity And Ecotoxicity Studies. *Applied Catalysis B: Environmental* **2021**, 282, 119556.
26. Monteiro, C. J. P.; Pereira, M. M.; Pinto, S. M. A.; Simões, A. V. C.; Sá, G. F. F.; Arnaut, L. G.; Formosinho, S. J.; Simões, S.; Wyatt, M. F., Synthesis Of Amphiphilic Sulfonamide Halogenated Porphyrins: MALDI-TOFMS Characterization And Evaluation Of 1-Octanol/Water Partition Coefficients. *Tetrahedron* **2008**, 64 (22), 5132-5138.
27. Simões, A. V. C.; Adamowicz, A.; Dąbrowski, J. M.; Calvete, M. J. F.; Abreu, A. R.; Stochel, G.; Arnaut, L. G.; Pereira, M. M., Amphiphilic Meso(Sulfonate Ester Fluoroaryl)Porphyrins: Refining The Substituents Of Porphyrin Derivatives For Phototherapy And Diagnostics. *Tetrahedron* **2012**, 68 (42), 8767-8772.
28. Monteiro, C. J. P.; Pereira, M. M.; Gonçalves, N. P. F.; Carvalho, C. G.; Neves, Â. C. B.; Abreu, A. R.; Arnaut, L. G.; Silva, A. M. S., Separation And Atropisomer Isolation Of Ortho-Halogenated Tetraarylporphyrins By HPLC: Full Characterization Using 1D And 2D NMR. *Journal of Porphyrins and Phthalocyanines* **2012**, 16 (03), 316-323.

29. Kooriyaden, F. R.; Sujatha, S.; Arunkumar, C., Synthesis, Spectral, Structural And Antimicrobial Studies Of Fluorinated Porphyrins. *Polyhedron* **2015**, *97*, 66-74.
30. Carrilho, R. M. B.; Dias, L. D.; Rivas, R.; Pereira, M. M.; Claver, C.; Masdeu-Bultó, A. M. J. C., Solventless Coupling of Epoxides and CO₂ in Compressed Medium Catalysed by Fluorinated Metalloporphyrins. *Catalysts* **2017**, *7*, 210.
31. Moschona, F.; Savvopoulou, I.; Tsitopoulou, M.; Tataraki, D.; Rassias, G., Epoxide Syntheses and Ring-Opening Reactions in Drug Development. *Catalysts* **2020**, *10* (10), 1117.
32. Wang, L.-H.; Lin, Y.-Y.; Chen, J.-C. J. R.; Pharmacy, R. J. o.; Sciences, P., Study the Photochemical of Fragrance Allergens of Eugenol Derivatives in Commercial Essential Oils and Containing Clove Drugs Using Gas Chromatography and Liquid Chromatography-Mass Spectrometry. *Research and Reviews: Journal of Pharmacy and Pharmaceutical Sciences* **2016**, *5*, 2322-0112.
33. Kurniawan, M. A.; Matsjeh, S.; Triono, S., Conversion Of Eugenol To Methyleugenol: Computational study and experimental. *AIP Conference Proceedings* **2017**, *1823* (1), 020109.
34. Carrilho, R. M. B.; Dias, L. D.; Rivas, R.; Pereira, M. M.; Claver, C.; Masdeu-Bultó, A. M., Solventless Coupling of Epoxides and CO₂ in Compressed Medium Catalysed by Fluorinated Metalloporphyrins. *Catalysts* **2017**, *7* (7), 210.
35. Bausch, M.; Schultheiss, C.; Sieck, J. B., Recommendations for Comparison of Productivity Between Fed-Batch and Perfusion Processes. *Biotechnology Journal* **2019**, *14* (2), 1700721.
36. Ekinci, E. K.; Gündüz, G.; Oktar, N., Activity Comparison Of Acidic Resins In The Production Of Valuable Glycerol Acetates. *International Journal of Chemical Reactor Engineering* **2016**, *14* (1), 309-314.
37. Zare, M.; Golmakani, M.-T.; Sardarian, A., Green Synthesis Of Banana Flavor Using Different Catalysts: A Comparative Study Of Different Methods. *Green Chemistry Letters and Reviews* **2020**, *13* (2), 83-92.
38. Rigo, D.; Fiorani, G.; Perosa, A.; Selva, M., Acid-Catalyzed Reactions Of Isopropenyl Esters And Renewable Diols: A 100% Carbon Efficient Transesterification/Acetalization Tandem Sequence, From Batch To Continuous Flow. *ACS Sustainable Chemistry & Engineering* **2019**, *7* (23), 18810-18818.

39. Sikora, E.; Hajdu, V.; Muránszky, G.; Katona, K. K.; Kocserha, I.; Kanazawa, T.; Fiser, B.; Viskolcz, B.; Vanyorek, L., Application Of Ion-Exchange Resin Beads To Produce Magnetic Adsorbents. *Chemical Papers* **2021**, *75* (3), 1187-1195.
40. Bonacci, S.; Iriti, G.; Mancuso, S.; Novelli, P.; Paonessa, R.; Tallarico, S.; Nardi, M., Montmorillonite K10: An Efficient Organo-Heterogeneous Catalyst For Synthesis Of Benzimidazole Derivatives. *Catalysts* **2020**, *10* (8), 845.
41. Alekseeva, O.; Noskov, A.; Grishina, E.; Ramenskaya, L.; Kudryakova, N.; Ivanov, V.; Agafonov, A., Structural and Thermal Properties of Montmorillonite/Ionic Liquid Composites. *Materials (Basel, Switzerland)* **2019**, *12* (16), 2578.
42. Dias, L. D.; Batista de Carvalho, A. L. M.; Pinto, S. M. A.; Aquino, G. L. B.; Calvete, M. J. F.; Rossi, L. M.; Marques, M. P. M.; Pereira, M. M., Bioinspired-Metalloporphyrin Magnetic Nanocomposite As A Reusable Catalyst For Synthesis Of Diastereomeric (-)-Isopulegol Epoxide: Anticancer Activity Against Human Osteosarcoma Cells (MG-63). *Molecules* **2019**, *24* (1), 52.
43. Calvete, M. J. F.; Piñeiro, M.; Dias, L. D.; Pereira, M. M., Hydrogen Peroxide and Metalloporphyrins in Oxidation Catalysis: Old Dogs With Some New Tricks. *ChemCatChem* **2018**, *10* (17), 3615-3635.
44. Dias, L. D.; Carrilho, R. M. B.; Henriques, C. A.; Calvete, M. J. F.; Masdeu-Bultó, A. M.; Claver, C.; Rossi, L. M.; Pereira, M. M., Hybrid Metalloporphyrin Magnetic Nanoparticles As Catalysts For Sequential Transformation Of Alkenes And CO₂ Into Cyclic Carbonates. *ChemCatChem* **2018**, *10* (13), 2792-2803.
45. Gonsalves, A. M. d. A. R.; Johnstone, R. A. W.; Pereira, M. M.; Shaw, J., Metal-Assisted Reactions. Part 21. Epoxidation Of Alkenes Catalysed By Manganese-Porphyrins: The Effects Of Various Oxidatively-Stable Ligands And Bases. *Journal of the Chemical Society, Perkin Transactions 1* **1991**, (3), 645-649.
46. Rebelo, S. L. H.; Gonçalves, A. R.; Pereira, M. M.; Simões, M. M. Q.; Neves, M. G. P. M. S.; Cavaleiro, J. A. S., Epoxidation Reactions With Hydrogen Peroxide Activated By A Novel Heterogeneous Metalloporphyrin Catalyst. *Journal of Molecular Catalysis A: Chemical* **2006**, *256* (1), 321-323.
47. Neves, C. M. B.; Rebelo, S. L. H.; Faustino, M. A. F.; Neves, M. G. P. M. S.; Simões, M. M. Q., Second-Generation Manganese(III) Porphyrins Bearing 3,5-Dichloropyridyl Units: Innovative Homogeneous And Heterogeneous Catalysts For The Epoxidation Of Alkenes. *Catalysts* **2019**, *9* (11), 967.

48. Mahamat Ahmat, Y.; Madadi, S.; Charbonneau, L.; Kaliaguine, S., Epoxidation Of Terpenes. *Catalysts* **2021**, *11* (7), 847.
49. Punniyamurthy, T.; Velusamy, S.; Iqbal, J., Recent Advances In Transition Metal Catalyzed Oxidation Of Organic Substrates With Molecular Oxygen. *Chemical Reviews* **2005**, *105* (6), 2329-2364.
50. Wentzel, B. B.; Alsters, P. L.; Feiters, M. C.; Nolte, R. J. M., Mechanistic Studies On The Mukaiyama Epoxidation. *The Journal of Organic Chemistry* **2004**, *69* (10), 3453-3464.
51. Murahashi, S.; Oda, Y.; Naota, T., Iron- And Ruthenium-Catalyzed Oxidations Of Alkanes With Molecular Oxygen In The Presence Of Aldehydes And Acids. *Journal of the American Chemical Society* **1992**, *114* (20), 7913-7914.
52. Finney, N. S.; Pospisil, P. J.; Chang, S.; Palucki, M.; Konsler, R. G.; Hansen, K. B.; Jacobsen, E. N., On The Viability Of Oxametallacyclic Intermediates In The (Salen)Mn-Catalyzed Asymmetric Epoxidation. *Angewandte Chemie International Edition in English* **1997**, *36* (16), 1720-1723.
53. Groves, J. T.; Lee, J.; Marla, S. S., Detection And Characterization Of An Oxomanganese(V) Porphyrin Complex By Rapid-Mixing Stopped-Flow Spectrophotometry. *Journal of the American Chemical Society* **1997**, *119* (27), 6269-6273.
54. Guo, M.; Seo, M. S.; Lee, Y.-M.; Fukuzumi, S.; Nam, W., Highly Reactive Manganese(IV)-Oxo Porphyrins Showing Temperature-Dependent Reversed Electronic Effect in C-H Bond Activation Reactions. *Journal of the American Chemical Society* **2019**, *141* (31), 12187-12191.
55. Mohammed, T. P.; Sankaralingam, M., Reactivities Of High Valent Manganese-Oxo Porphyrins In Aqueous Medium. *Tetrahedron* **2022**, *103*, 132483.
56. Wu, J.; Kozak, J. A.; Simeon, F.; Hatton, T. A.; Jamison, T. F., Mechanism-Guided Design Of Flow Systems For Multicomponent Reactions: Conversion Of CO₂ And Olefins To Cyclic Carbonates. *Chemical Science* **2014**, *5* (3), 1227-1231.
57. Calmanti, R.; Selva, M.; Perosa, A., Tandem Catalysis: One-Pot Synthesis Of Cyclic Organic Carbonates From Olefins And Carbon Dioxide. *Green Chemistry* **2021**, *23* (5), 1921-1941.
58. Li, H.-J.; Wu, Y.-C.; Dai, J.-H.; Song, Y.; Cheng, R.; Qiao, Y., Regioselective Electrophilic Aromatic Bromination: Theoretical Analysis and Experimental Verification. *Molecules* **2014**, *19* (3), 3401-3416.

Experimental section

This chapter contains all the information regarding reagents, solvents, techniques, instruments and experimental procedures used during the experimental work. It is divided into four main sections: Solvents and reagents (section 3.1); Instrumentation (section 3.2); Synthesis of metalloporphyrin-based catalysts (section 3.3) and Synthesis of eugenol derivatives (section 3.4).

3.1. Solvents and reagents

All the solvents and reagents were purchased from Merck, Fluka, Strem, Fluorochem or Sigma Aldrich. Air-sensitive reagents were kept under an argon atmosphere. The solvents were purified through distillation and dried as needed, following the standard procedures, described below.

Tetrahydrofuran (THF), 2-methyltetrahydrofuran (2-MeTHF), n-Hexane and toluene

In a round-bottom flask, THF, 2-MeTHF, n-hexane or toluene was mixed with metallic sodium flakes and benzophenone and then kept under reflux until the solution became dark blue. The blue solution was then distilled and collected into a previously dried flask with activated molecular sieves (4Å) and stored under argon atmosphere.

Dichloromethane and chloroform

Chlorinated solvents were placed in a round-bottom flask, with calcium hydride and stirred under reflux for two hours. After that period, the solvent was distilled and passed through a column of basic alumina (grade I). The dry solvent was stored under argon atmosphere in a sealed flask containing activated molecular sieves (4Å).

Ethyl acetate

The solvent was mixed with anhydrous calcium chloride in a round-bottom flask. Then, the solution was kept under reflux for 2 hours and distilled. The solvent was additionally passed through a basic alumina (grade I) column before being stored in a flask containing molecular sieves (4Å).

3.2. Instrumentation

Thin layer chromatography (TLC)

Thin layer chromatography (TLC) was performed using aluminium plates coated with silica gel 60 with fluorescent indicator UV₂₅₄.

Ultraviolet-Visible Spectroscopy (UV-Vis)

All UV-VIS spectra were obtained using a Hitachi U-2001 spectrophotometer, using a 10 mm quartz cell and CH₂Cl₂ as solvent.

Mass spectrometry

High-resolution electrospray mass spectra (HRMS (ESI)) were recorded with a Micromass Quatro LC instrument; nitrogen was employed as a drying and nebulizing gas. The mass spectrometry was provided by the Mass Spectrometry Unit (UniMS), ITQB/iBET, Oeiras, Portugal.

Nuclear Magnetic Resonance (NMR)

The ¹H and ¹³C NMR spectra were recorded on a 400 Bruker Avance III NMR spectrometer (400.13 for ¹H and 100.62 MHz for ¹³C), All spectra were recorded using deuterated chloroform (Chloroform-d) as the solvent, also the signal from the vestigial non-deuterated solvent was used as a chemical shift reference in all NMR spectra (δ = 7.26 ppm). ¹H and ¹³C chemical shifts are expressed in ppm and indicated in the following

order: Nucleus (apparatus, solvent): chemical shift (δ , ppm), the signal multiplicity is indicated as follows: s - singlet, d - doublet, t - triplet, q - quartet, dd - double doublet, ddt - doublet of doublet of triplets, p – pentet, m – multiplet. Followed by the coupling constant (J, in Hertz) and relative intensity (nH as the number of protons).

Gas chromatography (GC)

GC-FID

Gas chromatography was performed using an Agilent-7820 apparatus equipped with a nonpolar HP-5 capillary column (5% diphenyl and 95% dimethylpolysiloxane), 30 m length and with an internal diameter of 0.32 mm using nitrogen as carrier gas. The signal acquisition was done using a flame ionization detector (FID).

GC-Method:

- Initial Temperature: 100 °C; (hold 10 min)
- Heating rate: 60 °C/min;
- Final temperature: 300 °C; (hold 3 min)
- Gas Flow: 1.63 mL/min;

Conversion, chemoselectivity, and regioselectivity of the catalytic experiments were calculated using the following equations:

$$\text{Conversion (\%)} = \left(\frac{\text{Area}(\text{substrate} + \text{products}) - \text{Area}(\text{substrate})}{\text{Area}(\text{substrate} + \text{products})} \right) \times 100$$

$$\text{Chemoselectivity (\%)} = \left(\frac{\text{Area}(\text{all products from a functional group})}{\text{Area}(\text{all products})} \right) \times 100$$

$$\text{Regioselectivity (\%)} = \left(\frac{\text{Area}(\text{major isomer from a functional group})}{\text{Area}(\text{all products from that functional group})} \right) \times 100$$

GC-MS

The GC-MS analysis was realised by Itecons-Coimbra, using a SCION 456-GC (Bruker) chromatograph equipped with an Rtx-5 column (5% phenyl / 95% methyl polysiloxane, 30 m x 0.25 mm DI x 0.25 μm coating, Restek). The mass spectra were acquired using an MS EVOQ TQ mass detector.

Inductively coupled plasma optical emission spectroscopy (ICP-OES)

The percentage of manganese in the **CAT1@NHSiO₂** was determined by an Inductively Coupled Plasma (ICP) using a Thermo X Series spectrometer (Department of Chemistry, University of Aveiro, Portugal).

Centrifuge

Isolation and recovery of the heterogenous catalyst **CAT1@NHSiO₂** was executed in a Selecta Centromix-BLT. The samples were centrifuged at 4000 rpm for 30 minutes.

Thermogravimetry (TG)

Thermogravimetric analyses were made using a TG-DSC Perkin-Elmer STA6000 with a heating rate of 10 °C min⁻¹ to a maximum temperature of 800 °C and 20 mL min⁻¹ nitrogen flux (Department of Physics, University of Coimbra)

High-pressure gas line

All the catalytic *batch* reactions that required CO₂ gas were performed in a stainless steel reactor connected to a high-pressure system belonging to the Chemistry Department at the University of Coimbra (Figure 3.1).



Figure 3.1. High-pressure system for catalytic reactions (Chemistry Department, University of Coimbra).

Flow Chemistry

The continuous-flow reactions were performed on a Vapourtec E-series apparatus, belonging to the Chemistry Department, University of Coimbra (Figure 3.2). The equipment standard configuration is three V3 peristaltic pumps, a chemical reactor (tubular, column and/or chip type) and a back-pressure regulator. The residence times were calculated using the default Vaportec software.

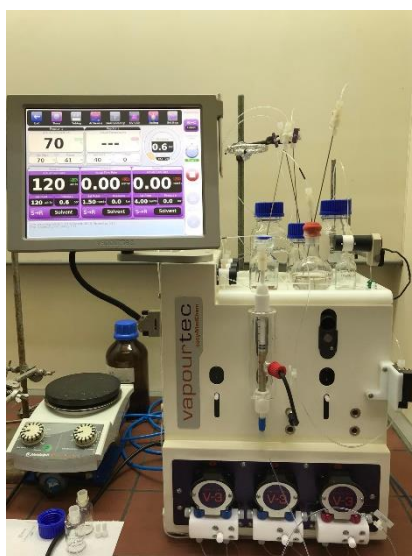


Figure 3.2. Continuous flow chemistry apparatus from the Catalysis and fine chemistry laboratory (Chemistry Department, University of Coimbra).

3.3. Synthesis of metalloporphyrin-based catalysts

Metalloporphyrin-based catalysts **CAT1** and **CAT2** were prepared by the synthesis of the correspondent porphyrins (**TDCPP** and *p*-**CF₃TPP** respectively), followed by the complexation with the desired metal salt. The heterogeneous catalyst **CAT1@NHSiO₂** was prepared by chlorosulfonation reaction of **TDCPP** (precursor of **CAT1**), followed by immobilization onto aminated silica particles and complexation with manganese acetate. All the procedures are described as follows.

3.3.1. Porphyrin synthesis

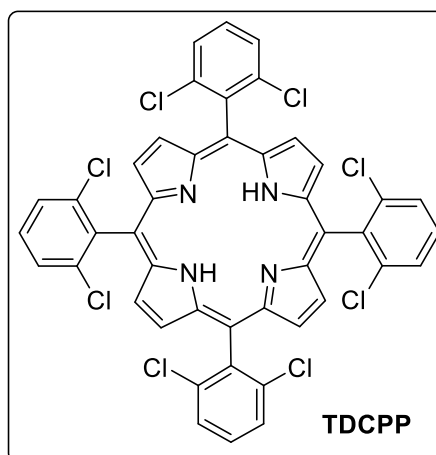
General procedure for porphyrin synthesis: To a mixture of glacial acetic acid (210 mL) and nitrobenzene (105 mL) under stirring at 150 °C, aldehyde (60 mmol) and pyrrole (60 mmol; 4.2 mL) were added dropwise, then the reaction was left for 2 h. After that period, cold methanol (200 mL) was added and the mixture was kept at 5 °C overnight. On the next day, the solid was filtrated using a D4 silica filter and washed several times with cold methanol. The final product was dried in an oven at 70 °C. The resulting powder was analysed by UV-Vis and ¹H NMR.

Synthesis of 5,10,15,20-tetra(2,6-dichloro-phenyl)porphyrin (TDCPP)

TDCPP was prepared following the general procedure for porphyrin synthesis using 2,6-dichlorobenzaldehyde as aldehyde. The desired product was obtained as a purple powder in 4.5% (480 mg) isolated yield. The product was then characterized by UV-Vis and ^1H NMR and the data are in good agreement with the literature.¹

^1H NMR (400 MHz, Chloroform-d) δ (ppm) = 8.68 (s, 8H, β -H), 7.83-7.62 (m, 12H, ArH), -2.57 (s, 2H, NH)

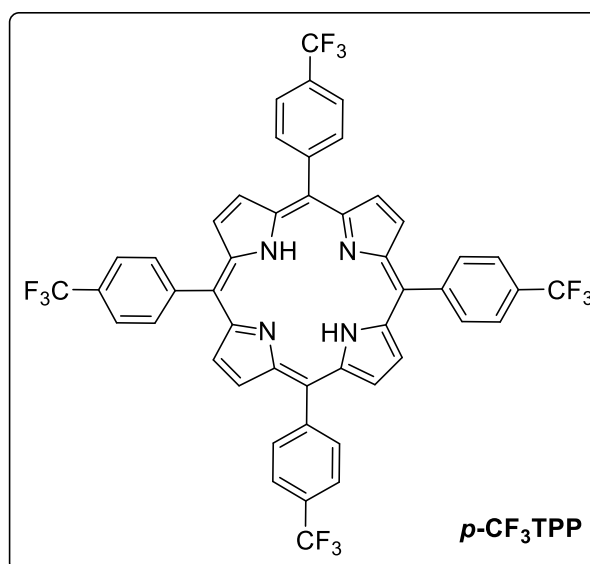
UV-VIS: 417.5 nm (Soret band)



Synthesis of 5,10,15,20-tetra(4-trifluoromethylphenyl)porphyrin (*p*-CF₃TPP)

Following the general procedure described above, using 8.2 mL of 4-(Trifluoromethyl)benzaldehyde (0.06 mol). The final product was obtained as a purple powder in 14% (4.912 g) isolated yield. The product was then characterized by UV-Vis and ^1H NMR and the data are in good agreement with the literature.²

^1H NMR (400 MHz, Chloroform-d) δ (ppm) = 8.81 (s, 8H, β -H), 8.34 (d, J = 7.9 Hz, 8H, ArH), 8.05 (d, J = 8.0 Hz, 8H, ArH), -2.83 (s, 2H, NH).



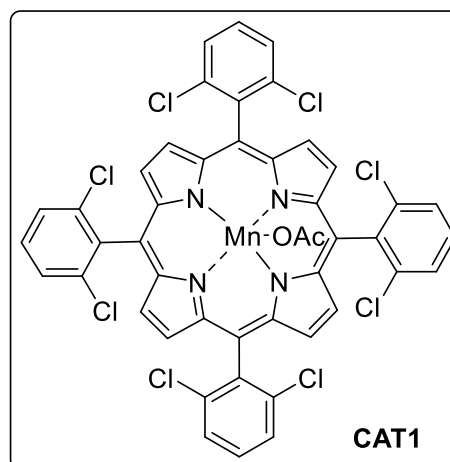
^{19}F NMR (400 MHz, Chloroform-d), δ (ppm) = -62.08 ppm (s, 9F)

UV-VIS: 416 nm (Soret band)

3.3.2. Preparation of CAT1

Synthesis of 5,10,15,20-tetra(2,6-dichlorophenyl)porphyrinat manganese Acetate

In a round-bottom flask, 100 mg of **TDCPP** (0.1 mmol) and 117 mg of manganese (II) acetate (0.7 mmol) were dissolved in 1 mL of DMF and the reaction was kept under reflux (180 °C). The reaction progress was controlled with UV-VIS. After 24 hours, the Soret band corresponding to metal-free **TDCPP** (417.5 nm) was no longer observed and the reaction was stopped. DMF was evaporated under reduced pressure and 20 mL of CH_2Cl_2 was added. The reaction crude was washed with 200 mL of distilled water several times and the organic phase was recovered and dried over anhydrous sodium sulfate, the solvent was then evaporated under reduced pressure. Finally, the concentrated reaction crude was purified by silica gel column chromatography using mixtures of $\text{CH}_2\text{Cl}_2/n$ -hexane and CH_2Cl_2 /ethyl acetate as eluents. **CAT1** was dried under reduced pressure resulting in a greenish solid with 88% isolated yield (88 mg) and characterized by MS and UV-Vis and the data are in good agreement with the literature.³



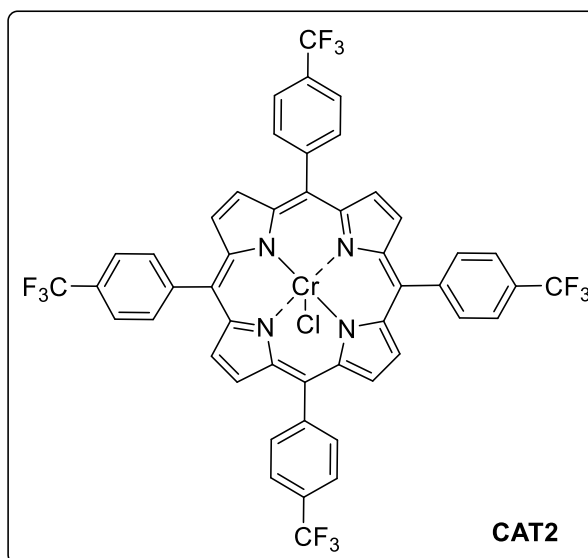
MS (MALDI-TOF): $m/z = 997.872$ $[\text{M}]^+$

UV-VIS: 469 nm (Soret band)

3.3.3. Preparation of CAT2

Synthesis of 5,10,15,20-tetra(4-trifluoromethylphenyl)porphyrinatochromium Chloride

In a round bottom flask, 500 mg of *p*-CF₃TPP was dissolved in 2 mL of DMF, the mixture was heated until boiling, then 74 mg of chromium (II) chloride was added, and the reaction was left under reflux (180 °C) for 2 hours. The reaction progress was controlled through UV-VIS. After 2 hours, the Soret band corresponding to free-base *p*-CF₃TPP (416 nm) was still present in the UV spectra, and more



chromium(II) chloride (40 mg) was added and the reaction was left under reflux. After 24 hours the reaction mixture was cooled to room temperature, 20 mL of CH₂Cl₂ were added and the reaction crude was washed with 200 mL of distilled water four times. The organic phase was evaporated in a rotary evaporator, and a silica gel column chromatography, using mixtures of CH₂Cl₂/*n*-hexane and CH₂Cl₂/ethyl acetate as eluents, was done to purify the complex. The desired fraction was collected and the solvent was evaporated under reduced pressure and oven dried at 70 °C for 2 hours. The desired product was obtained as dark green crystals in 64% isolated yield (0.347 g). **CAT2** was characterized by HRMS and UV-Vis and the data are in good agreement with the literature.⁴

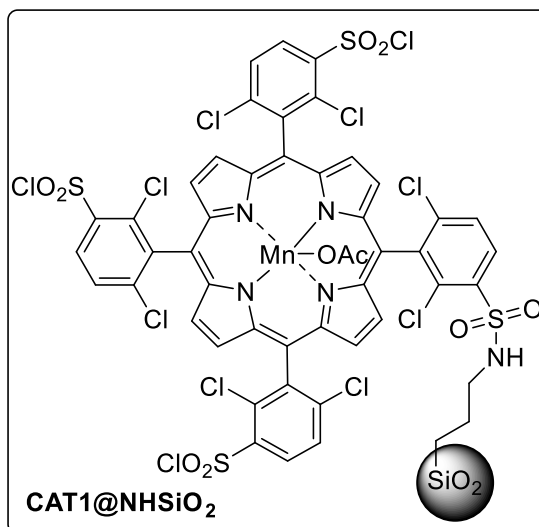
HRMS (ESI): *m/z* 891.1512 [M+2Na]⁺ calculated for C₄₄H₂₀ClCrF₈N₄Na₂ = 891.0448

UV-VIS: 447 nm (Soret band)

3.3.4. Preparation of CAT1@NHSiO₂

The heterogeneous catalyst **CAT1@NHSiO₂** was prepared following a synthetic route of chlorosulfonation of **TDCPP** followed by immobilization onto aminated silica particles and complexation with manganese acetate.

First, **TDCPP** (300 mg, 0.3 mmol) was dissolved in chlorosulfonic acid (12 mL) and the reaction was left for 2 h under reflux at 160 °C. After this period, chloroform (200 mL) was added to the solution. A continuous water extraction was carried out, with stirring, until neutralization using a sodium hydrogen carbonate solution. The chloroform was then evaporated under reduced pressure.



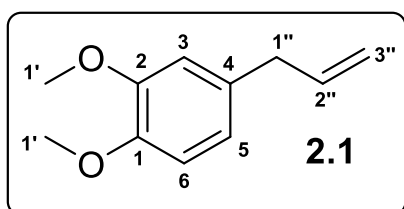
The chlorosulfonated porphyrin

TDCPPS was used without further purification. Next, 3 g of 3-aminopropyl functionalized silica (containing 1 mmol NH₂/g) were placed in a 100 mL round flask. Then the sulfonated porphyrin was dissolved in 42 mL of triethylamine and the reaction was further stirred for 48 h, at 25 °C. After that period the reaction crude was centrifuged (4000 rpm, 30 min) and the solvent was removed by decantation. This procedure was repeated two times with CH₂Cl₂, and then twice with acetone. Next, the obtained particles were dispersed in acetic acid and manganese (II) acetate (1 g, 6 mmol) and sodium acetate (300 mg, 4 mmol) were consecutively added. Then, the mixture was brought to 120 °C and left for another 48 h. Afterwards, the reaction was cooled to room temperature, centrifuged and the supernatant carefully removed. The obtained solid was dispersed in 15 mL of CH₂Cl₂ by stirring. After stirring for 10 min, it was centrifuged (4000 rpm, 30 min) and the solvent was removed by decantation. This procedure was repeated two times with CH₂Cl₂, ethanol and acetone each. The hybrid material was collected and dried in an oven at 25 °C for 24 h. After characterization with TG, ICP and UV-Vis. The TGA indicated a mass difference between the aminated silica and the **CAT1@NHSiO₂** of 3.3% corresponding to 2.75×10^{-5} mol of immobilized porphyrin. ICP analysis reported 2 mg of manganese per gram of functionalized silica. The data is in good agreement with the literature.⁵

3.4. Synthesis of eugenol derivatives

3.4.1. Methyl eugenol synthesis (2.1)

To a round-bottomed flask 2 mL of iodomethane (30.0 mol), 5 mL of DME and 1 mL of eugenol (6.1 mmol) were mixed and then 4.21 g of potassium carbonate (30 mmol) were stirred for 48 hours at 25 °C. After confirming the full eugenol conversion via GC-FID, 20 mL of DME was added to the reaction crude and the organic phase was extracted by work-up with a 1 M hydrochloric acid solution and then with water. After the organic phase was dried using anhydrous sodium sulphate it was evaporated under reduced pressure. The resulting product, methyl eugenol (**2.1**), a light-yellow liquid, was isolated in a 74% yield (0.7854 g). The characterization are in good agreement with the literature.⁶



¹H NMR (400 MHz, Chloroform-d) δ (ppm) = 6.78 (*d*, J = 8.6 Hz, 1H, H₆), 6.73-6.69 (*m*, 2H, H₅ and H₃), 5.95 (*ddt*, J = 16.8, 10.1, 6.6 Hz, 1H, H_{2''}), 5.10 – 5.01 (*m*, 2H, H_{3''}), 3.84 (*s*, 3H, H_{1'}), 3.83 (*s*, 3H, H_{1'}), 3.32 (*d*,

J = 6.7 Hz, 2H, H_{1''}).

¹³C NMR (101 MHz, Chloroform-d) δ (ppm) = 148.8, 147.3, 137.6, 132.6, 120.4, 115.5, 111.8, 111.2, 55.8, 55.7, 39.7.

3.4.2. Acetyleugenol synthesis (2.2)

Acetyleugenol (**2.2**) was prepared following 2 different approaches, classical batch conditions and under alternative continuous flow conditions using two different catalysts (K10 and sulfuric acid).

Batch conditions

Sulfuric acid as catalyst: In a round bottom flask, 10 mL of CH₂Cl₂, eugenol (1 mL, 6.5 mmol) and acetic anhydride (1.2 equivalents, 0.75 mL, 7.8 mmol) were added. Then three droplets of sulfuric acid (~1 mmol) were slowly added while stirred. After 5 min the solution was washed with a sodium bicarbonate aqueous solution and filtered through

a small silica plug to remove the colored products. After the residual solvents were evaporated and dried under vacuum overnight, acetyeugenol (**2.2**) was obtained as a colorless oil with 82% isolated yield and analyzed via ^1H and ^{13}C NMR. The characterization are in good agreement with the literature.⁷

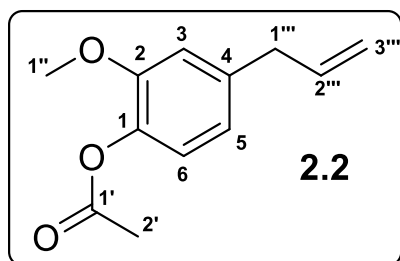
K10 or IRA-120H catalyst: To a round-bottomed flask 6 mL of acetic anhydride (10 eq., 65 mmol), 1 g of eugenol (6.5 mmol), 0.25 g of K10 or IRA-120H (25% wt/wt), and 10 mL of CH_2Cl_2 as solvent. The reaction was heated until boiling and left for reflux for 3 h. After that period, GC analysis was performed indicating full conversion. The reaction was stopped, and the K10 was filtered and washed several times with CH_2Cl_2 . Then, several extractions were done using a bicarbonate solution, and distilled water. Finally, the solvent was removed from the organic phase through evaporation and acetyeugenol (**2.2**) with 96% isolated yield.

Continuous flow conditions

Sulfuric acid as catalyst: Two solutions were prepared in CH_2Cl_2 , one of eugenol (0.23 M) and acetic anhydride (0.27 M) and another with sulfuric acid (1.84 mol). Then, the reaction was carried out in a 1.5 mL microchip using two peristaltic pumps and a volumetric ratio of 1 to 10 of sulfuric acid/olefin solution. The optimal conditions are 1 minute residence time at 25 °C. The crude reaction was then analyzed via GC, obtaining 83% yield for acetyeugenol (**2.2**).

K10 as catalyst: A column reactor was filled with 1.78 g of K10 clay. The clay was previously activated in a heated oven overnight at 250 °C. The resulting dead volume was 2 mL. A solution of eugenol (0.23 M) with acetic anhydride (2.3 M) was prepared in CH_2Cl_2 and then pumped through the reactor, pressurized to 8 bar. The best results were obtained with 20 min residence time at 70 °C. The GC yield was 98%.

4-allyl-2-methoxyphenyl acetate (2.2)



$^1\text{H NMR}$ (400MHz, Chloroform-d) δ (ppm) = 6.96 (*d*, $J = 8.0$ Hz, 1H, H6), 6.81 (*d*, $J = 1.9$ Hz, 1H, H3), 6.78 (*dd*, $J = 8.0$ Hz, 1.9 Hz, 1H, H5), 5.97 (*ddt*, 16.8, 10.1, 6.7, 1H, H2'''), 5.15 – 5.08 (*m*, 2H, H3'''), 3.82 (*s*, 3H, H1''), 3.39 (*d*, $J = 6.8$ Hz, 2H, H1'''), 2.31 (*s*, 3H, H2').

$^{13}\text{C NMR}$ (101 MHz, Chloroform-d) δ (ppm) = 169.2 (C1'), 150.9 (C2), 139.0 (C1), 138.0 (C4), 137.1 (C2'''), 122.6 (C6), 120.7 (C5), 116.2 (C3'''), 112.8 (C3), 55.8 (C1''), 40.1 (C3'''), 20.7 (C2').

3.4.3. Acetylugenol epoxide synthesis

Acetylugenol epoxide (2.3) was prepared following 2 different approaches, classical batch conditions and continuous flow, using a Prilejaev epoxidation with mCPBA as oxidant.

Batch conditions

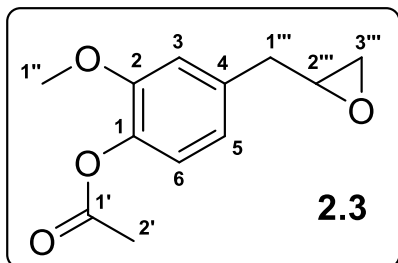
To a round-bottomed flask, 0.82 g of acetylugenol (3.9 mmol), 0.82 g of *meta*-chloroperoxybenzoic acid (1.2 eq., 4.8 mmol) and 20 mL of CH_2Cl_2 were added. The mixture was stirred for 30 h at 25 °C, then the reaction was quenched with sodium bisulfite. The organic solution was then washed several times with a bicarbonate solution and water. Then, the solvent was dried using sodium sulfate and evaporated under reduced pressure, resulting in yellow oil. The isolated yield was 91% yield (0.7821 g). The compound was then characterized using $^1\text{H NMR}$, $^{13}\text{C NMR}$ and HRMS (ESI). The resulting data are in good agreement with the literature.⁷

Continuous flow conditions

Two different solutions were pumped into a 10 mL tubular reactor, one with mCPBA (0.23 M) in CH_2Cl_2 , and another with acetylugenol (0.23 M) also in CH_2Cl_2 .

The volumetric ratio of the acetyeugenol/mCPBA solution was 1.2, residence time of 40 minutes, 8 bar of pressure, and 100 °C. The GC yield was of 83%.

[2-methoxy-4-(oxiran-2-ylmethyl)phenyl acetate] (2.3)



¹H NMR (400 MHz, Chloroform-d) δ (ppm) = 6.96 (*d*, *J* = 8.0 Hz, 1H, H6), 6.86 (*d*, *J* = 1.9 Hz 1H, H3), 6.82 (*dd*, *J* = 8.0, 1.9 Hz, H5), 3.82 (*s*, 3H, H1''), 3.17 – 3.12 (*m*, 1H, H2'''), 2.83 (*d*, *J* = 5.5 Hz, 2H, H1'''), 2.79 (*dd*, *J* = 4.8, 4.0 Hz, 1H, H3'''), 2.54 (*dd*, *J* = 4.9, 2.6 Hz, 1H, H3'''), 2.30 (*s*, 3H, H2').

¹³C NMR (101 MHz, Chloroform-d) δ (ppm) = 169.2 (C1'), 151.0 (C2), 138.5 (C1), 136.3 (C4), 122.7 (C6), 121.1 (C5), 113.2 (C3), 55.9 (C1''), 52.3 (C2'''), 46.8 (C3'''), 38.7 (C1'''), 20.7 (C2')

HRMS (ESI) m/z: obtained 245.0784 [M+Na]⁺ calculated for C₁₂H₁₄O₄Na⁺ 245.0790

3.4.4. Methyl eugenol epoxidation

Batch conditions

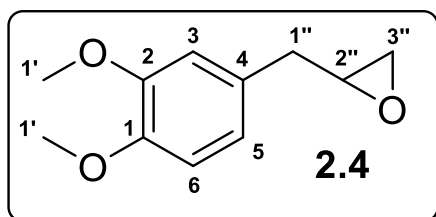
Molecular oxygen: A glass vial was charged with the methyl eugenol (0.5 mmol) and 1 mg **CAT1** (1 μ mol), CH₃CN (2 mL), isobutyraldehyde (0.18 g; 2.5 mmol). The reaction was conducted under vigorous stirring, at 25 °C for 90 minutes, with molecular oxygen constant bubbling. The GC-MS yield was 28%.

Hydrogen peroxide: The olefin substrate (0.5 mmol), MnOAcTDCPP (**CAT1**) (1 μ mol) and imidazole (0.25 mmol) or ammonium acetate (0.25 mmol) were dissolved in acetonitrile (2 mL). The mixture was introduced into a glass vial and 4 equivalents (2 mmol) of hydrogen peroxide (35 %), diluted with acetonitrile (1:10), and slowly added over 30 minutes using a syringe pump. The reaction was conducted at 25 °C, under stirring, for 3 hours. The GC yield was 83%.

Continuous flow conditions

Hydrogen peroxide: A solution of methyl eugenol **2.1** (0.23 M), **CAT1** (4 mM) and imidazole (0.11 M) was prepared in CH₃CN. Another solution containing 35% hydrogen peroxide and CH₃CN, in a ratio 1:1 was also prepared. The two solutions were connected to the flow system and pumped through a 10 mL column reactor with a volumetric ratio of 1:0.5 for the methyl eugenol **2.1**/hydrogen peroxide solutions. At the end of the reactor, another portion of the peroxide solution was added with a volumetric ratio of 0.5 and the solution entered to another 10 mL tubular reactor. The total residence time was 50 minutes, and the reaction was carried out at 25 °C. The crude was analyzed by GC-MS and ¹H NMR (good agreement with the literature)⁸, obtaining 77% yield.

[2-(3,4-dimethoxybenzyl)oxirane] (**2.4**)



¹H NMR (400 MHz, Chloroform-d) δ (ppm) = 6.80 – 6.75 (*m*, 3H, H₃, H₅ and H₆), 3.85 (*s*, 3H, H_{1'}), 3.83 (*s*, 3H, H_{1'}), 3.14 – 3.08 (*m*, 1H, H_{2''}), 2.79 (*d*, *J* = 5.4 Hz, 2H, H_{1''}), 2.79 – 2.75 (*m*, 1H, H_{3''}), 2.52 (*dd*, *J* = 5.0, 2.7 Hz, 1H, H_{3''}). (from a

reaction crude with 77% purity)

GC-MS (*m/z*): 194.1 [M]⁺, 180.1, 165.0, 137.1, 123.0, 107.1, 91.1, 69.0.

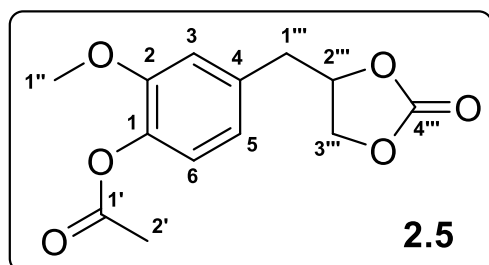
3.4.5 Acetyeugenol carbonate synthesis

Batch conditions

In a stainless steel reactor, 8.8 mg of **CAT2** (0.2 mol%, 10 μmol) was added to 6.1 mg of PPNC1 (0.2 mol%, 10 μmol). The reactor was closed and put under vacuum at 80 °C, for 1 hour to remove any moisture. Then, acetyeugenol epoxide (4.6 mmol, 1.015 g) and 3 mL of CH₂Cl₂ were added. High-purity carbon dioxide was introduced to the reactor until 30 bar was reached. After 24 hours the resulting crude was analyzed by GC-FID, obtaining full conversion and >99% selectivity for the desired carbonate. Silica-gel chromatography was done to remove the catalyst and co-catalyst, using CH₂Cl₂ as the eluent. The solvent was evaporated under reduced pressure, resulting in a light-yellow

powder. The powder was then characterized using ^1H NMR, ^{13}C NMR and HRMS (ESI) analysis. The isolated yield was 91% (1.095 g).

[2-methoxy-4-((2-oxo-1,3-dioxolan-4-yl)methyl)phenyl acetate] (2.5)



^1H NMR (400 MHz, Chloroform-*d*) δ (ppm) = 6.99 (*d*, J = 8.0 Hz, 1H, H6), 6.83 (*d*, J = 1.7 Hz, 1H, H3), 6.78 (*dd*, J = 8.0, 1.9 Hz, 1H, H5), 4.91 (*p*, J = 6.5 Hz 1H, H2'''), 4.46 (*t*, J = 8.2 Hz, 1H, H3'''), 4.15 (*dd*, J = 8.6, 6.8 Hz, 1H, H3'''), 3.82 (*s*, 3H, H1''), 3.11

(*dd*, J = 14.4, 6.5 Hz, 1H, H1'''), 2.96 (*dd*, J = 14.3, 6.2 Hz, 1H, H1'''), 2.30 (*s*, 3H, H2').

^{13}C NMR (101 MHz, Chloroform-*d*) δ (ppm) = 169.1 (C1'), 154.8 (C4'''), 151.4 (C2), 139.3 (C1), 133.1 (C4), 123.2 (C6), 121.5 (C5), 113.5 (C3), 76.8 (C2'''), 68.6 (C3'''), 56.0 (C1''), 39.5 (C1'''), 20.7 (C2')

HRMS (ESI) m/z : obtained 289.0683 $[\text{M}-\text{Na}]^+$ calculated for $\text{C}_{13}\text{H}_{14}\text{O}_6\text{Na}^+$ $[\text{M}-\text{Na}]^+$ 289.0688

3.4.6 Oxidative carboxylation

Continuous flow conditions

A solution of acetyeugenol (**2.1**) (0.33M), NBS (0.40M), and NH_4OAc (0.033M) in H_2O and acetone, 1:2 ratio, were pumped through a tubular reactor for 30 minutes at 40 °C. Then, in a T-mixer, 3 volumetric equivalents of carbon dioxide at 8 bar and an aqueous solution of DBU (0.43M) were added to a 3.2 mL microchip at 100 °C, with a residence time of 10 minutes. The crude was analyzed via ^1H NMR, concluding that 50% conversion for cyclic carbonate was obtained. Additionally, GC-MS analysis from the reaction crude was performed to elucidate the chemical structure of the reaction major products.

4-(4-hydroxy-3-methoxybenzyl)-1,3-dioxolan-2-one (**2.6**) **GC-MS (m/z):** 224 $[\text{M}]^+$, 137, 122, 107, 94, 77, 65, 51, 43, 29

4-(2-bromo-4-hydroxy-5-methoxybenzyl)-1,3-dioxolan-2-one (2.7) GC-MS
(m/z): 304 [M+2]⁺, 302 [M]⁺, 217, 215, 202, 200, 174, 172, 137, 122, 107, 94, 77, 65, 51, 43, 29.

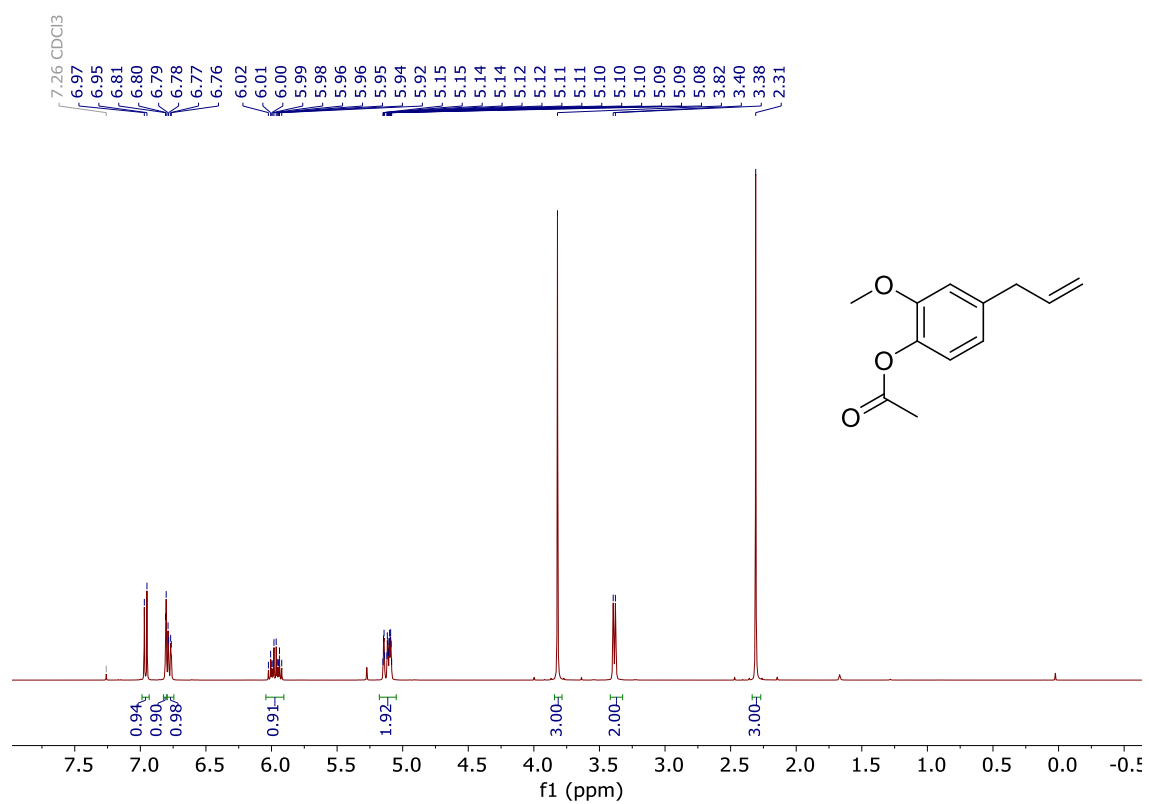
3.5. Cytotoxic: MTT Assay

The MTT assay was used to do a preliminar study on the toxicity of acetyeugenol cyclic carbonate (2.5). MCF12A cell cultures were established in 24-well plates (1 mL/well). Cells were allowed to attach for 24 h, treated with three different concentrations (200, 100 and 50 mM) and incubated in a humidified atmosphere (5% CO₂), at 37 °C. All experiments were carried out in triplicate, and 2.5 was solubilized in DMSO (0.1% concentration (v/v)). After 4 and 24 hours of exposure, the cells were washed with a solution of PBS (1 mL), and a MTT solution in PBS (0.5 mg/mL – 500 µL) was added to each well. Then, the plates were incubated for 3 h. The violet MTT formazan precipitate was then solubilized by the addition of DMSO (500 µL) to each well and absorbance was measured at 570 nm on a microplate reader BioRad Xmark spectrophotometer.

3.6. References

1. Gonsalves, A. M. d. A. R.; Pereira, M. M.; Serra, A. C.; Johnstone, R. A. W.; Nunes, M. L. P. G., 5,10,15,20-Tetrakisaryl- And 2,3,7,8,12,13,17, 18-Octahalogeno-5,10,15,20-Tetrakisarylporphyrins And Their Metal Complexes As Catalysts In Hypochlorite Epoxidations. *Journal of the Chemical Society, Perkin Transactions 1* **1994**, (15), 2053-2057.
2. Kooriyaden, F. R.; Sujatha, S.; Arunkumar, C., Synthesis, Spectral, Structural And Antimicrobial Studies Of Fluorinated Porphyrins. *Polyhedron* **2015**, *97*, 66-74.
3. Cuesta-Aluja, L.; Castilla, J.; Masdeu-Bultó, A. M.; Henriques, C. A.; Calvete, M. J. F.; Pereira, M. M., Halogenated Meso-Phenyl Mn(III) Porphyrins As Highly Efficient Catalysts For The Synthesis Of Polycarbonates And Cyclic Carbonates Using Carbon Dioxide And Epoxides. *Journal of Molecular Catalysis A: Chemical* **2016**, *423*, 489-494.
4. Carrilho, R. M. B.; Dias, L. D.; Rivas, R.; Pereira, M. M.; Claver, C.; Masdeu-Bultó, A. M. J. C., Solventless Coupling of Epoxides and CO₂ in Compressed Medium Catalysed by Fluorinated Metalloporphyrins. *Catalysts* **2017**, *7*, 210.
5. Piccirillo, G.; Moreira-Santos, M.; Válega, M.; Eusébio, M. E. S.; Silva, A. M. S.; Ribeiro, R.; Freitas, H.; Pereira, M. M.; Calvete, M. J. F., Supported Metalloporphyrins As Reusable Catalysts For The Degradation Of Antibiotics: Synthesis, Characterization, Activity And Ecotoxicity Studies. *Applied Catalysis B: Environmental* **2021**, *282*, 119556.
6. Nicolau, E. d. S.; Ribeiro, L. d. P.; Ansante, T. F.; Fernandes, J. B.; Forim, M. R.; Vieira, P. C.; Vendramim, J. D.; Da Silva, M. F. d. G. F., Isolation Of Chavibetol And Methyleugenol From Essential Oil Of *Pimenta Pseudocaryophyllus* By High Performance Liquid Chromatography. *Molecules* **2018**, *23* (11), 2909.
7. da Silva, F. F. M.; Monte, F. J. Q.; de Lemos, T. L. G.; do Nascimento, P. G. G.; de Medeiros Costa, A. K.; de Paiva, L. M. M., Eugenol Derivatives: Synthesis, Characterization, And Evaluation Of Antibacterial And Antioxidant Activities. *Chemistry Central Journal* **2018**, *12* (1), 34.
8. Jeyakumar, K.; Chand, D. K., Ring-Opening Reactions of Epoxides Catalyzed by Molybdenum(VI) Dichloride Dioxide. *Synthesis* **2008**, *2008* (05), 807-819.

NMR spectra of acetyl eugenol (2.2)

Figure A1. ^1H NMR of acetyleneugenol (2.1).

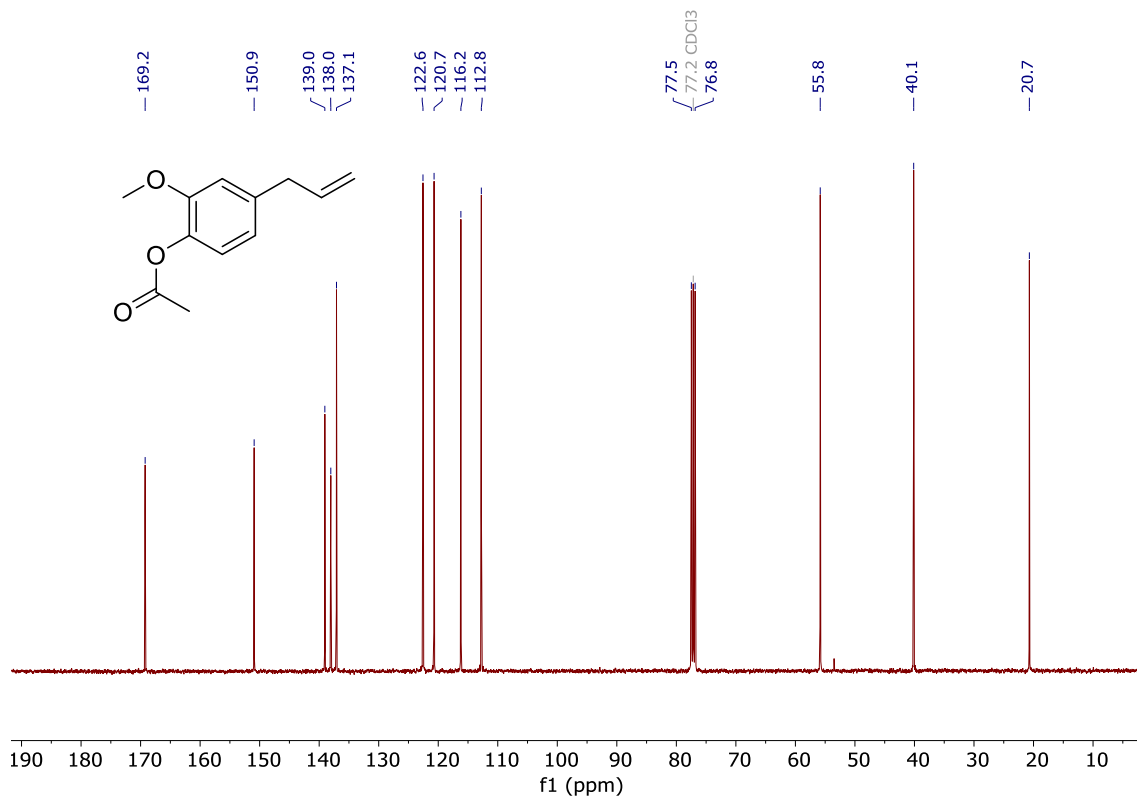


Figure A2. ^{13}C NMR of acetylugenol (2.1).

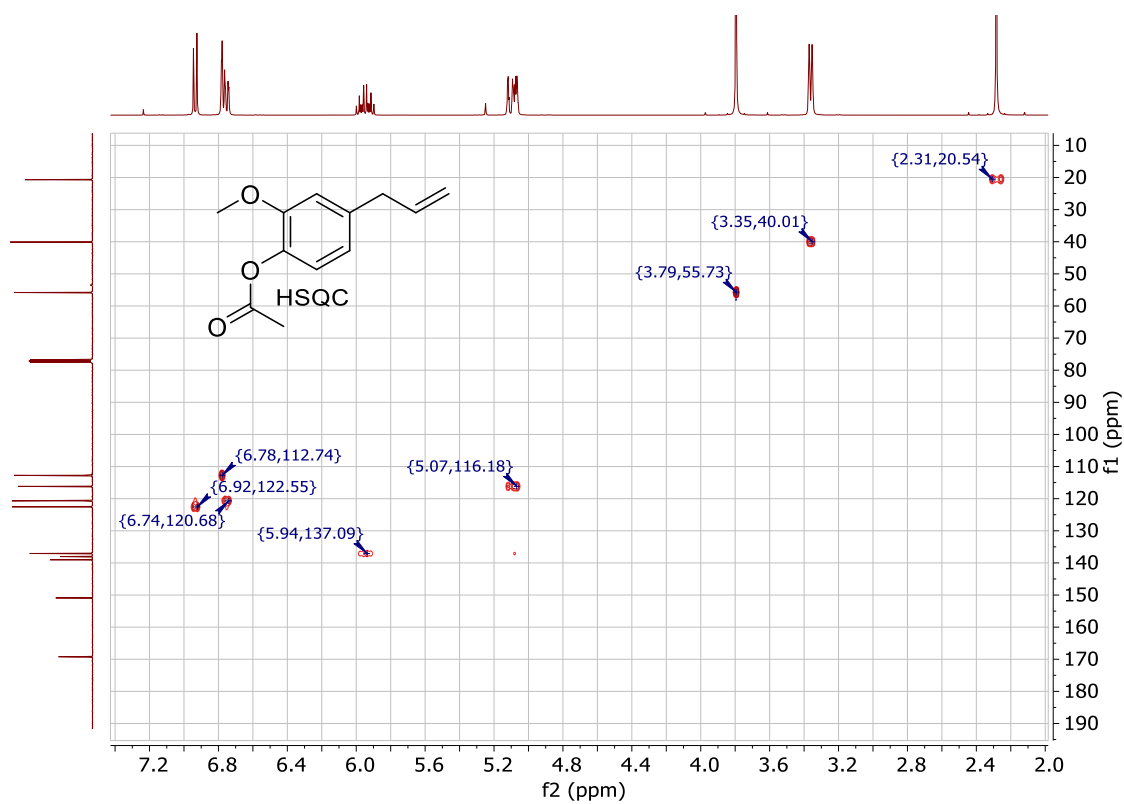


Figure A3. HSQC NMR of acetylugenol (2.1).

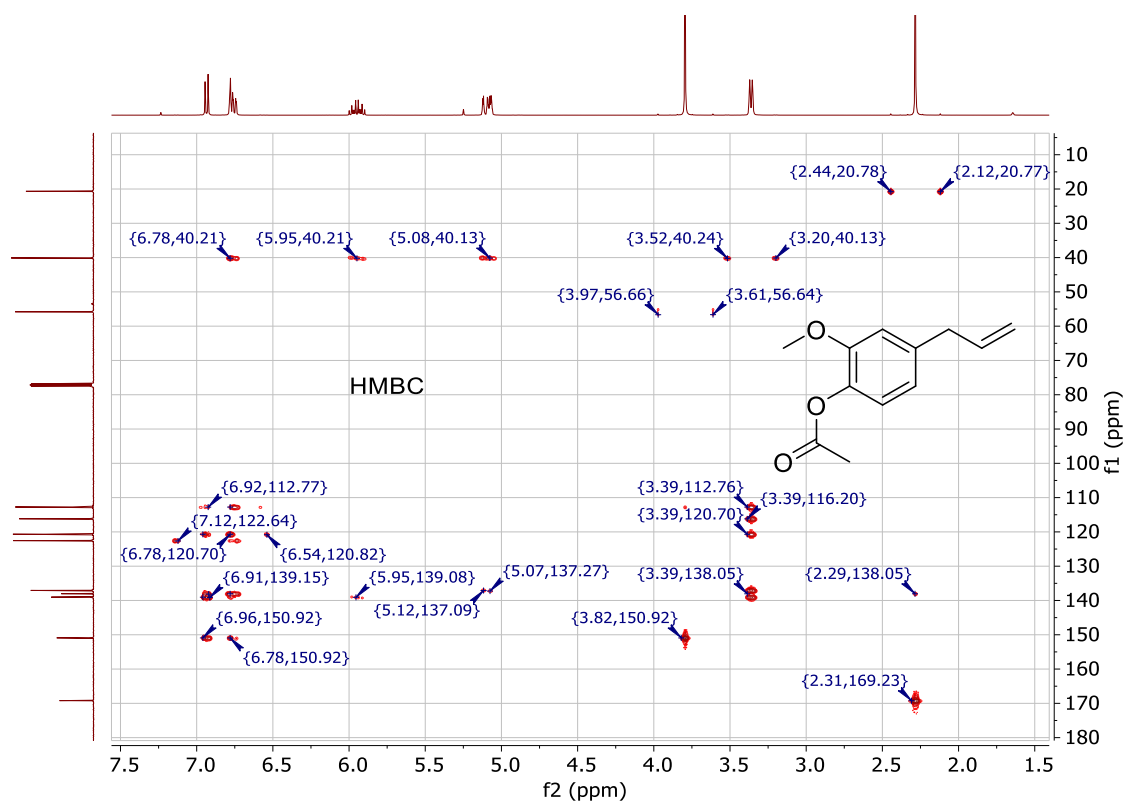


Figure A4. HMBC NMR of acetylugenol (2.1).

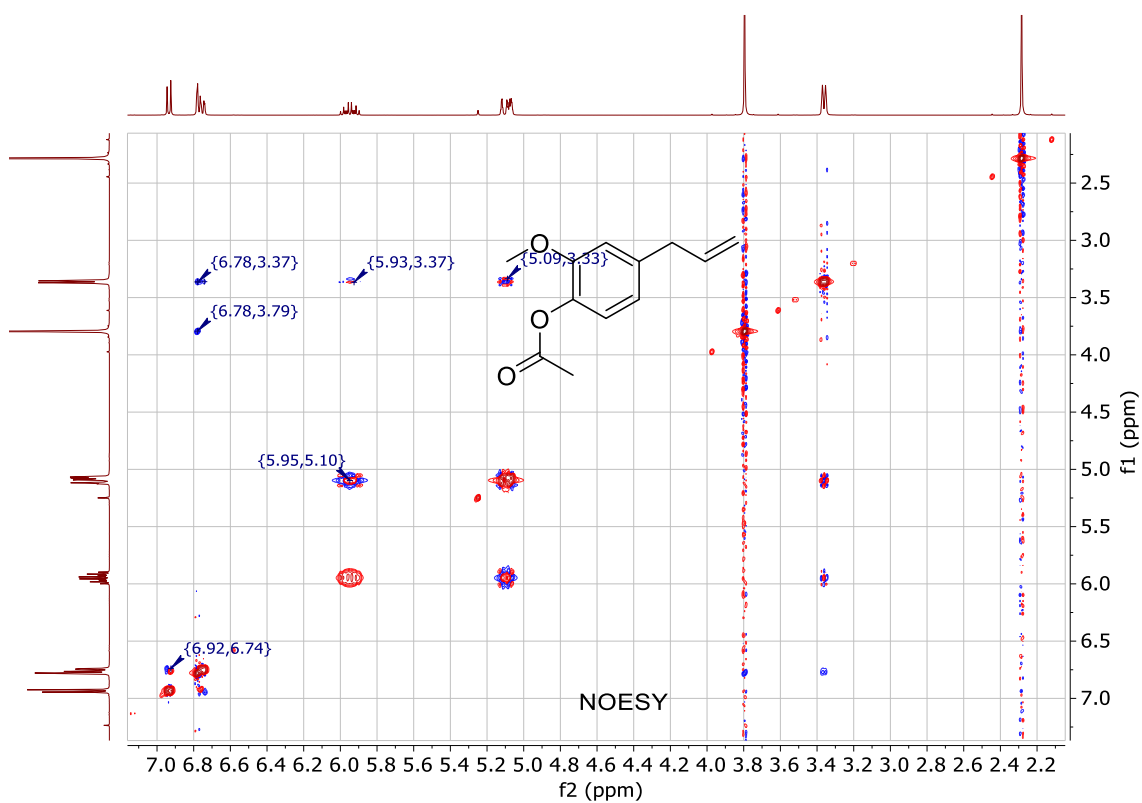


Figure A5. NOESY NMR of acetylugenol (2.1).

NMR spectra for acetyl eugenol epoxide (**2.3**)

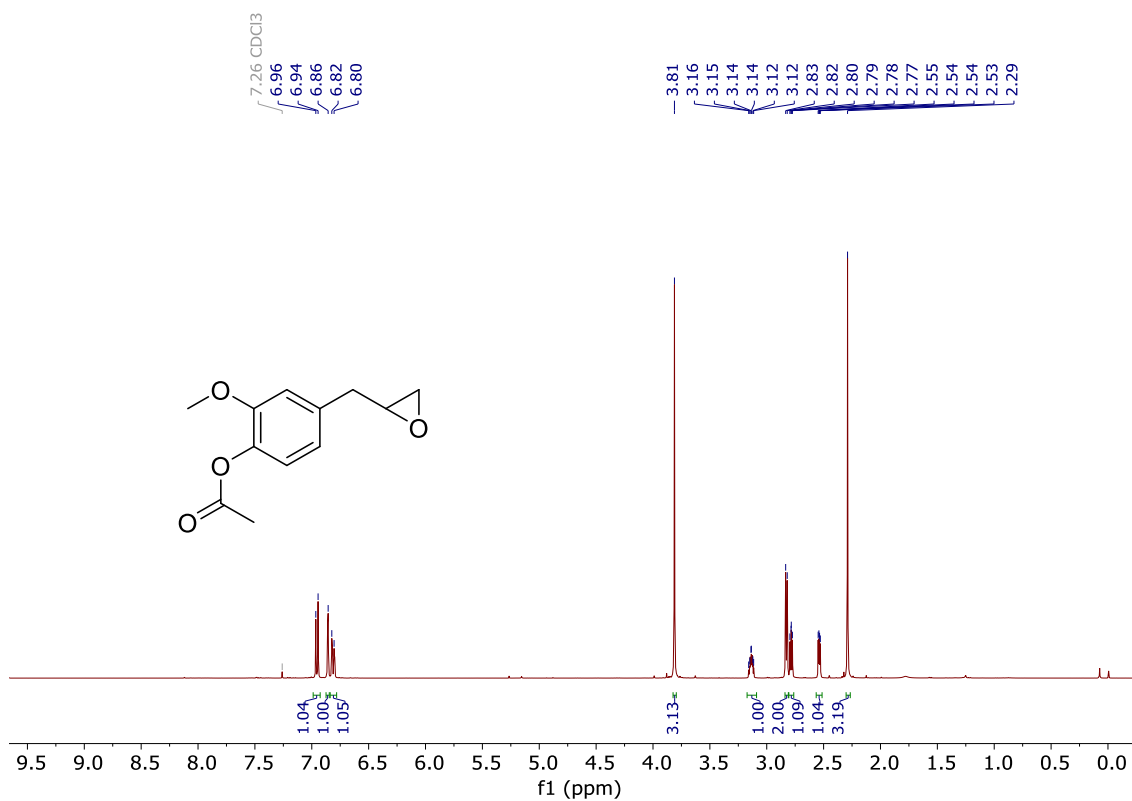


Figure A6. ¹H NMR of acetyleneugenol epoxide (**2.3**).

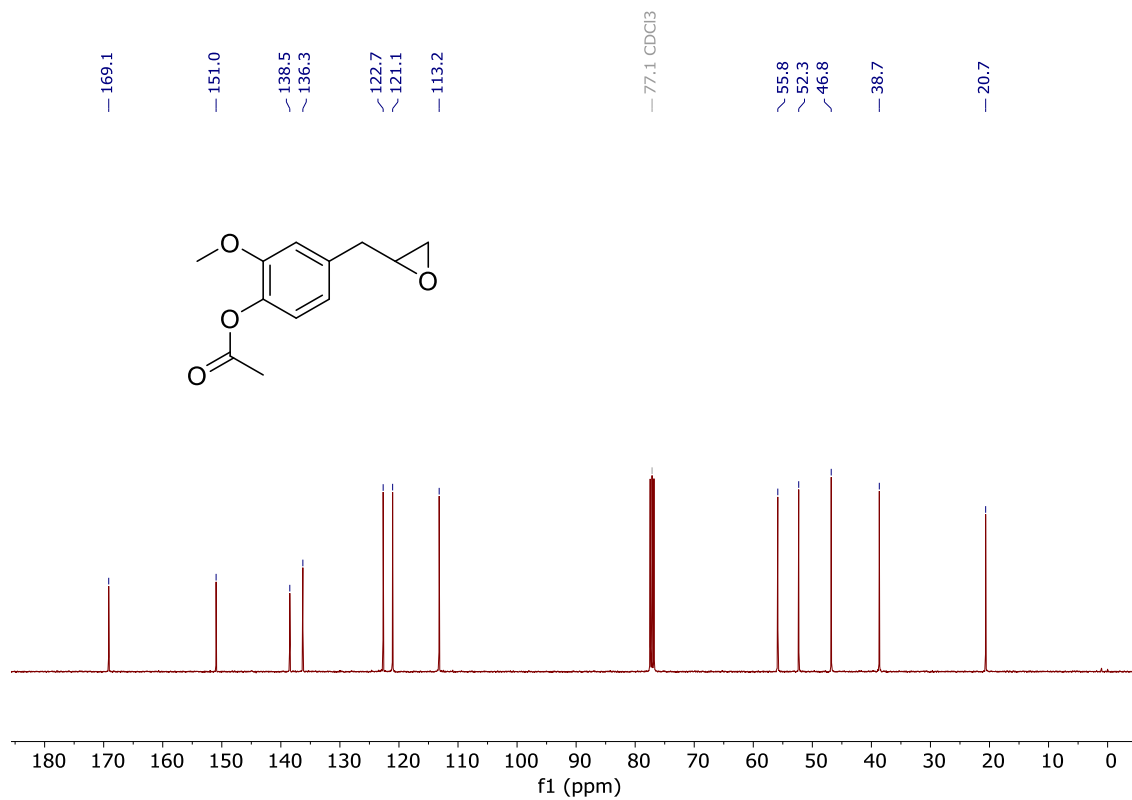


Figure A7. ¹³C NMR of acetyleneugenol epoxide (**2.3**).

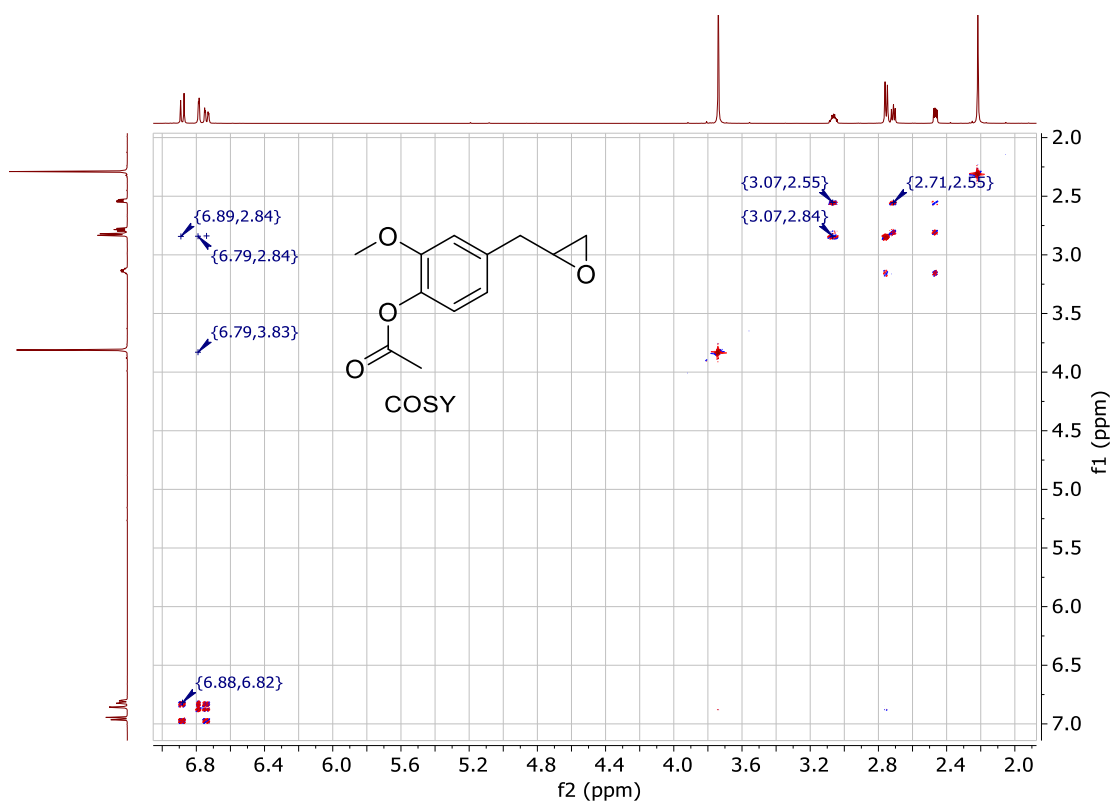


Figure A8. COSY NMR of acetylugenol epoxide (**2.3**).

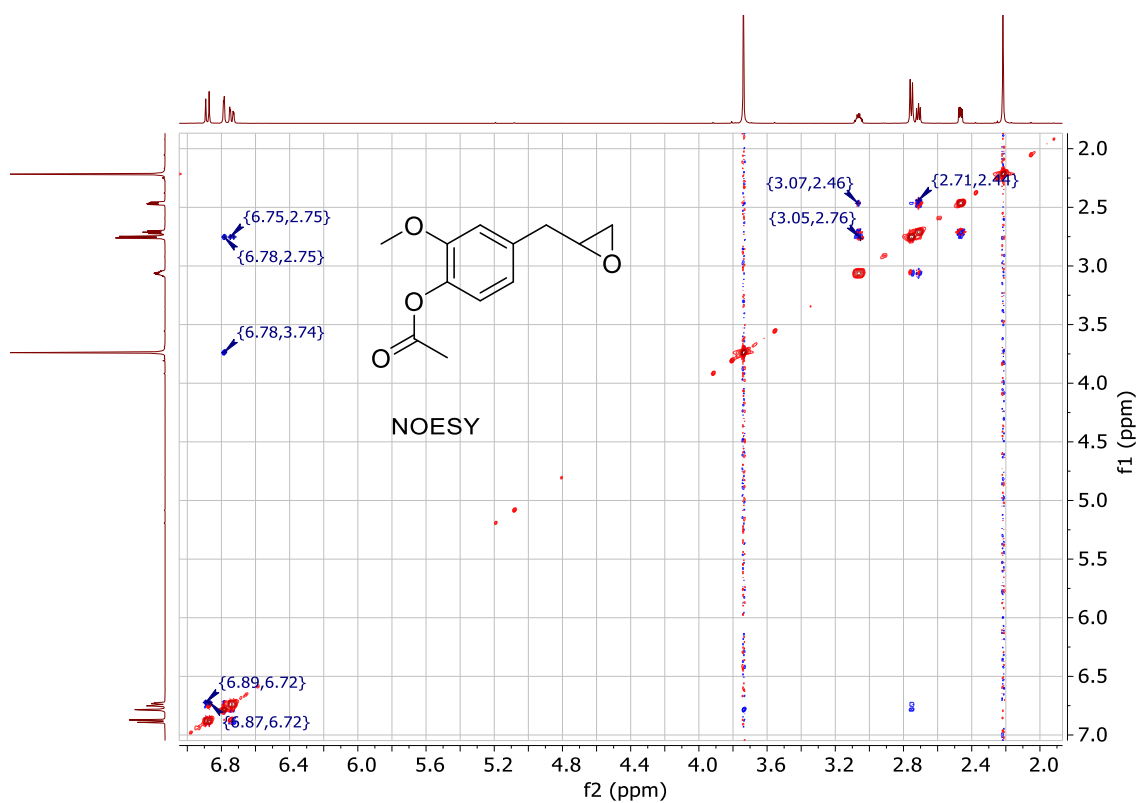


Figure A9. NOESY NMR of acetylugenol epoxide (**2.3**).

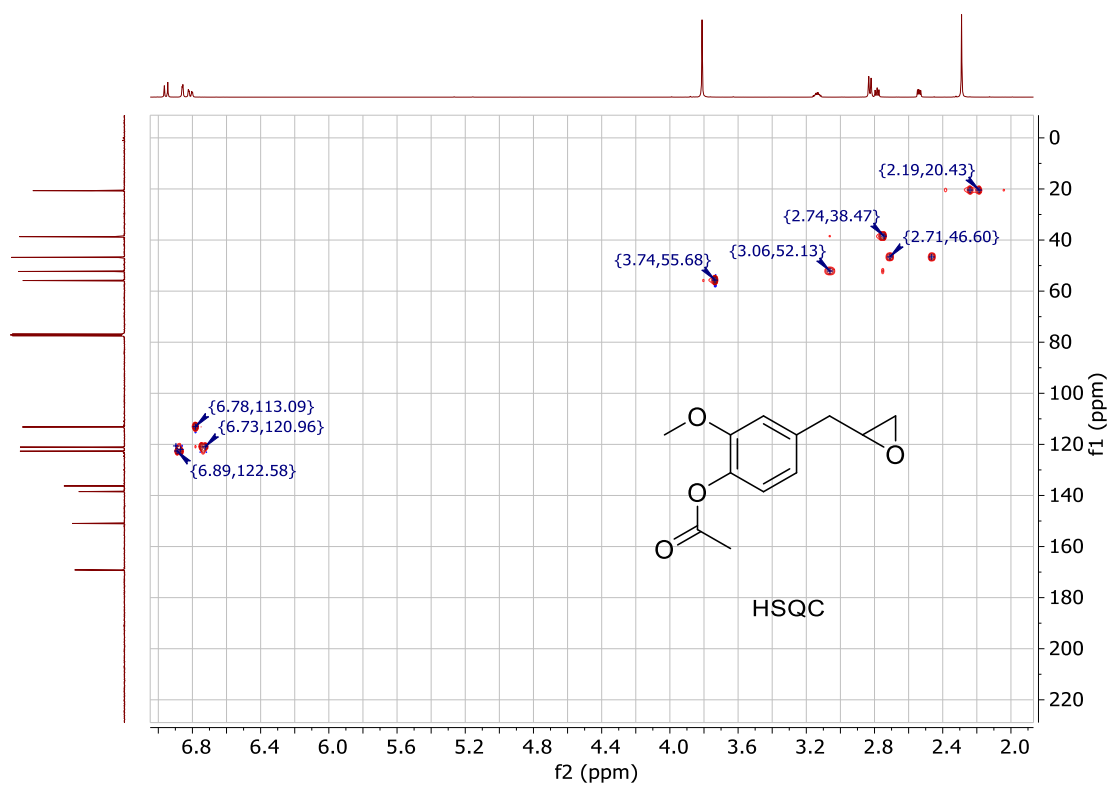


Figure A10. HSQC NMR of acetylugenol epoxide (**2.3**).

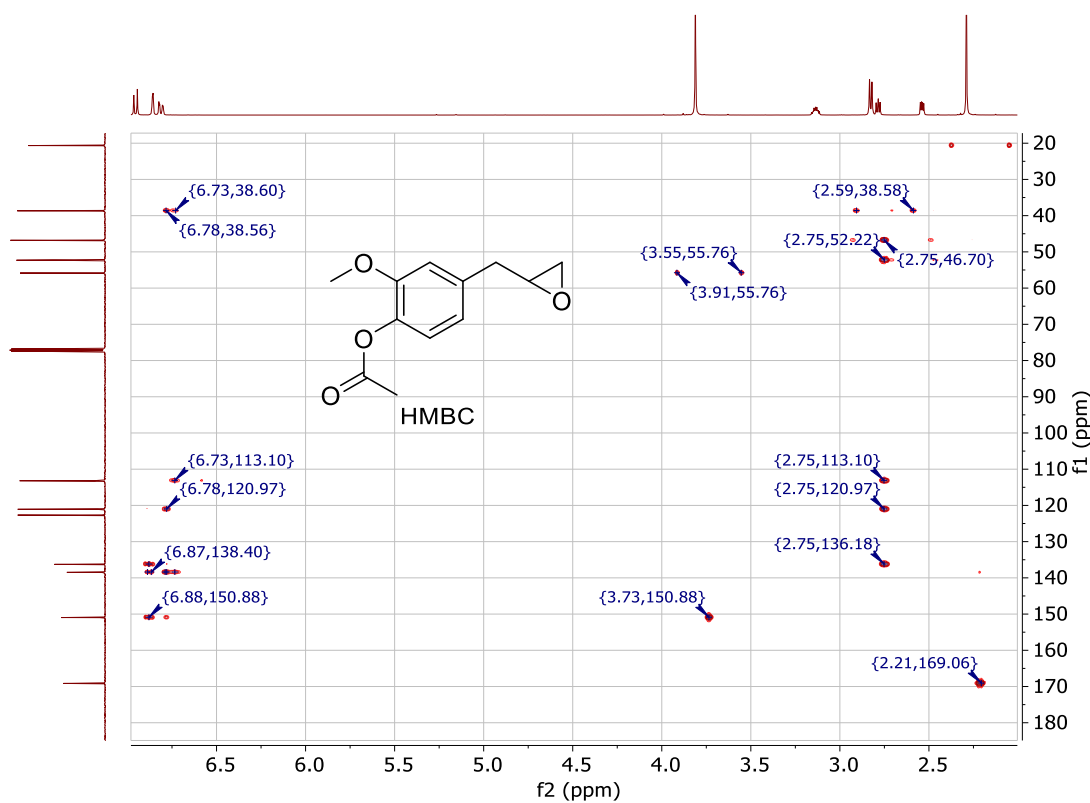


Figure A11. HMBC NMR of acetylugenol epoxide (**2.3**).

NMR data for acetylugenol cyclic carbonate (2.5)

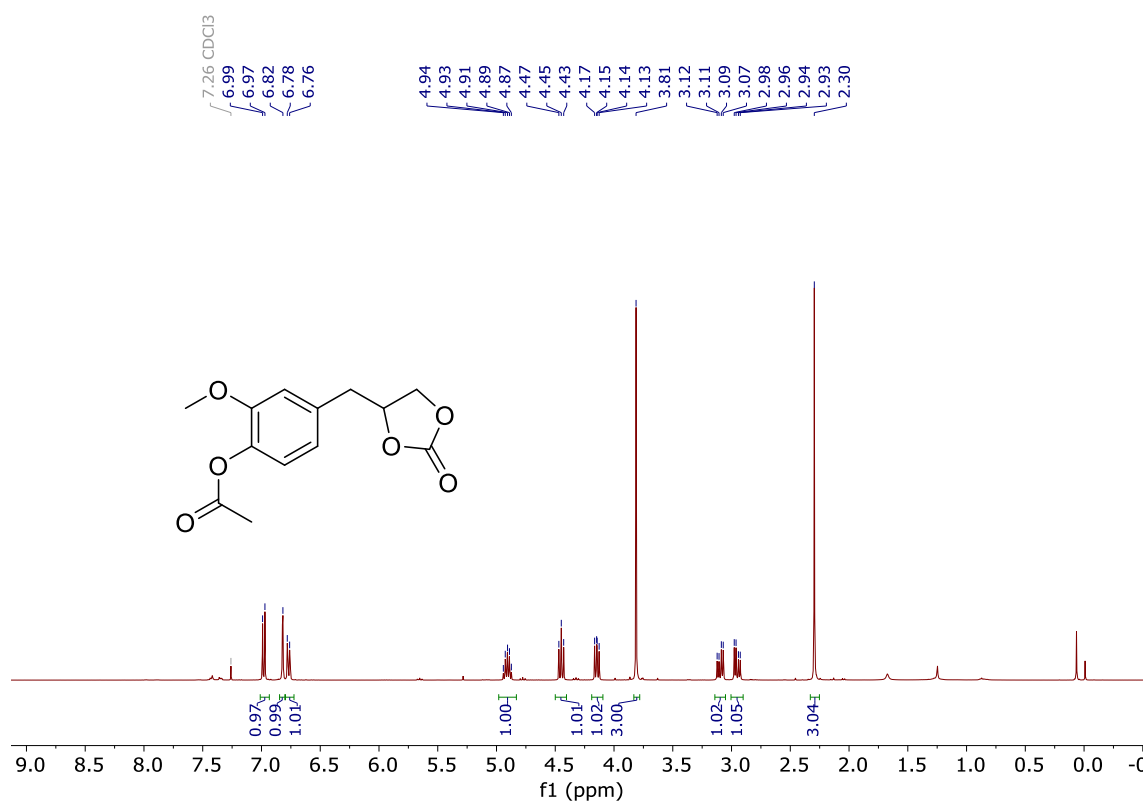


Figure A12. ¹H NMR of acetylugenol cyclic carbonate (2.5).

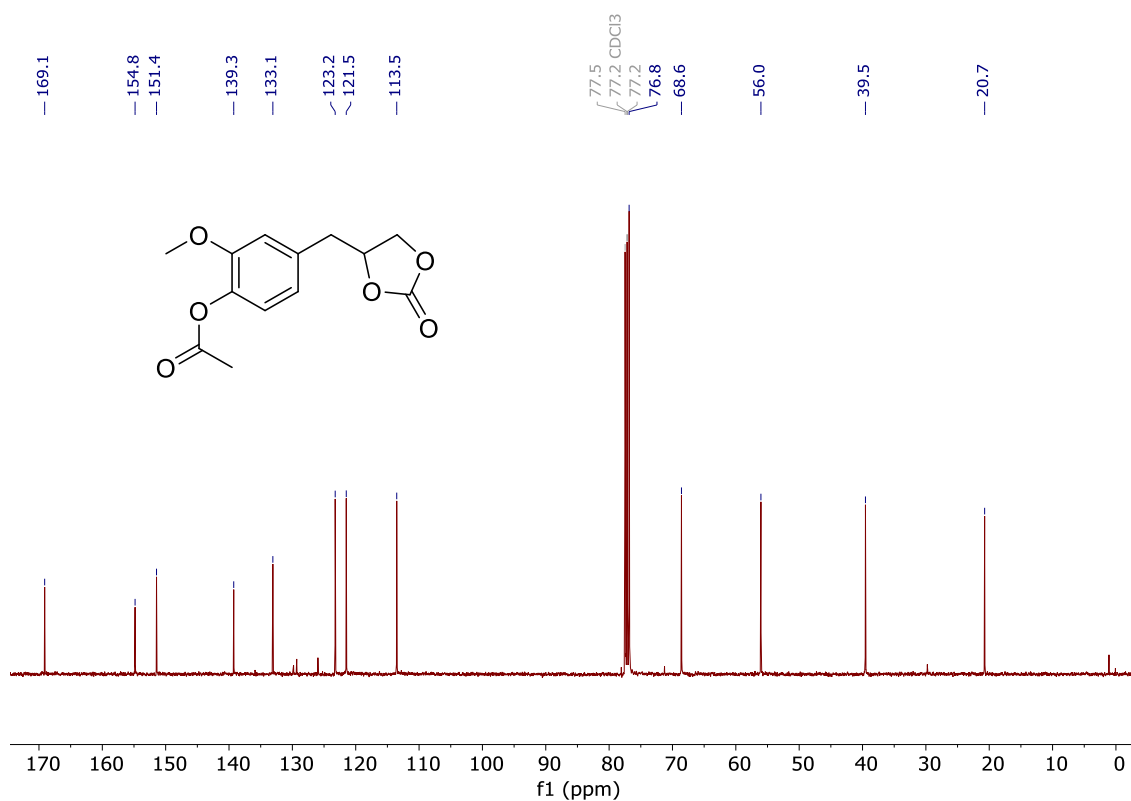


Figure A13. ¹³C NMR of acetylugenol cyclic carbonate (2.5).

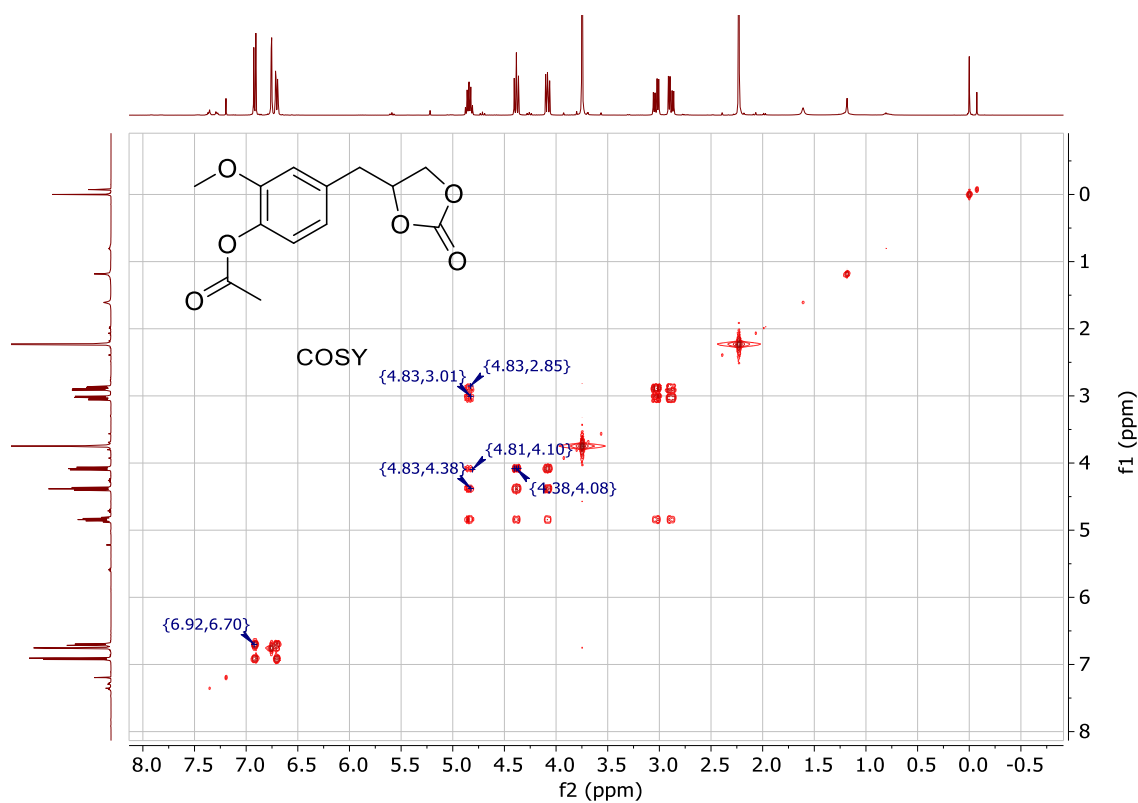


Figure A14. COSY NMR of acetylugenol cyclic carbonate (**2.5**).

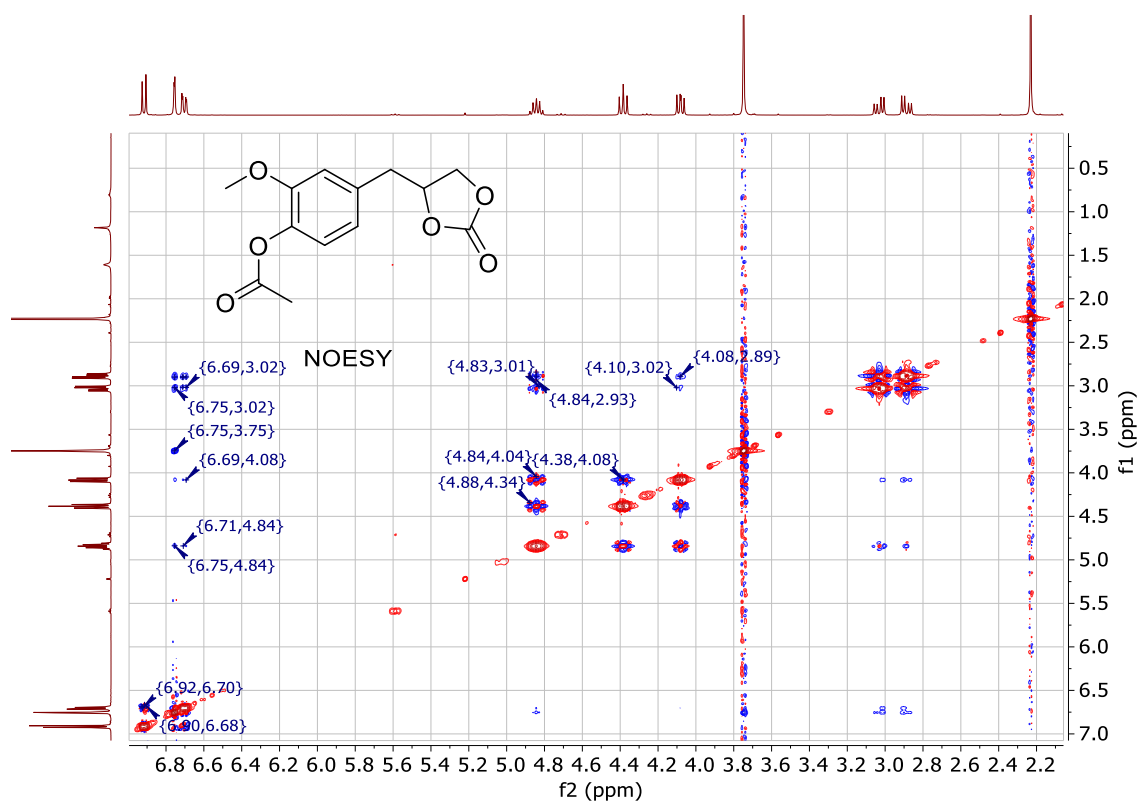


Figure A15. NOESY NMR of acetylugenol cyclic carbonate (**2.5**).

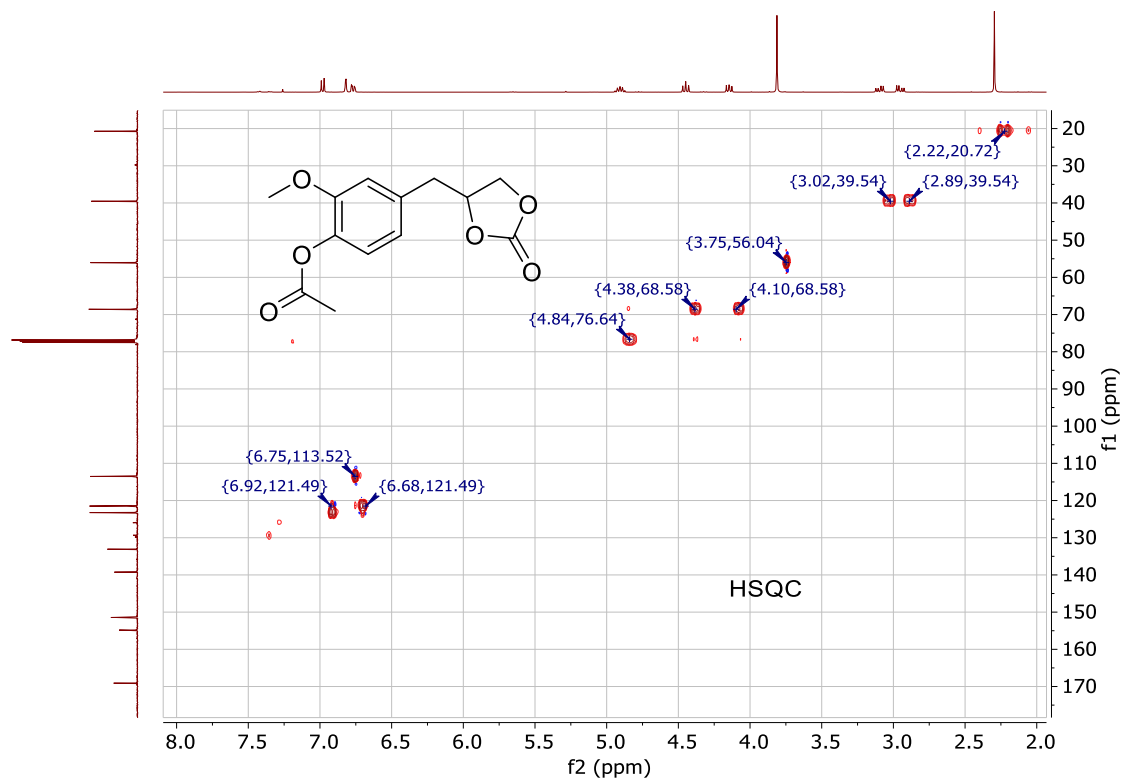


Figure A16. HSQC NMR of acetylugenol cyclic carbonate (2.5).

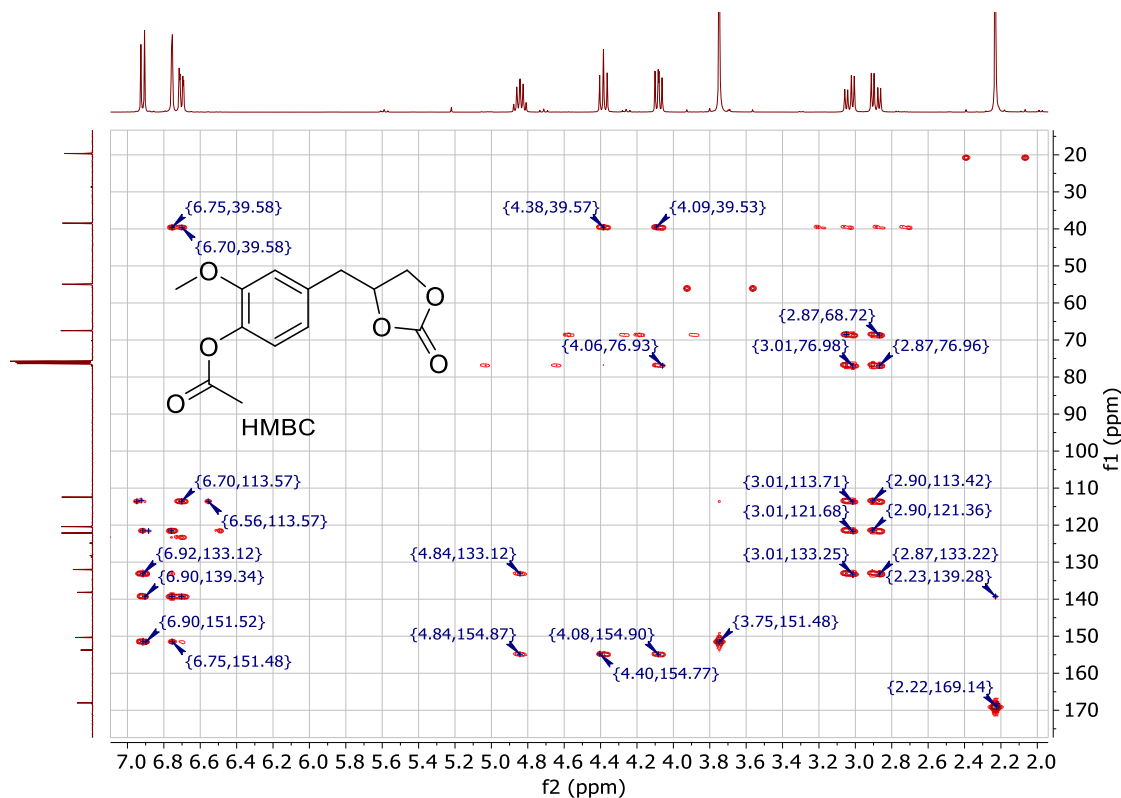


Figure A17. HMBC NMR of acetylugenol cyclic carbonate (2.5).